Expression of RNase L in Prostate Cancer

Thesis submitted to

Jawaharlal Nehru University

for the award of the degree of

DOCTOR OF PHILOSOPHY

KUMAR SANDEEP

SCHOOL OF LIFE SCIENCES

JAWAHARLAL NEHRU UNIVERSITY

NEW DELHI -110067

INDIA

January, 2013

School of life sciences

Jawaharlal Nehru University

New Delhi -110067

INDIA

CERTIFICATE

The Research work included in this thesis entitled **"Expression of RNase L in Prostate Cancer"** has been carried out by Mr. Kumar Sandeep in the School of Life Sciences, Jawaharlal Nehru University (JNU), New Delhi. This work is original and has not been submitted so far, in part or full for any other degree or diploma of any other university.

Kumar Sandeep
(Candidate)

Prof. Neera B. Sarin
(Dean)

Prof. Pramod C. Rath
(Supervisor)

ACKNOWLEDGEMENTS

labmate and friend. I thank them for always being with me. I must thank Dr. Kanchan Singh for teaching me mouse castration. I thank my juniors Jitendra, Sukhleen, Naseem and Vineet for providing a congenial environment and work experience to me for carrying out the work. I also extend my thanks to short term lab trainees Shefali, Joiselle and Amit.

Friends are the most precious gift of life. I thank to Vijayan, Abhishek, Vibhor, Shafat, Manish, Anil, Akhil, Shafat, Sitaram, Ram Babu Ajeet, Bhawana, Sanjveeni, Sudhuman, Naveen, Malika, Pooja, Saima, Shweta and Vijayata for the memorable time, I spent with them. Presence of seniors like Antresh, Vinay, Vishnu, Ashutosh, Pritesh, and friends like Surendra, Sanjay, Nikhil, Deepak, Pradeep, Nishant, Anuradha and Sudhuman, from Himachal Pradesh University in and around JNU formed a strong emotional support in the hours of need.

I would also like to extend huge, warm thanks to my Chandrabhaga hostel residents Pankaj, Avinash and Indresh for providing a joyful and fun filled environment at the hostel.

No word is sufficient to express my deepest sense of regards to my parents for their understanding, affection and love and as of my source of inspiration. I take this opportunity to thank my brother and sister for all the love and affection they shared with me, for being there for me at all times and for encouraging me throughout in all my endeavours.

And, I have no word to express and explicate the thanks to the GOD for blessing because words are not sufficient.

Kumar Sandeep

ABBREVIATIONS

-/-	Knockout
°C	Degree celsius
μg	Microgram
μl	Microliter
2-5A	2`-5`oligoadenylate
2-5OAS	2`-5`oligoadenylate synthetase
a.a.	Amino Acid
$A_{260/280}$	Absorbance at 260/280 nm wavelength
AMP	Adenosine monophosphate
ATP	Adenosine triphosphate
bp	Base pairs
cDNA	Complementary DNA
conc.	Concentration
COX-2	Cyclooxygenase-2
ddw	Double distilled water
DEPC	Diethylpyrocarbonate
DHT	5α-Dihydrotestosterone
DMSO	Dimethylsulphoxide
DNA	Deoxyribonucleic acid
ds	Double stranded
dsRNA	Double stranded RNA
e.g.	Example
EDTA	Ethylenediamine tetra acetic acid
EtBr	Ethidium bromide
Fig.	Figure
g	Gram
GAPDH	Glyceraldehyde 3-phosphate dehydrogenase
HIV-1	Human Immunodeficiency Virus-1
HPC-1	Hereditary prostate cancer-1
hr	Hour
hRNase L	Human Ribonuclease L
i.e.	That is

IDV	Integrated density value
IFN	Interferon
kb	Kilobase
kDa	Kilo Dalton
LB	Luria broth
M	Molar
mg	Milligram
min	Minutes
ml	Milliliters
mM	Milimolar
MMLV	Moloney Murine Leukemia Virus
mRNA	Messenger RNA
mRNase L	Mouse RNase L
N	Normal
NCBI	National Center for Biotechnology Information
ng	Nanogram
nm	Nanometer
nt	Nucleotide
O.D.	Optical density
O/N	Overnight
OD_X	Optical Density at Wavelength X
PAGE	Polyacrylamide Gel Electrophoresis
PAMPs	Pathogen-associated molecular patterns
PBS	Phosphate buffered saline
PCR	Polymerase Chain Reaction
pg	Picogram
PRRs	Pattern recognition receptors
PTEN	Phosphatase and tensin homolog
RNA	Ribonucleic Acid
RNase L	2'-5'A dependent endoribonuclease L
ROS	Reactive oxygen species
rpm	Revolutions per minute
rRNA	Ribosomal RNA
RT	Room temperature

RT-PCR	Reverse Transcription Polymerase Chain Reaction
sec	Second
siRNA	Small interfering RNA
STAT1	Signal Transducers and Activators of Transcription 1
TNF-α	Tumor necrosis factor-alpha
U	Unit
UTR	Untranslated region
v/v	Volume/volume
w/v	Weight /volume
XMRV	Xenotropic murine leukemia virus-related virus

CONTENTS

I

Summary

I. SUMMARY

RNase L was originally identified as a non-specific endoribonuclease, which degraded viral and cellular single-stranded RNAs after being activated by 2-5A cofactor(s) in response to viral-infection and interferon (IFN) treatment of mammalian cells. RNA degradation by RNase L led to apoptosis of virus-infected cells thus producing antiviral effects. Later, RNase L was identified as a tumor suppressor as well as a human prostate cancer (HPC-1) susceptibility locus. It was argued that a homozygous mutation (R462Q) in the RNase L gene (RNASEL) increased the risk for prostate cancer in human patients. A human gammaretrovirus, xenotropic murine leukemia virus-related virus (XMRV), that was detected at high frequency in patients homozygous for the RNase-L mutation but was found at significantly reduced rates in heterozygous or wild type individuals. Like other retroviruses, XMRV probably promotes tumorigenesis by integrating adjacent to cellular genes and changing their expression; in fact, mapping of XMRV integration sites in prostate cancer revealed a preference for cancer-associated genes and regions (Kim et al., 2010). Stable knockdown of RNase-L increased tumor size and number as compared to the control cells in the nude mouse xenografts of human cervical cancer cells and ectopic expression of RNase L reduced tumorigenesis in a murine xenograft model (Liu et al., 2007). While most studies described a tumor suppressor role for RNase L, it was reported to be upregulated in premalignant familial adenomatous polyposis polyps and adenocarcinomas as compared to the colon epithelium (Wang et al., 1995). Androgens play an important role in the development of prostate. Androgen ablation therapy is recommended in many prostate cancer cases. RNase L interacted with androgen receptor (AR) in a ligand-dependent manner. In transient transfection experiments, overexpression of wild-type or R462Q-mutated RNase L differentially affected the ability of IFN to antagonize 5α-dihydrotestosterone (DHT) mediated transactivation. Furthermore, it was also shown that IFN-insensitive cells could become sensitive to IFN upon down-regulation of AR-expression by siRNA (Bettoun et al., 2005).

In the meantime, earlier studies in our laboratory reported that the human RNase L when expressed as a recombinant protein in *E. Coli* caused degradation of the RNAs and inhibited cell growth without exogenous 2-5A cofactor (Pandey and Rath, 2004). This human RNase L protein was degraded in *E. Coli* cells, later this was stabilized and purified by expressing a GST-hRNase L fusion protein, which was biochemically active

against cellular rRNAs *in vitro* in a 2-5A dependent manner (Gupta and Rath, 2012). But a RNase-domain deleted / dominant negative form of the mouse RNase L (homologous to the human RNase L) not only did not degrade the RNAs but also it stimulated the *E. Coli* cell growth. Earlier, this dominant negative mouse RNase L (DN-mRNase L) cDNA was reported to inhibit RNA degradation and apoptosis caused by the human RNase L cDNA in the mammalian cells, and this was explained as, since the DN-mRNase L protein bound and sequestered the 2-5A cofactors, the hRNase L protein was less active (Naik et al, 1998). Later, it was found out in our laboratory that the DN-mRNase L protein was highly degraded when expressed in *E. Coli* and it stimulated expression of some *E. Coli* proteins, which might have stimulated the *E. Coli* cell growth (Gupta and Rath, 2009, unpublished), this informed about a role of RNase L similar to the opposite effect of a tumor-suppressor in terms of cell growth, proliferation of mammalian cells. A study in our laboratory, for the first time showed that the RNase-domain deleted RNase L may have other cellular functions/ effects; this is analogous to the gain-of-function mutation effect(s) of a tumour-suppressor. Yet another study from our laboratory showed that cellular RNase L protein expression was induced by a number of stressors like the anticancer drugs, dsRNA, H_2O_2, $CaCl_2$ and inflammatory cytokine (TNF-α) in the human cervical carcinoma (HeLa) cells, this correlated with RNA-degradation, DNA-fragmentation and apoptosis in the cells (Pandey et al., 2004), suggesting for the first time that RNase L is a stress-responsive gene factor and it may be involved in normal cellular functions other than its well-established antiviral role.

In another study from our laboratory, a number of cellular proteins were identified from the mouse spleen which interacted with RNase L (Gupta, 2009). It was also found that the RNase L mRNA was constitutively expressed in the mouse tissues with higher levels in the spleen and thymus, the two immunological tissues (Gupta, 2009). This stimulated us to explore the link between RNase L expression and prostate cancer, if any.

With this background the present study was designed to address the following questions

A. What is the status of RNase L expression in mouse tissues under normal conditions?

B. What is the effect(s) of endogenous and exogenous androgen(s) on the expression of RNase L in the prostate tissue of mouse under *in vivo* conditions?

2

C. What is the status of RNase L expression in an androgen-responsive and androgen-unresponsive human prostate cancer cell lines?

D. What is the effect(s) of androgen on RNase L expression in the above two human prostate cancer cell lines?

E. What is the effect(s) of oxidative stress (H_2O_2) on RNase L expression in above two human prostate cancer cell lines?

In our study it was found that, RNase L mRNA is constitutively expressed in the mouse tissues under normal physiological conditions, with 3X fold higher level in the spleen and 2X fold higher level in thymus, when compared to other tissues, i.e. prostate, suggesting housekeeping function(s) of RNase L in the tissues as well as its immunological role(s) in the spleen and thymus. This is a new information, as RNase L has been long known as mainly an antiviral RNA-degrading enzyme induced by viruses, interferons and dsRNA in mammalian cells.

RNase L mRNA may not be primarily regulated by endogenous androgen in normal mouse prostate tissue, exogenous androgen also did not show any major significant effect on RNase L mRNA level, at the best, it may negatively regulate RNase L expression to some extent, possibly, through a cryptic androgen response element (ARE) in the RNase L promoter at -51 to -63 nucleotide, which needs to be established.

Human prostate cancer cell lines, e.g. the androgen-unresponsive DU145 and the androgen-responsive 22Rv1 cells showed differential effects of androgen in regulating the levels of RNase L mRNA and protein. In 22Rv1 cells, androgen caused cell proliferation of nearly 1.5X fold at 48 hr, and down-regulation of the level of RNase L mRNA (0.46X fold) as well as protein, while in DU145 cells no effect of testosterone was observed either on cell proliferation or on expression of RNase L mRNA and protein. Here, negative regulation of RNase L positively correlated with cell proliferation in response to androgen.

Oxidative stress by H_2O_2 caused cytotoxic/apoptotic effect on both DU145 and 22Rv1 cells and up regulated the RNase L mRNA and protein level in both the androgen-responsive and unresponsive cell lines, 22Rv1 and DU145 cell lines, respectively. There was an increase of 5.75X fold for DU145 and 1.51X fold for 22Rv1 in the RNase L mRNA expression in response to H_2O_2. Here, again positive regulation of RNase L negatively correlated with cell proliferation.

RNase L expression in the human prostate cancer cells may be exploited to cause inhibition of cell growth/proliferation and oxidative stress-inducing agents like H_2O_2 may be exploited to induce RNase L expression in order to cause cytotoxicity/apoptosis in both androgen-responsive and androgen-unresponsive human prostate cancer cells. Further investigation is necessary to dissect the molecular details of these cellular effects of androgen and H_2O_2 in the context of RNase L gene expression.

Although our study have revealed the regulation RNase L mRNA and protein in androgen-responsive and androgen-unresponsive human prostate cancer cells DU145 and 22Rv1, respectively, by androgen and oxidative stress inducing agent H_2O_2, further investigation is necessary to establish the molecular details of these cellular effects.

II

Introduction

II. INTRODUCTION

The mammalian innate immune system is the first line of defense against pathogens such as viruses, bacteria, fungi and parasites that encounter passive physical barriers like the skin and mucosal tissues. If the pathogen crosses this barrier, the innate immune systems will recognize the agent and generate active anti-viral and antimicrobial responses at the cellular level by producing pro-inflammatory cytokines and interferons (IFNs) (Stark et al., 1998). Interference to viral growth was first reported by Issacs and Lindenman (1957) in the chick chorioallantoic egg membranes pre-exposed to heat inactivated influenza virus. The secreted factor from the chorioallantoic membranes responsible for interference with virus (inhibition) was named as "interferon" (IFN). Atanasiu and Chany (Atanasiu and Chany, 1960) demonstrated that pre-treatment of hamsters with IFN preparations prior to inoculation of Polyoma Virus delayed appearance of the tumors. Paucker (Paucker et al., 1962) argued that murine IFN inhibited cell growth and the activity was independent of its antiviral action; Gresser (Gresser et al., 1969) demonstrated that treatment of IFN could inhibit tumor growth in animals. These properties of IFNs were later proved by recombinant IFNs in 1980s and later.

IFNs are a family of cytokines that have anti-viral, anti-proliferative and immunomodulatory effects on many cell types. The classification of the IFN family of proteins is based mainly on their sequence, chromosomal location and receptor specificity (Chelbi-Alix and Wietzerbin, 2007). There are mainly three types of interferons, Type I, II and III. The type I IFNs consist of IFN-α, -β, -ω, -ε, -κ, -δ, -τ and -ζ (limitin) (Pestka et al., 2004). Some of these like IFN-δ, -τ and -ζ are only detected in pigs/cattle, ruminants and mice respectively. All these members are induced in virally infected cells to induce an antiviral state in the uninfected cells. Most of the studies on interferons have focused mainly on IFN-α/β. IFN-α/β also shows a variety of important immunomodulatory roles in the innate immune response and also in the adaptive immune response. Additionally, a direct or indirect tumor suppression is one of the major therapeutic activities of IFN-α/β. All of the members transmit signals through a receptor complex composed of two subunits, IFNAR-1 and IFNAR-2 (Takaoka and Yanai, 2006). Type II IFN comprises of IFN-γ. This cytokine is strongly produced by activated macrophages, T cells and NK cells. IFN-γ signaling is essential for the activation of macrophages to constitute the effective form of innate immunity to intracellular

microorganisms, and it also contributes to the development of CD4+ Th1 cells and cytotoxic CD8+ T cells (Ikeda et al., 2002). IFN-γ signals through a pair of receptor subunits, IFNGR-1 and IFNGR-2. The type III IFN consists of IFN-λs or IL-28/29. In humans, this group includes three homologous proteins, IFN-λ1-3 (IL-28A, IL-28B and IL-29). Similar to type I IFNs, they are induced upon viral infection for their antiviral activity by inducing IFN-stimulated genes e.g., OAS (2',5'-Oligoadenylate synthetase), PKR (Protein Kinase R, double stranded RNA-dependent) and MxA, through activation of Jak kinase(s), Signal Transduction and Activator of Transcription (STAT) factors and subsequent formation of the IFN-stimulated (ISGF) complex (Vilcek, 2003). However, the major differences are that they are structurally distinct from type I IFNs and they utilize their specific receptor subunit, IFN-λR1 or IL-28Rα, together with IL-10R2 is known to be a shared receptor subunit among IL-10, IL-22 and IL-26. In this regard, they might be separated into the third group (type III IFNs).

IFNs act in the cell through the Janus-Kinase Signal Transduction and Activation of Transcription (JAK-STAT) pathway by induction of a subset of genes, called IFN stimulated genes (ISGs). The ISGs are known to cause anti-viral, cell cycle inhibitory, anti-angiogenic, and pro-apoptotic effects (Chawla-Sarkar et al., 2003). Genes induced by IFNs include the 2', 5'-oligoadenylate synthetases (OAS), located on chromosome 12q24.2, which encodes 8-10 latent isoforms of OAS by alternative splicing (Rebouillat and Hovanessian, 1999). In human, three OAS genes (OAS1-3) and a related enzymatically inactive gene OASL are known (Justesen et al., 2000). Double stranded RNA activates OAS proteins to catalyze the 2'-specific adenosine nucleotidyl transfer reactions using ATP as a substrate. OAS1 and OAS2 proteins produce mainly 2-5A trimer or longer oligomers, all of which stimulate RNase L. However, OAS3 proteins produce predominantly 2-5A dimer, which does not stimulate RNase L (Rebouillat et al., 1999).

IFN inhibits virus replication in higher vertebrates, this is effected by causing cells to transcribe genes encoding anti-viral proteins, including the 2'-5' oligoadenylate synthetases (OAS) (Kerr and Brown, 1978; Mashimo et al., 2003). The viral double-stranded RNA (dsRNA) produced by viral infections, which acts as pathogen associated molecular pattern (PAMP), activates OAS to produce 5'-phosphorylated, 2', 5'-linked oligoadenylates (2-5A) from ATP. The known function of 2-5A is to activate latent and ubiquitous RNase L, which is a ubiquitous 83 kDa protein that dimerizes into its

catalytically active form upon 2-5A binding (Dong and Silverman, 1995; Zhou et al., 1993). The 2-5A cofactor must have at least one (in human) or two (in mice) 5'-phosphoryl groups and a minimum of three adenylyl residues in 2', 5' linkage (Cayley et al., 1984). Upon activation, RNase L degrades both viral and cellular single-stranded RNA, which leads to suppression of virus replication. Anti-viral role of the 2-5A system was understood by *in vivo* studies with RNase L knock-out mice, which have increased susceptibility to virus compared to wild type mice (Flodstrom-Tullberg et al., 2005; Samuel et al., 2006; Zhou et al., 1997). The 2-5A/RNase L pathway is implicated in mediating apoptosis in response to viral infect ions. Thus, sustained activation of RNase L triggers a mitochondrial pathway of apopsosis by activating the stress-activated protein kinases, c-jun NH2-terminal kinases (JNKs) to eliminate virus-infected cells (Castelli et al., 1997; Li et al., 2004; Malathi et al., 2004; Zhou et al., 1997). RNase L-mediated apoptosis is accompanied by cytochrome c release from the mitochondria and requires caspase-3 activity (Rusch et al., 2000). The caspase-dependent signaling cascade recruits Fas-associated death domain (FADD) and caspase-8 to activate the effectors caspase-3 and caspase-7. These caspases cleave their substrates such as poly(ADP-ribose) polymerase (PARP), Rb, ρ-GDI, and lamins, ultimately leading to cell death (Almasan and Ashkenazi, 2003).

Prostate cancer is a major cause of cancer related deaths in the human males in the western world and it is increasing in India. One of the first evidences of association of RNase L to prostate cancer came from identification of *RNASEL* (gene encoding RNase L) as a candidate gene for human prostate cancer 1 (HPC1) (Carpten et al., 2002; Silverman, 2003). Several germline mutations or variants in the *HPC1/RNASEL* gene have been observed among hereditary prostate cancer cases. A controlled sib-pair study implicated the RNase L R462Q variant in up to 13% of unselected prostate cancer cases (Casey et al., 2002). One and two copies of the mutated gene increased the risk of prostate cancer by about 150% and 200%, respectively. The RNase L "Q" variant at residue 462 in the kinase-like region had a 3X fold decrease in the catalytic activity compared to the wild-type enzyme, due to an impairment in dimerization (Xiang et al., 2003). However, while several case-controlled genetic and epidemiologic studies support the involvement of *RNASEL* (and notably the R462Q variant) in prostate cancer etiology others do not (Silverman, 2003) suggesting that population differences and environmental factors, such as viral infection, may modulate the impact of *RNASEL* on

7

prostatic carcinogenesis. Therefore, there is a possibility that the linkage of RNase L alterations to *HPC* might reflect enhanced susceptibility to a viral agent.

The direct evidence that RNase L is able to inhibit tumour growth *in vivo* was provided by Liu and coworkers (Liu et al., 2007). To directly measure the effect of RNase L on tumour growth in the absence of other IFN-induced proteins, human RNase L cDNA was stably expressed in P-57 cells, an aggressive mouse fibrosarcoma cell line. Three clonal cell lines were isolated in which the overexpression of RNase L was 15–20-fold higher than the endogenous level. Groups of five nude mice were subcutaneously injected with either the human RNase L overexpressing clones or the control cells transfected with an empty vector. Tumour growth by the two types of cell lines was monitored by measuring the tumour volumes. In the human RNase L overexpressing group, tumour formation was significantly delayed and the tumours grew much slower compared to the control group.

Correlation of RNase L to prostate cancer encouraged researchers to look for its role in other cancers. As prostate cancer occurs in some familial cases of pancreatic cancer, Bartsch and co-workers evaluated the role of two variants of *RNASEL* gene: E265X and R462Q in the etiology of pancreatic cancer (Bartsch et al., 2005). The study showed that the *RNASEL* R462Q variant might be associated with an increased risk for sporadic pancreatic cancer and with more aggressive tumors in familial pancreatic cancer. The R462Q variant of RNase L correlated with earlier age of onset of the hereditary non-polyposis colorectal cancer (Kruger et al., 2005). Elevated levels of RNase L in the colorectal cancer were observed compared to the corresponding normal mucosa (Wang et al., 1995). Interestingly, it was found that, in the lung cancer, the expression of RNase L was 3- and 9- fold higher in its mRNA and protein levels, but there was a significant decrease of its enzymatic activity when compared to that in corresponding normal lung cells. Further it was also found that the 2-5A-induced dimerization of the RNase L protein, a necessary prerequisite for the activation of RNase L, was inhibited, as a result of that RLI, a specific inhibitor of RNase L, was remarkably up-regulated in the cancer cells (Yin et al., 2012).

Thus, considering the available literature the RNase L is an unique molecule having broad range of functions, including its role in cancer in general. Its role in prostate cancer is an active area of research in the last few years. The scientific evidence for its role in prostate cancer have been growing, but many areas, particularly androgen,

its corelation with androgen status, its regulation by androgen with respect to prostate cancer and normal prostate cells remains less-investigated. A careful and detailed analysis is required to understand the relationship between prostate cancer. RNase L and androgen.

III

Review of literature

III. REVIEW OF LITERATURE

III.1. Interferons

The interferons are well known cytokines with antiviral, antiproliferative and immunomodulatory molecules. Virus infection or interferon treatment of mammalian cells induces the expression of the protein kinase (PKR), 2`-5` Oligoadenylate synthetases (OAS), adenosine deaminase acting on RNA (ADAR1), Mx, apolipoprotein B mRNA-editing enzyme catalytic polypeptide like editing complex (APOBEC), Fv, and tripartite motif (TRIM) proteins (Samuel et al., 2006). Among the IFN-induced proteins believed to affect virus multiplication are PKR, which inhibits translation initiation through phosphorylation of the protein synthesis initiation factor eIF-2α; the OAS synthetase family and RNase L, which mediates RNA degradation; the family of Mx protein GTPases, which appear to target viral nucleocapsids and inhibit RNA synthesis; and ADAR, which edits double-stranded RNA by deamination of adenosine to inosine.

III.2. Antiviral pathways

Release of interferon after recognition of viral signal to cell, induces the expression of a set of interferon stimulated genes (ISGs). ISGs activate antiviral pathways including amplification of interferon signaling, production of cytokines that activation of adaptive immunity, and many factors that directly inhibit viruses. ISGs with direct antiviral functions are an active area of research, largely because they are virus-specific and can have multiple mechanisms. The major known Antiviral pathways induced by interferons are described below.

III.2.1. The protein kinase R (PKR) pathway

The Protein kinase R (PKR) was discovered by its property of inhibition of protein synthesis in cell free lysates on treatment with dsRNA, interferon or viruses (Ehrenfeld and Hunt, 1971; Kerr et al., 1974; Meurs et al., 1990). PKR is also known by several other names in the literature like DAI, dsI, P1 kinase or TIK (for the mouse enzyme). Besides PKR, the other protein kinases that phosphorylate eIF2α and regulate the protein synthesis are the hemin controlled repressor (HCR/EIF2αK1), PERK (EIF2αK3) and GCN2 kinase (EIF2αK4) (Williams, 1999).

The PKR molecule contains an N-terminal dsRNA binding domain (consisting of two tandem copies of a conserved dsRNA binding motif, dsRBM1 and dsRBM2) and a C-terminal kinase domain (Nanduri et al., 1998). PKR is generally expressed constitutively at very low basal levels in almost all the tissues however, its expression is enhanced by type I and type III interferons (Ank et al., 2006). PKR is activated by viral dsRNA, polyanionic molecules like heparin (George et al., 1996), ceramide (Ruvolo et al., 2001) and protein activators (Patel and Sen, 1998) by relieving the inhibition of its C-terminal kinase domain by N-terminal RNA binding domain. Binding of the dsRNA activates the PKR by conformational switching leading to its homdimerization and autophosphorylation at several residues (Dar et al., 2005). The active PKR molecule then phosphorylates the eIF2α at serine residue 51, resulting in its sequesteration by eIF2β (Roberts et al., 1976).

PKR interacts with mainly three proteins *viz*; the TRAF family of adaptor molecules that are associated with the TLR signaling (Gil et al., 2004); the protein activator of PKR called as PACT (also known as PRKRA) (Patel and Sen, 1998) and the cleavage of its N-terminal RNA binding domain by caspases (caspase 3, caspase 7 and caspase 8) generating a constitutively active, truncated kinase domain (Gil and Esteban, 2000; Saelens et al., 2001). Gene targeting studies in mice have demonstrated PKR to have antiviral actions against several RNA viruses like HCV, hepatitis D virus, WNV, HIV-1, sindbis virus, EMCV and foot and mouth virus and also some DNA viruses like HSV-1 (Sadler and Williams, 2008). The constitutive expression of PKR at low levels also indicates that it functions as a double-stranded RNA specific PRR in addition to its role as an antiviral effector molecule.

III.2.2. The Mx GTPase pathway

The Mx family of GTPases, highly induced in response to type I IFNs, upon induction is assembled into constitutively active oligomers. They are responsible for the antiviral state against influenza virus infection in mice (Pavlovic et al., 1992). This class of protein consists of four families of proteins *viz*; the p47 guanylate-binding proteins (GBPs), the p65 GBPs, the very large inducible GTPases and the Mx proteins, among which only Mx proteins are known to antiviral functions (Haller et al., 1980).

The Mx family of GTPases, comprise of MxA and MxB present on chromosome 21 in humans and are localized in the cytoplasm of the cell (Aebi et al., 1989). Similarly,

the mouse Mx1 and Mx2 genes are present on chromosome 16; the Mx1 resides in the nucleus while the Mx2 is present in the cytoplasm. Sensitivity of mouse strains to orthomyxovirus was solely due to mutations in the Mx gene locus which was could be restored by Mx1 expression (Arnheiter et al., 1990; Lindenmann, 1962).

The family of viruses that are susceptible to Mx proteins are orthomyxoviruses, paramyxoviruses, rhabdoviruses, togaviruses and bunyaviruses (Andersson et al., 2004). The Mx proteins consist of a large N-terminal GTPase domain, a central interacting domain (CID) and the C-terminal leucine zipper (LZ) domain. They are present near the smooth endoplasmic reticulum and bind viral structures like the nucleocapsid domain through the CID and LZ domains (Kochs and Haller, 1999). They mediate vesicle trafficking to trap essential viral components at early part of the infection and they also bind to influenza virus polymerase (PB2) subunits to block viral gene transcription (Accola et al., 2002; Turan et al., 2004).

III.2.3. RNase L pathway

The 2-5A pathway is constituted by 2-5A synthetases, (2-5OAS), 2-5A cofactor and the RNase L. The 2-5A cofactor activates RNase L to degrade RNAs. The 2-5OAS synthesizes the 2-5A from ATP. Virus, dsRNA, interferons induce and activate 2-5OAS, 2-5A and RNase L for the antiviral defence. Discovery of 2-5A (Kerr and Brown, 1978) as low molecular weight inhibitor of protein synthesis, on incubation of the cytoplasmic extracts from interferon-treated cells with dsRNA and ATP, led to the curiosity about the role of this small unusual oligonucleotides. The 2-5A was later shown to induce a nuclease activity (Hovanessian et al., 1979). The specificity of the 2-5A dependent endoribonuclease to UA and UU sequences was shown later (Wreschner et al., 1981). Two years later, it was shown that Interferon treatment of mouse JLS-V9R cells resulted in a 10- to 20-fold increase in the levels of the 2-5A (ppp(A2'p)nA)-dependent RNase. The nuclease was monitored in cell extracts by covalent and non-covalent binding of ^{32}P-labeled 2-5A derivatives to the nuclease and by the appearance of 2-5A-mediated ribosomal RNA cleavage products. The 2-5A dependent RNase was purified (Silverman et al., 1988) by affinity labeling of the proteins with a ^{32}P-labeled 2-5A derivative, which revealed that, the mouse 2-5A dependent RNase is a 80kDa protein.

The viral pathogen associated molecular pattern (PAMP), double-stranded RNA (dsRNA) produced by viral infections, activates OAS to produce 5'-phosphorylated, 2',

5'-linked oligoadenylates (2-5A) [px5'A(2'p5'A)n; x = 1-3; n≥2] from ATP. Examples of viral dsRNA include replicative intermediates of many single-stranded RNA viruses, such as picornativuses (Gribaudo et al., 1991). In addition, many DNA viruses, such as poxvirus, vaccinia virus, produce dsRNA by annealing of complementary RNAs transcribed from viral DNA strands (Colby and Duesberg, 1969). The known function of 2-5A is to stimulate pre-existing, latent and ubiquitous RNase L, a ubiquitous 83 kDa protein that dimerizes into its catalytically active form upon 2-5A binding (Dong and Silverman, 1995; Zhou et al., 1993). RNase L activation degrades both viral and cellular single-stranded RNA leads to suppression of virus replication. In vivo evidence for the anti-viral role of the 2-5A system was provided by studies with RNase L -/- mice, which have increased susceptibility to the picornaviruses, encephalomyocardit is virus, and Coxsackievirus, or the flavivirus West Nile virus compared to wild type mice (Flodstrom-Tullberg et al., 2005; Samuel et al., 2006; Zhou et al., 1997).

III.2.3.1. 2-5OAS

The 2', 5'-Oligoadenylate synthetases (2-5OAS) are the only known enzyme, which can catalyze the synthesis of 2' to 5' linked phosphodiester bond rather than the usual 3' to 5' phosphodiester bond formation as catalyzed by conventional nucleotide polymerases. These family proteins were discovered by their property to synthesize small molecule inhibitors of protein synthesis in cell free lysates on treatment with dsRNA, interferon or viruses along with PKR (Ehrenfeld and Hunt, 1971; Kerr et al., 1974; Meurs et al., 1990). Also activated in presence of the dsRNA on viral infection or IFN treatment and then they utilize ATP as substrate to synthesize unique and labile oligomers of adenosine, collectively referred to as 2-5A with the general formula $pppA(2'p5'A)_n$, $n \geq 1$. 5OAS proteins are constitutively expressed at low basal levels in healthy individuals, therefore it is believed that they can function as PRRs for the presence of viral dsRNA in the cytoplasm as well as also involved in some other physiological functions of the normal cell (Kerr et al., 1977). Apart from 2-5A synthesis, partially purified 2-5OAS preparations can also catalyze *in vitro* transfer of a nucleotide monophosphate moiety to the 2'-OH end of a preformed 2-5A molecule or to a nucleotide with the structure RpA like NAD^+, tRNA, and 5',5''-linked Ap4A or Ap3A (Cayley and Kerr, 1982; Turpaev et al., 1997). In addition to humans and mice, the 2-5OAS is also found in various species such as rat, pig, chicken (Truve et al., 1994), and even in the lowest multicellular organisms like the marine sponges (Schroder et al.,

2008) where the activity of the enzyme is not dependent on dsRNA (Lopp et al., 2002). On LPS treatment in sponges, the 2-5OAS mRNA and activity are increased, thus suggesting that the 2-5OAS is involved the mechanism of defense against microorganisms (Schroder et al., 2008). In humans, the 2-5OAS is expressed in peripheral blood mononuclear cells (PBMCs) where it is used as marker to monitor the immediate response of patients to IFN-treatment (Witt et al., 1990).

OAS genes are four types in humans referred as - OAS1 (small), OAS2 (medium), OAS3 (large) and OASL (OAS-like), which are clustered on chromosome 12q24.2. in humans and chromosome 5 in mice (Hovanessian and Justesen, 2007; Sadler and Williams, 2008). Sequence comparison of human 2-5OAS with OAS from other species revealed the presence of a conserved domain of 346 a.a. called the OAS unit. OAS1, OAS2 and OAS3 proteins encode for one, two and three OAS domains, respectively. *OAS1* (small) has two alternatively spliced forms in humans (eight in mice) that produce two proteins of 40 and 46 kDa (coded by 1.6 and 1.8 kb mRNA) that differ at their C termini by 18 and 54 amino acids, respectively. Similarly, *OAS2* (medium) produces four alternatively spliced transcripts (4.5, 3.9, 3.3 and 2.8 kb) that encode two proteins of 69 and 71 KDa while *OAS3* (large) encodes a single transcript of 7 kb that produces a 100 KDa protein. OASL is the most distinct form of the OAS proteins (Benech et al., 1985; Marie and Hovanessian, 1992; Rebouillat et al., 1999). *OASL* has two transcripts (2 and 1.8 kb) expressed, which produce two proteins of 30 and 59 KDa. The 30 KDa protein is present in the cytoplasm while the higher molecular weight (59 KDa) OASL protein contains a putative nuclear-localization signal (RKVKEKIRRTR) at its C terminus, thus localizing to both cytoplasm and the nucleus. The OASL protein also has an OAS domain which is inactive due to mutations at key residues that disable its catalytic function. In addition, the OASL protein also contains a tandem repeat of 160 a.a. ubiquitin-like domains at its C-terminal end which helps in its ISGylation to other cellular proteins following type I interferon treatment (Hartmann et al., 1998; Rebouillat et al., 1998).

A tripeptide motif (CFK) present within the OAS domain helps in the oligomerization of the proteins; hence the OAS1 and OAS2 are tetramers and dimers respectively. Mutations within the tripeptide motifs of OAS3 and OASL do not allow them to oligomerize hence, they function as monomers (Ghosh et al., 1997). OAS3 specifically synthesizes dimeric molecules of 2', 5'-linked oligomers of adenine whereas

OAS1 and OAS2 can synthesize trimeric and tetrameric oligomers of adenine (Hartmann et al., 2003; Sarkar et al., 2002). The dimeric forms of 2-5A have a lower affinity than the oligomeric molecules to bind and activate the RNAse L (Dong et al., 1994). Thus, if the dimeric forms of 2-5A are functional, they must act via another mode of action and it has been demonstrated that analogues of dimeric forms of 2-5A exert a negative impact on the transcription profile in breast carcinoma cells (Latham et al., 1996), which is in agreement with previous reports showing that low concentrations of 2-5A can regulate gene expression and DNA replication by direct inhibition of DNA topoisomerase I (Castora et al., 1991). Thus, the preferential 2-5A dimer production and OAS3 induction in response to IFN raises the possibility for the implication of OAS3 in alternative mechanisms other than the antiviral action of interferon. GTP can also be an alternative substrate for 2-5OAS as donor as well as acceptor molecule. However, GTP has a higher affinity for donor site of OAS in presence of ATP and it can be transferred to a 2-5A matrix in presence of ATP (Marie et al., 1997). This suggests a potential role for OAS3 in pre-mRNA splicing (Sperling et al., 1991) by producing 2', 5' phosphodiester bond in the intermediate lariat structure, where the 5' terminal guanosine residue of the intron is covalently joined to a conserved adenosine at the 3' end of the intron.

III.2.3.2. RNase L: Historical perspective

Discovery of 2-5A (Kerr and Brown, 1978) as low molecular weight inhibitor of protein synthesis, on incubation of the cytoplasmic extracts from interferon-treated cells with dsRNA and ATP, led to the curiosity about the role of this small unusual oligonucleotides. The 2-5A was later shown to induce a nuclease activity (Hovanessian et al., 1979). The specificity of the 2-5A dependent endoribonuclease to UA and UU sequences was shown later (Wreschner et al., 1981). Two years later, it was shown that Interferon treatment of mouse JLS-V9R cells resulted in a 10- to 20-fold increase in the levels of the 2-5A (ppp(A2'p)nA)-dependent RNase. The nuclease was monitored in cell extracts by covalent and non-covalent binding of ^{32}P-labeled 2-5A derivatives to the nuclease and by the appearance of 2-5A-mediated ribosomal RNA cleavage products. The 2-5A dependent RNase was purified (Silverman et al., 1988) by affinity labeling of the proteins with a ^{32}P-labeled 2-5A derivative, which revealed that, the mouse 2-5A dependent RNase is a 80kDa protein.

Expression of RNase L had been established in different tissues much before it was cloned or antibodies were raised against it. This was possible by radiolabeling of 2-5A. Presence of RNase L in rabbit liver, kidney, spleen and reticulocyte (Krause and Silverman, 1993; Nilsen et al., 1981) mouse liver, kidney, lungs, intestine, spleen, brain, testis, thymus, intestine and heart (Floyd-Smith and Denton, 1988; Nilsen et al., 1981; Silverman et al., 1988) was shown in absence of IFN. RNase L peaks soon during postnatal development in many organs and gradually decreases as the animal ages (Floyd-Smith and Denton, 1988). Determination of RNase L using monoclonal antibody showed the presence of RNase L in normal colonic mucosa with elevated levels in the colorectal tumors and polyps (Wang et al., 1995). In 2005 Zhou and co-workers mapped the promoter of RNase L and also determined and compared RNase L levels in different human and rodent cancers and normal cell types using a radiolabeled 2-5A derivative. In addition, levels of RNase L were established in various normal human tissues and cell types by immunoblotting and immunohistochemistry (Zhou et al., 2005).

III.2.3.3. Cloning of RNase L

Zhou et al in 1993 cloned RNase L cDNA where they used murine L929 cells and enhanced the mRNA level by treating with cycloheximide and interferon. The cDNA library was screened by bromine substituted ^{32}P-labeled 2-5A analogue (2-5A probe). A single plaque ZB1 was selected from 3×10^6 plaques and the protein was expressed from the clone by *in vitro* translation. The plaque showed the reactivity to both 2-5A and highly purified polyclonal antibody. Migration of the translational product in wheat germ extract showed an apparent molecular weight of 74kDa as opposed to 80kDa purified previously. Further analysis showed that ZB1 was a partial cDNA clone encoding 74kDa polypeptide made up of 656 amino acid residues (Zhou et al., 1993).

The ZB1 was then used to screen various human libraries containing genomic DNA as well as cDNA clones, to obtain a composite human RNase L cDNA clone. The screening resulted in the partial cDNA HZB1 from human kidney cDNA library in λgt11, which was used to pick an overlapping clone HZB22. The HZB22 was then used as a probe to screen a human placenta cosmid library in the vector pWZC5 to pick the 5'-region of the coding sequence in a Sac 1-fragment. Fusion of the Sac1-fragment upstream of the Nco 1 site in ZC1 produced the clone ZC3. The coding sequences along with some flanking sequences was then subcloned into pBluescript KSII(+), resulting in

the clone pZC5, whose predicted amino acid sequence resulted in an ORF encoding a polypeptide of 741 residues (83,539 Daltons) representing the human RNase L.

III.2.3.4. Biochemical properties of RNase L

RNase L is an IFN-inducible endoribonuclease for single stranded RNA.

Its general biochemical properties are:

S. No.	Property	Comments
1	Size	83.5kDa, 741aa (human) 80kDa, 735aa (mouse)
2	Functional definition	single stranded RNA binding endoribonuclease activated by 2-5A
3	Specificity	cleaves 3'- of UU, UA sequences, shows substrate specificity for ISG43 and ISG15 mRNA
4	Divalent ion effect	Mg^{++} and Mn^{++} ions enhance 2-5A binding and ribonuclease activity
5	ATP effect	ATP moderately enhances RNase L activity

III.2.3.5. Structure of RNase L

RNase L has a bipartite structure with a N-terminal regulatory domain and a C-terminal functional domain (Dong and Silverman, 1995). The structural motifs are as follows-

III.2.3.5.1. Ankyrin repeats

The ankyrin repeat was first identified in the yeast cell cycle regulator, Swi6/Cdc10 and the *Drosophila* signaling protein, Notch (Breeden and Nasmyth, 1987), and was eventually named for the cytoskeletal protein ankyrin, which contains 24 copies of this repeat (Lux et al., 1990). Ankyrin repeat containg proteins are present in all three superkingdoms including bacteria, archaea, and eukarya, as well as in a number of viral

genomes. However, a phylogenetic breakdown of the organisms that contain ankyrin repeats indicates that the majority are found in eukaryotes. Modular protein domains. such as the ankyrin repeat, that act as a scaffold for molecular interactions are likely to be important for development of numerous signaling pathways necessary to evolve a more complicated multicellular organism (Marcotte et al., 1999).

The primary structure analysis of RNase L suggested that RNase L had nine ankyrin repeats, but the ninth ankyrin repeat is incomplete (Hassel et al. 1993). However, this prediction for RNase L differs from the crystal structure of ANK (Tanaka et al., 2004), which consists of eight ankyrin repeats (R1–R8). Residues 306-333, corresponding to the incomplete ninth repeat (Hassel et al., 1993) are disordered. As in other ankyrin repeat proteins (Sedgwick and Smerdon, 1999), each repeat is formed by 33 amino-acid residues and consists of pairs of antiparallel α-helices stacked side by side and are connected by a series of intervening β-hairpin motifs. In general, the structure is shaped similar to a cupped hand (Jacobs and Harrison, 1998). There is a noticeable curvature across the 'palm', such that the surface created by the β-hairpins (fingers) and the α1 'inner' helices is concave, whereas that formed by the α2 'outer' helices, that is, the back of the cupped hand, is convex . The 2-5A molecule fits in the concavity and directly interacts with ankyrin repeats 2 and 4. The N-terminal ankyrin repeats serve as the regulatory domain of RNase L, since 2-5A binds to the ankyrin repeats 2 and 4 and activates RNase L.

III.2.3.5.2. 2-5 A binding

Tanaka et al, (2004) crystallized 1–333 amino acids of the N-terminal ankyrin repeat domain of human RNase L with 5'-O-monophosphoryladenylyl(2'-5')adenylyl(2'-5')adenosine (p5'(A2'p5')$_2$A), a 2-5A trimer with 5'-monophosphate. The crystal structure showed that the first AMP moiety of the 2-5A directly interacts with the fourth repeat of ANK. The 5'-phosphate group of the first AMP (phosphate1) forms bifurcated salt bridge with the side chain of Arg155. The side chain of Arg155 is fixed by bifurcated salt bridge with the side chain of Asp174. The adenine ring of the first AMP (adenine1) is stacked between the side chain of Phe126 and the adenine ring of the second AMP (adenine2), and is fixed by bifurcated hydrogen bonds with the side chain of Glu131, that is, OE1(Glu131)—N6(Adenine1) and OE2(Glu131)—N1(Adenine1). The side chain of Phe126 also stacks with the guanidine group of the side

chain of Arg155, forming a quadruplex (Arg155–Phe126–Adenine1–Adenine2) of stacking interactions (Tanaka et al., 2004).

The second AMP moiety of 2-5A interacts only slightly with ANK. The 5'-phosphate group of the second AMP (phosphate2) is exposed to solvent, and no direct interactions are found between phosphate2 and the surface of ANK. The adenine ring of the second AMP (adenine2) is stacked with adenine1 as described above, and is fixed by a single hydrogen bond with the side chain of Tyr135, that is, OH(Tyr135)—N1(adenine2). The 3'-OH group of the second AMP is involved in a hydrogen bond network and is fixed on the protein surface via water molecules. The second AMP appears to be rather weakly fixed on the ANK surface relative to the two ends of the 2-5A molecule.

The third AMP moiety of 2-5A directly interacts with the second repeat (R2) of ANK. The 5'-phosphate group of the third AMP (phosphate3) forms a salt bridge with the side chain of Lys89. The adenine ring of the third AMP (adenine3) is stacked with the side chain of Trp60, and is fixed by a hydrogen bond network involving the side chains of Gln68 [OE1(Gln68)—N6(Adenine3) and NE2(Gln68)—N1(Adenine3)] and Asn65 [OD1(Asn65)—N6(Adenine3)], as well as a water molecule [O(Water)—N7(Adenine3)] and [O(Water)— ND2(Asn65)]. The side chain of Trp60 also stacks with the CD–CE–NZ bonds of the side chain of Lys89, forming a triplex (Lys89–Trp60–Adenine3) of stacking interactions.

Interestingly, the 2-5A binding residues in the R4 and R2 of ANK are located at the structurally equivalent positions of the ankyrin repeats and these residues play a functionally equivalent role. The side chains of Arg155 in R4 and Lys89 in R2 form salt bridges with phosphate1 and phosphate3, respectively. The side chains of Phe126 in R4 and Trp60 in R2 stack with Adenine1 and Adenine3, respectively. Furthermore, a quadruplex (Arg155–Phe126– Adenine1–Adenine2) and a triplex (Lys89–Trp60–Adenine3) of stacking interactions are observed at R4 and R2, respectively. The side chains of Glu131 in R4 and Asn65 in R2 form hydrogen bonds with Adenine1 and Adenine3, respectively.

Based on the structure given by Tanaka et al., (2004), Nakanishi et al., (2005) used structure-based site-directed mutagenesis to identify the residues of human RNase L crucial for the recognition and binding of 2–5A. Substitution for either Trp60 or Phe126

significantly hampered the 2–5A binding ability of RNase L, as well as inactivating 2–5A-dependent RNase activity, indicating that the π-π stacking interactions of Trp60-Adenine3 and Phe126-Adenine1 are critical for 2–5A binding. Mutations of the residues Lys89 and Arg155 also led to inactivation of RNase L, indicating the importance of electrostatic interactions between Lys89-Phos3 and Arg155-Phos1 for 2–5A binding(Nakanishi et al., 2005; Tanaka et al., 2004).

III.2.3.5.3. Protein kinase homology domain

RNase L bears significant homology to protein kinase domain VI and VII and some additional protein kinases in its C-terminal region. One of the opinions about the ribonuclease is that the ribonuclease evolved in part from a protein kinase which somehow lost its kinase function during evolution (Dong and Silverman, 1999). The proposed kinase domains of RNase L are either incomplete or they differ substantially from the domains of protein kinases. Domain I bears little similarity to the canonical protein kinase domain I sequence (hGXGXXGXVh, Where h is any hydrophobic residue) and in motif VII, an aspartate residue is replaced by a conserved glycine residue, in motif VIII, a glutamine replaces an invariant glutmate, in motif IX and a conserved arginine is present in human RNase L but not in murine RNase L.

In protein kinases, a conserved lysine residue in the domain II serves to bind the α- and β-phosphoryl groups of ATP, whereas the conserved aspartate residue in domain VII serves to chelate Mg^+ complexed with ATP. In RNase L, both of these residues are present. In fact in presence of ATP, there is enhanced RNase L activity (Krause et al., 1986; Wreschner et al., 1982). Despite the homology, however, no protein kinase activity has been detected during activation and RNA-cleavage reactions with human RNase L (Dong and Silverman, 1999). Similarly, the kinase plus ribonuclease domain of RNase L produces no detectable protein kinase activity in contrast to the phosphorylation obtained with homologous domain of the related kinase and endoribonuclease, i.e., the yeast Ire1p. In addition, neither ATP nor pA(2'p5'A)3 is hydrolyzed by RNase L. To further investigate the function of the kinase homology in RNase L, the conserved lysine residue at 392 in the protein kinase-like domain II was replaced with an arginine residue, the resulting mutant, RNase L K392R, showed >100-fold decrease in 2-5A-dependent ribonuclease activity without reducing 2-5A- or RNA-binding activities (Dong and

Silverman, 1999). The greatly reduced activity of RNase LK392R was correlated to a defect in the ability of RNase L to dimerize.

Within the protein kinase region of RNase L is present a high cysteine content region (Zhou et al., 1993). The spacing of these cysteine residues ($CX_4CX_3CX_{17}CX_3C$, residues 401-436 in human RNase L) bears resemblance to some Zinc fingers, protein/nucleic acid binding domains (Dong et al., 1994). Interestingly, an argnine to glutamine mutation at 462 position in the protein kinase homology domain has been shown to be associated with prostate cancer risk or aggressiveness (Casey et al., 2002). To determine the effect of this mutations on the enzyme activity, the wild-type and mutant RNase L were compared after expression in mouse JM03 cells, isolated from a spontaneous rhabdomyosarcoma from RNase L$^{-/-}$, p53$^{-/-}$ double gene-knockout mice. The R462Q variant showed approximately one-third of the wild-type RNase L activity (Xiang et al., 2003). The deficiency in RNase L R462Q activity was correlated with a reduction in its ability to dimerize into a catalytically active form. Furthermore, RNase L R462Q was deficient in causing apoptosis in response to 2–5A which was consistent with its possible role in the prostate cancer development.

III.2.3.5.4. RNase domain

With the cloning of partial murine clone pZB1, which lacked 89 amino acids from the C-terminal as well as RNase activity, it was clear that the RNase activity resides in the C-terminus of the molecule (Zhou et al., 1993). In 1997, Silverman and coworkers (Dong and Silverman, 1997) constructed a series of truncated RNase L proteins and found that the C-terminal 31 residues of RNase L are critical for the catalytic function of the enzyme. RNase L CΔ31, lacking residues 711–741, showed neither ribonuclease nor substrate binding activities. In contrast, RNase L CΔ21 (1-720) had full activity in presence of 2-5A. These findings clearly showed that the residues 711–720, EYRKHFPQTH, are essential for the RNA binding and ribonuclease activity of the enzyme. Later in 2001, the same group (Dong et al., 2001) mutated the amino acid residues found conserved in RNase L and *Ire1* superfamily. They found that the RNase L mutants W632A, D661A, R667A and H672A lacked ribonuclease activity. To dissect the function of the residues 711–720, EYRKHFPQTH, Nakanishi and coworkers preformed scanning mutagenesis over the 10 residues of glutathione S-transferase (GST)-fusion RNase L (Nakanishi et al., 2004). Among the single amino acid mutants examined,

TH 23276

Y712A and F716A resulted in a significant decrease of RNase activity with a reduced RNA binding acitivity. The loss of the RNase activity was not restored by its conservative mutation, whereas the RNA binding activity was enhanced in case of Y712F. These results indicated that both Tyr712 and Phe716 provide the enzyme with a RNA binding activity and catalytic environment.

III.3. RNase L and prostate cancer

Prostate cancer is believed to be caused by Aging, hormonal, environmental, and genetic factors acting independentaly or in combination. Sporadic prostate cancer displays an age-related increase in incidence, whereas familial prostate cancer often displays earlier-onset disease. Importence of RNase L in hereditary prostate cancer (HPC) has emerged from several genetic studies. The criteria for HPC are a family with three generations affected, three first-degree relatives affected, or two relatives affected before age 55. HPC accounts for approximately 43% of early onset cases (<55 years old) and 9% of all cases (Carter et al., 1993). In 1996, Smith et al. identified a region on chromosome 1, 1q24–25, as a susceptibility locus in familial prostate cancer (Smith et al, 1996). Since then, this gene has been widely studied. The main mutations in the RNase L gene related to prostate cancer are 3 missense mutations: D541E, R462Q, and I97L (Chen et al., 2003; Larson et al., 2008; Xiang et al., 2003). R462Q and D541E are non-synonymous variants showing a reduction in the enzymatic activity of RNase L (Beuten et al., 2010). I97L is a missense mutation located in the third and seventh repetition site of the ankyrin domain (Madsen et al., 2008). The R462Q or Arg462Gln variant is associated with an increased risk in prostate cancer in familial cases in the Finnish population (Rokman et al., 2002), among American Caucasians (Dagan et al., 2006), and among Japanese men (Dong, 2006). In the population in the south of Spain, the genotype A/A is associated with a worse prognosis (Alvarez-Cubero et al., 2012). Other variants within the RNase L gene which have been described, especially in exons 1 and 3 are, The most common mutations are E265X, 471delAAAG, M11, G59F, S113S, I221V, E262X, S406F and Y530C. Some of these mutations have been identified in several studies as related to hereditary or sporadic prostate cancer, although some of the studies presented inconclusive results (Dagan et al., 2006; Larson et al., 2008). The 471delAAAG is a null mutation associated with an increased risk of prostate cancer in Ashkenazi Jew males (Rennert et al., 2002). However, this finding remains controversial because studies by Dagan et al. reported low rates of the 471delAAAG mutation in the

22

Ashkenazi population that rejected the consideration as a major factor of cancer susceptibility in this population (Dagan et al., 2006). Several other studies, including a population-based study conducted in Swedish population (Wiklund et al., 2004) and in the German population (Dong, 2006), have found no association between the Arg462Gln polymorphism and sporadic prostate cancer. In vitro studies have indicated that the Gln variant results in the decreased enzyme activity of RNase L, which allow tumor cells to escape the apoptotic pathway, mainly, because RNase L acts as a true tumor suppressor (Kruger et al., 2005). D541E or Asp541Glu increase the risk of prostate cancer in some Japanese men (Nakazato et al., 2003). However, in other analyses, such as the ones performed in European populations, no correlation is described between D541E and prostate cancer (Casey et al., 2002; Rokman et al., 2002). With respect to I97L or Ile97Leu, although denoted as a major mutation in prostate cancer, most of the studies do not shown a clear correlation between this mutation and the risk of prostate cancer (Xiang et al., 2003). However, some reports of other mutations in prostate cancer, such as E265X, a truncation protein motif, or M1I, a missense mutation in the start codon are also described in individuals of African-American ancestry (Robbins et al., 2008; Shook et al., 2007).

III.3.1. RNase L, prostate cancer and virus

The antiviral and prostate cancer suppressor functions of RNase-L encouraged the Silverman and colleagues to search for viruses that may be associated with the R462Q RNase-L mutation in prostate cancer. Their work identified the first authentic human gammaretrovirus, xenotropic murine leukemia virus-related virus (XMRV), that was detected at high frequency in patients homozygous for the RNase-L mutation but was found at significantly reduced rates in heterozygous or wild type individuals. Like other retroviruses, XMRV probably promotes tumorigenesis by integrating adjacent to cellular genes and changing their expression; in fact, mapping of XMRV integration sites in prostate cancer revealed a preference for cancer-associated genes and regions (Kim et al., 2010). However, conflicting reports preclude a consensus on the role of XMRV in the etiology of prostate cancer and its association with RNase-L (Rusmevichientong and Chow, 2010; Silverman et al., 2010). These studies highlight the need for further investigations into the relationships between these parameters as risk factors and as potential therapeutic targets.

III.3.2. RNase L as tumor supressor

RNase-L functions as established tumor suppressor mechanisms that may mediate antitumor activity against a broader profile of malignancies. The compromised induction of apoptosis or senescence observed in RNase-L-deficient cells in culture is predicted to confer a survival advantage on tumor cells with inactivating mutations in RNase-L. In accordance with this idea, stable knockdown of RNase-L increases tumor size and number as compared to control cells in nude mouse xenografts of human cervical cancer cells and ectopic expression of RNase-L reduced tumorigenesis in a murine xenograft model (Liu et al., 2007). RNase-L can also influence the response of cancer cells to chemotherapeutic agents, as stable knockdown of RNase-L in prostate cancer cells conferred resistance to apoptosis induced by a combination of camptothecin and TRAIL (Malathi et al., 2004). Two recently identified targets of RNase-L regulation that may play important roles in its antitumor activity are the RNA binding proteins HuR and TTP. These proteins bind AU-rich elements in the 3'UTR of labile mRNAs including those encoding oncogenes, cytokines and growth factors. HuR stabilizes its targets resulting in increased expression and is elevated in human cancers (Lopez de Silanes et al., 2003). The antitumor activity of RNase-L thus appears to involve significant reprogramming of the gene expression profile with distinct mRNA subsets targeted in cancers of different origin or stage of progression.

While most studies describe a tumor suppressor role for RNase-L, it was reported to be upregulated in premalignant familial adenomatous polyposis polyps and adenocarcinomas as compared to colon epithelium (Wang et al., 1995). This observations suggested that RNase-L may play an oncogenic role in certain contexts. Indeed, opposing activities in tumor suppression and oncogenesis are observed for innate immune effectors in which a regulated inflammatory response mediates tumor suppression by recruiting and activating innate immune cells to kill tumor cells. In contrast, a dysregulated inflammatory response can result in tissue damage, chronic proliferative repair and increased tumor invasion to promote tumorigenesis (Grivennikov et al., 2010). Consistent with an inflammatory mechanism in RNase-L-associated prostate cancer, a mutation downstream of RNASEL was correlated with an increase in both prostate cancer risk and levels of inflammatory biomarkers (Meyer et al., 2010). The potential for pathologic effects in conditions of dysregulated RNase-L activity

suggests that pharmacologic RNase-L inhibitors may be effective as anti-inflammatory agents in certain contexts.

III.4. Functions of RNase L

III.4.1. RNA metabolism

The initial studies carried out to find the sequence preferences of RNase L using poly(rC), poly(rU), poly(rA), and poly(rG) as the substrates, showed that it preferentially cleaves only poly(U) (Floyd-Smith et al., 1981; Wreschner et al., 1981). The same group showed that the activated RNase L cleaved single stranded RNA after atleast three dinucleotides (UU, UA and UG) out of 16 possible combinations. In 1994, Dong and coworkers (Dong et al., 1994) expressed RNase L in insect cells and purified the protein through fast protein chromatography. Studies with purified protein revealed sequence specificity for poly (rU) on addition of 2-5A. In contrast, poly(rA), poly(rC), poly(rG), ssDNA, dsDNA were not cleaved by RNase L.

The mechanism of RNase L-mediated antiviral activity was investigated (Li et al., 1998) following encephalomyocarditis virus (EMCV) infection of cell lines in which expression of transfected RNase L was induced or endogenous RNase L activity was inhibited. RNase L induction markedly enhanced the anti-EMCV activity of IFN via a reduction in EMCV RNA. Inhibition of endogenous RNase L activity inhibited this reduction in viral RNA. RNase L induction reduced the rate of EMCV RNA synthesis, suggesting that RNase L may target viral RNAs involved in replication early in the virus life cycle. The RNase L-mediated reduction in viral RNA occurred in the absence of detectable effects on specific cellular mRNAs and without any global alteration in the cellular RNA profile. Extensive rRNA cleavage, indicative of high levels of 2-5A, was not observed in RNase L-induced, EMCV-infected cells; however, transfection of 2-5A into cells resulted in widespread degradation of cellular RNAs. These findings provide the first demonstration of the selective capacity of RNase L in intact cells and link this selective activity to cellular levels of 2-5A.

Differential display PCR analysis was used to identify mRNAs that were differentially expressed in N1E-vector and N1E-RNase-L cell lines and identified ISG43, ISG15 mRNA as negatively regulated by RNase L (Li et al., 2000). During the IFN-antiviral response in RNase L-null cells, PKR mRNA stability was enhanced, PKR

induction was increased and the phosphorylated form of eIF2α appeared with extended kinetics compared to similarly treated wild type cells. An enhanced IFN-response in RNase L-null cells was also demonstrated by monitoring inhibition of viral protein synthesis (Khabar et al., 2003). MyoD mRNA levels were decreased in C2 cells transfected with an inducible RNase L construct. The effect of RNase L activity on MyoD mRNA levels was relatively specific because expression of several other mRNAs was not altered in C2 transfectants (Bisbal et al., 2000). Le Roy and coworkers down-regulated RNase L activity in human H9 cells by stably transfecting (i) RNase L antisense-cDNA or (ii) RLI sense-cDNA constructs. In contrast to control cells, no post-transcriptional down-regulation of mitochondrial mRNAs and no cell growth inhibition were observed after IFN-α treatment in these transfectants. These results demonstratd that IFN-α exerts its antiproliferative effect on H9 cells at least in part via the degradation of mitochondrial mRNAs by RNase L (Le Roy et al., 2001). Similarily Chandrashekaran and coworkers showed RNase-L-dependent decrease in mtDNA-encoded mRNA transcript levels in monensin-treated mouse embryonic fibroblasts (MEFs) (Chandrasekaran et al., 2004).

III.4.2. Antiviral immunity

Induction of RNA decay by RNase L is one of the host cell responses to viral infection. The most important line of evidence that link the 2-5A system to specific antiviral effects were obtained by measuring: (1) 2-5A accumulation and RNase L activation in virus-infected cells (Hearl and Johnston, 1987); (2) antiviral effects in cells expressing 2-5A synthetase cDNA (Schroder et al., 1992); and (3) enhanced virus production and reduction of the antiviral effects of IFN, caused by inhibiting RNase L activity in cells. For instance, it was shown that expression of the 40kDa form of human 2-5A synthetase from a cDNA in chinese hamster ovary (CHO) cells provided resistance to the picornavirus, mengo virus (Chebath et al., 1987). Similarly, expression of the 40kDa human 2-5A synthetase cDNA in a human glioblastoma cell line, T98G, and expression of murine 43kDa 2-5A synthetase from a cDNA in mouse NIH 3T3 cells resulted in resistance to EMCV replication (Rysiecki et al., 1989). Another strategy to study the involvement of 2-5A/RNase L system in the antiviral activity of IFN was to use the 2-5A analog, $CH_3Sp(A2'p)2A2'pp3'OCH_3$, which binds to, but does not activate RNase L (Defilippi et al., 1986). Transfection of the analog into IFN-treated, EMCV-infected murine L929 cells inhibited rRNA cleavage and increased virus production by

upto 10 fold. Hassel and coworkers (Hassel et al., 1993) showed that expression of a dominant negative truncated RNase L in murine SVT2 cells blocked the rRNA cleavage and reduced the anti-EMCV effects of IFN about 250-fold compared with the IFN-treated, vector control cells. The RNase L knockout mice succumbed to EMCV and HSV-1(McKrae strain) infections more rapidly than the infected wild type mice (Zhou et al., 1997). RNase L knockout mice treated with IFN prior to EMCV infection also died several days earlier than the wild type mice with the same treatment. However, IFN treatment extended survival against EMCV infection of both the RNase L-wild-type and knockout mice, indicating multiple and overlapping antiviral pathways of IFN.

So far, RNase L has been shown to have antiviral effects against many viruses such as EMCV, vaccinia virus, reovirus, herpes simplex virus (HSV) and SV40 (Diaz-Guerra et al., 1997; Rivas et al., 1998). Austin and coworkers (2005) evaluated resistance to HSV-1 in RNase L-deficient mice, treated with IFN-α6 and IFN-β transgenes. In the absence of RNase L, the antiviral effectiveness of the IFN-transgene was lost (Austin et al., 2005). When RNase L activity was down-regulated in West Nile Virus (WNV) resistant cells via stable expression of a dominant negative RNase L mutant, 5- to 10-times higher yields of WNV were produced (Scherbik et al., 2006). PKR and RNase L act as important effector molecules against WNV infection. Mice lacking PKR and RNase L were significantly more susceptible to WNV infection and showed increased viremia and viral burden in peripheral tissues, early entry into the brain, and higher viral loads in the CNS than the wild-type mice (Samuel et al., 2006). However, viral evasion of the 2-5A/RNase L system was also reported. Vaccinia virus E3L proteins sequestered the dsRNA from 2-5A synthetase (Rivas et al., 1998), whereas reovirus S4 gene encodes a dsRNA-binding protein σ3 with the same function (Beattie et al., 1995).

III.4.3. Apoptosis

At the cellular level, the antiviral effects of IFN may be partly due to apoptosis. Indeed, activation of PKR and 2-5A synthetase by dsRNA have been shown to induce apoptosis. Several lines of studies link RNase L to apoptosis in cells in response to viral infection. RNase L-null mice showed enlarged thymuses and reduced levels of spontaneous apoptosis in both the thymus and spleen. In addition, thymocytes and lymphocytes from spleen of RNase L-null mice were resistant to apoptosis induced by staurosporine and irradiation (Rusch et al., 2000; Zhou et al., 1997). Furthermore, over

expression of dominant negative RNase L (mouse RNase L lacking the C-terminal 89 a.a.) in cells reduced apoptosis whereas over expression of wild type RNase L enhanced apoptosis in response to viral infection (Hassel et al., 1993). Malathi and coworkers showed that RNase L-deficient prostate cancer cells are remarkably resistant to apoptosis induced by Topoisomerase I inhibitors and tumor necrosis factor-related apoptosis-inducing ligand. TRAIL (Malathi et al., 2004). The apoptosis induced by RNase L involves cytochrome c release. it is caspase dependent. and inhibited by overexpression of Bcl-2 (Castelli et al.. 1997; Rusch et al., 2000; Silverman, 2003). A study revealed that RNase L mediates virus-induced apoptosis through activating c-Jun NH_2-terminal kinase (JNK) (Li et al., 2004). Naito et al found that down regulation of RNase L inhibited apoptosis induced by 1-(3-C-ethynyl-ß-D-ribo-pentofuranosyl) cytosine (ECyd). which inhibits RNA synthesis through competitive inhibition of RNA polymerase I (Naito et al., 2007).

III.4.4. Antiproliferative effect

Introduction of 2-5A into cells results in an inhibition of the growth rate, suggesting a role of RNase L in antiproliferation (Hovanessian and Wood, 1980). Furthermore, RNase L and 2-5A synthetase levels were reported to be elevated in growth-arrested or differentiated cells and reduced in rapidly dividing cells, indicating that RNase L may be involved in fundamental control of cell proliferation and differentiation (Jacobsen et al., 1983; Krause et al., 1985). Cells expressing a dominant negative form of RNase L (mouse RNase L lacking the C-terminal 89 a.a.) are resistant to the antiproliferative activity of IFN-α (Zhou et al., 1997).

III.4.5. Stress response

As early as 1991, the role of stress in RNase L expression was indicated by Krause and coworkers, they observed increased level of RNase L in murine L929 cells after exposure to 2.45-GHz continuous-wave microwaves (SAR = 130 mW/g) (Krause et al., 1991). In our Laboratory, different stressors were used to study the expression of RNase L and apoptosis in human cervical carcinoma (HeLa) cells (Pandey et al., 2004). Chemotherapeutic agents like cisplatin, doxorubicin. vinblastin and vincristine showed RNase L-induction, RNA degradation and apoptosis. RNase L was also shown as oxidative stress-inducible. H_2O_2 and doxorubicin, a potent inducer of H_2O_2 in cells, also induced RNase L. RNase L was also induced by $CaCl_2$ and TNF-α.

III.4.6. Small RNA generation

Malathi and co-workers have showen that activation of the antiviral endoribonuclease, RNase L, by 2`-5`-linked oligoadenylate (2-5A) produced small RNA cleavage products from self-RNA that initiated IFN production. Mice lacking RNase L produced significantly less IFN-β during viral infection than the infected wild-type mice (Malathi et al., 2007). This indicates RNase L is involved in RNA processing for the stimulation of innate immune response.

III.4.7. Interaction of RNase L with RNase L Inhibitor (RLI)

In 1995, Bisbal and coworkers cloned a novel protein from the human lymphoid daudi cells, expression of this protein led to the inhibition of RNase L activity and hence named RNase L inhibitor (RLI) (Bisbal et al., 1995). RLI is an exceptionally conserved protein found in all eukaryotes and archaea sequenced so far (Gabaldon and Huynen, 2004). For example, *Drosophila* ortholog *Pixie* and yeast *Rli1p* share 66% and yeast Rli1p and human RLI have 67% amino acid identities. RLI belongs to the ABCE subfamily of ABC proteins, which contain two nucleotide-binding domains and two N-terminal iron sulfur clusters. In contrast to most ABC domain proteins, members of this subfamily do not contain the membrane-spanning domains that would enable them to function as transporters (Kerr, 2004). RNase L is found in vertebrates, so the function of RNase L-inhibition by RLI does not account for conservation of RLI in invertebrates (Kerr, 2004). *Drosophila* ortholog of RLI, *Pixie* is known to interact with the translation initiation factor eIF3 and ribosomal protein. It was further observed that depletion of *pixie* resulted in impairment of translational initiation (Chen et al., 2006). RLI and its homologues are also thought to play a role in ribosome biogenasis, nuclear export, or both (Kispal et al., 2005). It has been found in the nuclei associated with the 40S and 60S subunits, as well as *Hcr1p*, a protein required for rRNA processing. It has been shown that the iron-sulfur (Fe/S) clusters are necessary for ribosome biogenesis and/or nuclear export, although the exact mechanism is unknown.

III.4.8. Interaction of RNase L with eRF3/RNBP – link to translation

RNase L was shown to interact with RNA binding protein (RNABP) (Le Roy et al., 2000). RNABP was later identified as a translation termination release factor (eRF3) (Le Roy et al., 2005). After activation by 2-5A, RNase L can interact with *eRF3*. This

association can either help to localize RNase L to its mRNA target or can modulate its function, but it is also a way to modulate *eRF3* activity. Importantly, the regulation of eRF3 activity depends on the 2-5A oligomer size activating RNase L. Binding of 2-5A$_3$ or 2-5A$_4$ induces a conformational change in RNase L that promotes its interaction with eRF3. In one conformational change, the eRF3- RNase L interaction brings RNase L into close association with the mRNA, where it can act as an endoribonuclease. But binding with 2-5A$_3$ can induce another conformational change leading to an RNase L-eRF3 complex that can modulate translation termination and promote ribosomal readthrough of a termination codon. Moreover, RNase L regulates the +1 frame shifting of the antizyme 1 mRNA in IFN-treated cells. This was the first report implicating a nuclease, RNase L, in the translational regulation of a cellular mRNA independent of its nuclease activity.

III.4.9. Interaction with androgen receptor

Functional crosstalk between IFN-signalling and dihydrotestosteron (DHT) was described by Bettoun and coworkers (Bettoun et al., 2005). They performed RNA microarray analysis to reveal an IFN-DHT antagonism in subset of genes. This effect was reproduced *in vitro* as IFN could antagonize the induction of a reporter gene by DHT in a cell type-specific manner. In an attempt to elucidate the mechanism underlying this cross-talk, co-immuno-precipitation and GST pulldown experiments were performed to show that RNase L interacted with androgen receptor (AR) in a ligand-dependent manner. In transient transfection experiment, overexpression of wild type or R462Q mutated RNase L differentially affected the ability of IFN to antagonize DHT-mediated transactivation. Furthermore, it was also shown that IFN-insensitive cells could become sensitive to IFN upon down-regulation of AR-expression by siRNA. This finding also indicated how the AR and RNase L pathways may be involved in development of protate cancer since both the molecules have been implicated in prostate cancer progression.

III.4.10. Interaction with mitochondrial translation initiation factor (IF2mt)

IF2mt is a nuclear-encoded translation factor that delivers N-formyl methionyl-tRNA to the P-site of the mitochondrial ribosome during initiation (Ma and Spremulli, 1996). IF2mt was isolated from a yeast two-hybrid screen using RNase-L as bait and the interaction was confirmed using IF2mt translated from rabbit reticulocyte lysate. Using human H9 T cell lymphoma cells in which IFNα induces RNase-L-dependent mt mRNA

degradation, antiproliferative effects and cell death, it was demonstrated that translation was necessary for a decrease in mt mRNA. When IF2mt was overexpressed to outcompete RNase-L-IF2mt binding in the translation initiation complex, the degradation of mt mRNA degradation was suppressed resulting in an increase in proliferation and decrease in apoptotic signaling (Le Roy et al., 2007). This observation demonstrated the functional significance of the RNase-L-IF2mt interaction and suggested that the mechanism of RNase-L-target recognition may involve mRNA translation status and ribosome association mediated in part by IF2mt.

III.4.11. Interaction with IQGAP1

The most recent addition to the list of RNase-L interactors is IQGAP1 (IQ motif-containing Ras GTPase-activating-like protein 1). IQGAP1 was identified as an RNase-L interactor through a screen searching for proteins that preferentially bound to RNase-L during 1-(3-C-ethynyl-β-D-ribo-pentofuanosyl) cytosine (ECyd) induced cell death (Sato et al., 2010). A previous report demonstrated that RNase-L is a key mediator of ECyd induced apoptosis, possibly through the activation of c-jun N-terminal kinase (JNK) and mitochondrial membrane damage (Naito et al., 2009). IQGAP1 immunoprecipitated with RNase-L and this binding was enhanced during ECyd treatment. IQGAP1 is a large, ubiquitously expressed scaffold protein that functions in cell-cell adhesion, migration, actin reorganization, cell polarization, proliferation, and differentiation.

III.4.12. RNase L and chronic fatigue syndrome

Chronic fatigue syndrome (CFS) is an illness characterized by long-lasting fatigue accompanied by non-specific symptoms. Several reports indicated the up-regulation of components of the 2-5A/RNase L pathway in extracts of peripheral blood mononuclear cells (PBMCs) from CFS patients as well as the accumulation of a low molecular weight 2-5A-binding protein of 37 kDa (Suhadolnik et al., 1997). This 37kDa protein could be a biochemical marker for CFS. The polypeptide is an apparent degradation product of the native RNase L due to an increased proteolytic activity in CFS PBMC extracts. An equivalent degradation of RNase L could be observed when recombinant RNase L was incubated with human leucocyte elastase *in vitro* (Demettre et al., 2002). The 2-5A trimer and tetramer binding appeared to stabilize RNase L in PBMC cell extracts from the CFS patients. These observations suggested that in CFS, there is

increased proteolytic activity in the PBMC's causing accumulation of the 37 kDa polypeptide (Fremont et al., 2005).

III.4.13. Induction of interferon by small RNA generation

RNase L regulates different types of viruses such as mostly RNA viruses by diverse mechanisms, which were dependent on the specific RNA substrates and ribonuclease activity (Silverman, 2007). Their sustained activities eliminate virus-infected cells through apoptosis (Castelli et al., 1997; Zhou et al., 1997). Even in case of some cellular RNAs cleavage, such as rRNA in intact ribosomes, likely contributes to their antiviral activity (Silverman et al., 1983; Wreschner et al., 1981). Some of the RNA cleavage products resulting from RNase L activity, named as "suppressor of virus RNA", which are either viral or cellular in origin and contributed to production of type I IFNs (Malathi et al., 2007; Malathi et al., 2010). Viral RNAs are specially recognized by different PRRs.For example, toll-like receptor 3 is a sensor for dsRNA in the endosomal compartment, whereas OAS for viral dsRNA in the cytoplasm. Similarly, Retinoic acid-inducible gene-I (RIG-I, also known as DDX58) and melanoma differentiation-associated gene-5 (MDA5, also known as IFIH1) are activated by triphosphorylated, double-stranded, or uridine and adenosine-rich viral RNAs also occurs in the cytoplasm (Saito et al., 2008). Activation of the PRRs trigger signalling cascades which stimulate transcription of type I IFN genes. Malathi and others observed that the role of RNase L in IFN induction was apparent on studies with mouse embryonic fibroblasts (deficient in RNase L), which showed reduced IFN-β production upon treatment with 2-5A, synthetic dsRNA [poly(rI):poly(rC)] and Sendai virus infection (Malathi et al., 2007). In IFN induction, the role of ribonuclease function of RNase L was essential with contributions from both RIG-I and MDA5. Total cellular RNA digested with RNase L or just the small cleaved RNA fragments, <200 nt, induced higher levels of IFN induction as compared to uncleaved RNA. RNase L produces small RNA cleavage products with 3'-monophosphate (3'-p) and 5'-hydroxyl (5'-OH) at the termini. The 3'-p of the cleaved RNAs function in the recognition by RIG-I or MDA5, as calf alkaline phosphatise (CIP) treatment compromised their ability to induce IFN. Cellular observations were validated in mice where injection of 2-5A caused IFN-β induction in wild-type mice but not in mice deficient in RNase L. Moreover, mice lacking RNase L had several-fold reduced levels of IFN induction after infections with EMCV and Sendai virus. Therefore, effects of the OAS/RNase L pathway extend beyond initially infected cells to support a

prolonged antiviral state in the organism. In case of need, RNase L converted self-RNA into small RNA products that appeared to the host cell as nonself RNA. It is also a critical component in IFN induction by a DNA virus, HSV-2 (Rasmussen et al., 2009).

III.4.14. Protection against virus-mediated demyelination

In mitigation of viral-induced demyelination (central nervous system), a novel protective role of RNase L has been demonstrated. It was showing that even when RNase L does not able to inhibit global viral replication, can still manage to protect from virus-mediated disease. A sub-lethal, demyelinating mouse hepatitis virus (the neutropic coronavirus strain JHM) was lethal to a majority of RNase L-deficient mice by 12 days postinfection (Ireland et al., 2009). In the absence, RNase L enhanced the morbidity rate without affecting overall viral replication in the brain of mice. Further, RNase L deficiency did not impair type I IFN production or interferon stimulated gene (ISG) expression after viral infection and neither alters the inflammatory response in central nervous system (CNS). Instead, there was early onset of severe demyelination with axonal damage in the brain stem and spinal cord of infected animals that lacked RNase L. Mice lack in RNase L has shown foci of infected microglia, sustained brain stem infection, and enhanced apoptosis. Therefore, RNase L prevents spread of virus to the microglia, leading to protection of the CNS from virus-induced demyelination. The authors suggest that by contributing to viral tropism in the CNS, RNase L affects the balance between neuroprotective and neurotoxic effects of microglia in the mice.

III.4.15. Cross-regulation of HuR and RNaseL impacts mRNA turnover

The cellular levels of RNase L are controlled in part by regulated turnover of its mRNA through sequences in its 3'-UTR and proteins, which are interacting to these elements (Li et al., 2007). The RNase L 3'-UTR contains 8 AU-rich elements (ARE), which have shown both positive and negative regulatory effects on their deletion. The RNase L 3'-UTR acted in cis form to destabilize a heterologous mRNA for β-globin; therefore, the overall effect of the RNase L 3'-UTR was to decrease the half life of the RNA. However, AREs 7 and 8 exerted a positive or stabilizing effect on the RNase L mRNA. In addition, the expression of ARE-binding protein, HuR, enhanced RNase L mRNA and protein levels through 3-UTR sequences in between and including AREs 7 and 8. HuR binds RNase L mRNA during myoblast differentiation as determined in RNP

immunoprecipitations. In case of, cellular stress induced by heat shock or UVC radiation leads to increases in RNase L levels that were dependent on the 3'-UTR.

HuR expression increases levels of RNase L, whereas expression of RNase L negatively affects the level of HuR as in an apparent feedback loop (Al-Ahmadi et al., 2009). Cell growth rates and HuR levels were both elevated in RNase L-null mouse embryonic fibroblasts. The increase in HuR protein levels was correlated positively to enhancement in the stability of its mRNA, in absence of RNase L. The RNase L inhibitory effect on HuR mRNA levels was mapped to the HuR 3'-UTR, which contains U-rich/ARE-like sequences. In summary, HuR stabilizes the RNase L mRNA through AREs 7 and 8, whereas RNase L destabilizes the HuR mRNA through AREs in its 3'-UTR. Posttranscriptional cross-regulation of these proteins determines cellular levels, and consequently cellular effects, between both proteins. The role of RNase L activity on HuR expression was found to be most prominent in confluent cells or cells arrested in G1 phase of cell cycle, during which time both proteins were in the cytoplasm.

III.4.16. Anti-bacterial role of RNase L

Previously, it was thought that RNase L played major role in terms of antiviral functions, but it provides also protection to mice against infections of *Bacillus anthracis* and *Escherichia coli* (Li et al., 2008). Incomparision, the mice lacking in RNase L had increased bacterial loads and higher mortality rates when infected with either type of bacteria than the identically WT mice. After bacterial infections in the RNase L-deficient mice reduced levels of pro-inflammatory cytokines, IL-1β and TNF-α, and IFN-β were observed. Also, *E. coli*–infected RNase L/macrophages has shown two fold reduction in IRF3 dimerization. Microarray analysis and subsequent experiments revealed a positive role of RNase L in regulation of Cathepsin E (Cat E), an endolysosomal aspartyl proteinase. Cat E mRNA was stabilized in macrophages lacking RNase L, which are leading to increased levels in the protein. Elevated Cat E levels correlated with reduction of lysosome-associated membrane proteins, LAMP1 and LAMP2, which are required for the terminal step in phagosome maturation. In this process late endosomes fuse with lysosomes to eliminate phagocytosed microbial cargo. Decreased expression of LAMP1/2 in macrophages from RNaseL-/- mice was also correlated to accumulated phagocytic vacuoles and ineffective clearance of bacteria. In addition, over-expression of Cat E mimicked in the absence of RNase L, which are impairing in the induction of IL-

1β after LPS treatment. These findings identify an essential role for RNase L in antibacterial immunity in which RNase L is required for the optimal induction of proinflammatory cytokines. In these processes RNase L, also regulating the Cat E, and associated endolysosomal functions, which is required for the elimination of phagocytosed bacteria. However, exactly how bacteria or LPS are signaling to RNase L, or whether, if fact, the ribonuclease activity of RNase L is required for its anti-bacterial role has not been reported. Curiously, while the IFN-inducible OAS/RNase L pathway is antibacterial, the type I IFNs themselves, which have been described in some studies to have probacterial effects (Rayamajhi et al., 2010).

A completely different line of investigation has indirectly linked the OAS/RNase L pathway to an innate immunity in case of bacterial infections. The nucleotide-binding and oligomerization domain-2 (NOD2) is a Nod-like receptor member that is activated by bacteria-derived muramyl dipeptide to trigger innate immunity by activating NF-kB and MAP kinases (Ting et al., 2010). Interaction between OAS2 p69 and NOD2 leads to enhanced RNase L activity in poly(rI):poly(rC)-treated human acute monocytic leukemia cell line THP-1 (Dugan et al., 2009). In addition, NOD2 recognizes viral ssRNA (fromrespiratory syncytial virus) and uses it to activate IRF3 (Sabbah et al., 2009).

III.4.17. RNase L and autophagy

Autophagy is a programmed homeostatic response to diverse types of cellular stress that disposes of long-lived proteins, organelles, and invading microbes within double-membraned structures called autophagosomes. Siddiqui and Malathi in 2012, Showed that RNase L coordinates the activation of c-Jun N-terminal kinase (JNK) and double-stranded RNA-dependent protein kinase (PKR) to induce autophagy with hallmarks such as accumulation of autophagic vacuoles, p62(SQSTM1) degradation and conversion of Microtubule-associated Protein Light Chain 3-I (LC3-I) to LC3-II. Accordingly, treatment of cells with pharmacological inhibitors of JNK or PKR and mouse embryonic fibroblasts (MEFs) lacking JNK1/2 or PKR showed reduced autophagy levels. Furthermore, RNase L-induced JNK activity promoted Bcl-2 phosphorylation, disrupted the Beclin1-Bcl-2 complex and stimulated autophagy. Viral infection with Encephalomyocarditis virus (EMCV) or Sendai virus led to higher levels of autophagy in wild-type (WT) MEFs compared with RNase L knock out (KO) MEFs. Inhibition of RNase L-induced autophagy using Bafilomycin A1 or 3-methyladenine

suppressed viral growth in initial stages; in later stages autophagy promoted viral replication dampening the antiviral effect. Induction of autophagy by activated RNase L is independent of the paracrine effects of interferon (IFN) (Chakrabarti et al., 2012; Siddiqui and Malathi, 2012).

III.4.18. Regulation of RNase L by micro RNA

RNase-L expression is controlled post-transcriptionally by its 3'-untranslated region (3' UTR), which exerts a strong negative effect on RNase-L levels. MicroRNAs (miRNAs) are a class of small noncoding RNAs that repress expression of target genes by binding to regions of complementarity often in the 3' UTR. The miR-29 family acts as a tumor suppressor in several cancers, including acute and chronic myelogenous leukemia (CML), and has many oncogenic targets. Using a luciferase reporter, Lee et al in 2013 showed that the miR-29 family represses RNase-L protein expression across several cell types and acts via 4 target sites within the RNASEL 3' UTR. Mutation of all sites is required for abrogation of miR-29 repression. In light of the reported tumor suppressive role of miR-29 in K562 CML cells and miR-29 repression of RNase-L in these cells, they generated K562 cells with stable RNase-L knockdown and demonstrated that loss of RNase-L inhibits proliferation in vitro as well as tumor growth in a xenograft model (Lee et al., 2013).

IV

Statement of problem

IV. STATEMENT OF THE PROBLEM

RNase L was originally identified as a non-specific endoribonuclease. which degraded viral and cellular single stranded RNAs after being activated by 2-5A cofactor(s) in response to viral infection and interferon treatment of mammalian cells. RNA degradation by RNase L led to apoptosis of virus-infected cells thus producing antiviral effects. Later, RNase L was identified as a tumor suppressor as well as a human prostate cancer (HPC-1) susceptibility locus. It was argued that a homozygous mutation (R462Q) in RNase L gene increased the risk for prostate cancer in human patients.

In the meantime, earlier studies in our laboratory reported that the human RNase L when expressed as a recombinant protein in *E. Coli* caused degradation of the RNAs and inhibited cell growth without exogenous 2-5A cofactor (Pandey et al., 2004). This human RNase L protein was degraded in *E. Coli* cells. later this was stabilized and purified by expressing a GST-hRNase L fusion protein, which was biochemically active against cellular rRNAs *in vitro* in a 2-5A dependent manner (Gupta and Rath, 2012). But a RNase-domain deleted / dominant negative form of the mouse RNase L (homologous to the human RNase L) not only did not degrade the RNAs but also it stimulated the *E. Coli* cell growth. Earlier, this dominant negative mouse RNase L (DN-mRNase L) cDNA was reported to inhibit RNA degradation and apoptosis caused by the human RNase L cDNA in the mammalian cells. and this was explained as, since the DN-mRNase L protein bound and sequestered the 2-5A cofactors, the hRNase L protein was less active (Naik et al, 1998). Later, it was found out in our laboratory that the DN-mRNase L protein was highly degraded when expressed in *E. Coli* and it stimulated expression of some *E. Coli* proteins, which might have stimulated the *E. Coli* cell growth (Gupta and Rath, 2009, unpublished), this informed about a role of RNase L similar to the opposite effect of a tumor suppressor in terms of cell growth, proliferation of mammalian cells. A study in our laboratory, for the first time showed that the RNase-domain deleted RNase L may have other cellular functions/ effects; this is analogous to the gain of function mutation effect(s) of a tumour suppressor. Yet another study from our laboratory showed that cellular RNase L protein expression was induced by a number of stressors like the anticancer drugs, dsRNA, H_2O_2, $CaCl_2$ and inflammatory cytokine (TNF-α) in the human cervical carcinoma (Hela) cells, this correlated with RNA-degradation, DNA-fragmentation and apoptosis in the cells (Pandey et al., 2004),

suggesting for the first time that RNase L is a stress-responsive gene factor ana it may be involved in normal cellular functions other than its well established antiviral role.

In another study from our laboratory, a number of cellular proteins were identified from the mouse spleen which interacted with RNase L (Gupta and Rath, 2009, unpublished). It was also found that the RNase L mRNA was constitutively expressed in the mouse tissues with higher levels in spleen and thymus, the two immunological tissues (Gupta and Rath, 2009, unpublished). This stimulated us to explore the link between RNase L expression and prostate cancer, if any.

With this background the present study was designed to address the following questions

A. What is the status of RNase L expression in mouse tissues under normal conditions?

B. What is the effect(s) of endogenous and exogenous androgen(s) on the expression of RNase L in the prostate tissue of mouse under *in vivo* conditions?

C. What is the status of RNase L expression in an androgen-responsive dependent and androgen-unresponsive human prostate cancer cell lines?

D. What is the effect(s) of androgen on RNase L expression in the above two human prostate cancer cell lines?

E. What is the effect(s) of oxidative stress (H_2O_2) on RNase L expression in above two human prostate cancer cell lines?

It was expected that this study may inform us about the status of RNase L expression in mouse tissues and its relationship with androgen and oxidative stress in prostate of mouse as well as in the human prostate cancer cell lines as experimental model system to correlate with RNase L expression with prostate cancer.

V

Materials and methods

V. MATERIALS AND METHODS

V. 1 Materials

V.1.1 Reagents

Acrylamide (30%)   Dissolved 29.0 g Acrylamide (Sigma, A-9099) and 1.0 g Bis N-N' Methylene-bis-acrylamide acrylamide (Sigma, M-7256) in double distilled water to final volume made upto 100.0 ml. Stored at 4°C.

Agarose   Routinely 1-2% agarose (Sigma, A-9539)/low melting agarose (Type VII, Sigma, A-9414) gels were made in 1X Tris-acetate-EDTA (TAE) or 0.5X Tris-borate-EDTA (TBE) buffer with a final concentration of 0.5 µg/ml EtBr, added later.

Antibodies   **Primary:**

1. Monoclonal mouse Anti hRNase L (Sigma, R-3529)

2. Monoclonal mouse anti-β actin (Sigma, A-5316)

Secondary: Rabbit anti-Mouse IgG HRP (Sigma, A-9044)

Aprotinin (1 mg/ml)   1.0 mg aprotinin (Sigma) added in 1.0 ml double distilled water. Stored at -20°C in aliquots.

APS (10%)   Dissolved 100.0 mg Ammonium persulfate (APS) (Sigma, A-9164) in 1.0 ml double distilled water. Stored at -20°C.

Benzamidine (250 mg/ml)   250 mg Benzamidine (Sigma, B-6506) dissolved in 1.0 ml double distilled water. Stored at –20°C.

Bradford reagent (5X)   50 mg Coomassie Brilliant Blue G-250 (S. D. Fine Chemicals, #54329) added to 25 ml 95% ethanol (Merck) and dissolve properly. Added 50 ml *ortho*-Phosphoric acid (85%) and final volume made upto 100 ml by double distilled water. Stored at 4°C.

BSA (10 mg/ml)	Dissolved 10 mg bovine serum albumin (BSA) (Fraction V, Sigma, A-9647) in 1.0 ml double distilled water. Stored at − 20°C in aliquots.
Cell culture	**(A) Reagents:**

1. Anibiotic-antimycotic solution, 100X concentration (Sigma, A-5955) and 1X final concentration to be used.
2. RPMI-1640 (Sigma, R-8758)
3. Dimethyl sulfoxide (DMSO) for cell freezing (Sigma, D-2650).
4. Dimethyl sulfoxide (DMSO) for MTT assay (Sigma D-8418).
5. Fetal bovine serum (FBS) (Sigma, F-4135, 500 ml or 100 ml).
6. Dextran-charcoal treated fetal bovine serum (FBS), (ThermoScientific, HyClone, SH30068.02HI)
7. Trypan blue (Sigma, T-8154)
8. Trypsin-EDTA (Sigma, T-4049, 100 ml)
9. Trypsin-EDTA (HiMedia, TCL007-100 ml)

(B) Plastic wares:

10. 24-well plate (Corning, CLS-3526)
11. 6-well plate (Corning, CLS-3506)
12. 96-well plate (Corning, CLS-3628)
13. Freezing vials (Sigma, V8130-100EA)
14. Polypropylcne Falcon 15 ml tube (Corning, CLS-430052)
15. Polypropylene Falcon 50 ml tube (Corning, CLS-430291)
16. T-25 flask (Corning, CLS-430639)

Deionized water	10 g Mixed Bed Resin (Sigma, M8157-100G) added to 100.0 ml double distilled water and kept at RT for overnight.

Aliquots the deionised water in eppendorf tube and autoclaved. Stored at -20°C (used for PCR etc.) as required.

DEPC water | Diethyl pyrocarbonate (DEPC) (Sigma. D-5758) added into double distilled water at final concentration of 0.1%, stored at 37°C for overnight and autoclaved. Stored at -20°C or RT.

DNA loading dye (6X) | 10 mM Tris-Cl (pH 7.5), 0.03% bromophenol blue (Alderich Inc. # 62625.28.9), 60% glycerol and 60 mM EDTA mixed well. Stored at 4°C.

DNA marker | O'GeneRuler™ 1 Kb DNA ladder (MBI Fermentas, #SM1163). Stored at -20^{0}C.

DTT, 1M | 771.3 mg Dithiothreitol (DTT) (Sigma, D-9779) dissolved in 4.0 ml double distilled water, final volume made upto 5.0 ml and aliquoted. Stored at -20°C. Repeated freeze-thaw prevented.

ECL reagent | SuperSignal® West Pico Chemluminescent Substrate (Thermo, #37077). Stored at 4°C.

EDTA, 0.5M pH 8.0 | 18.6 g Ethylenediaminetetraacetic acid (EDTA) (Sigma, E-5134) dissolved in 80 ml double distilled water. pH 8.0 was adjusted by 10 N NaOH and final volume made upto 100 ml and autoclaved. Stored at RT.

EGTA (0.5 M) | Ethylene glycol bis-[B-amino ethyl ether]- N, N, N', N' tetra acetic acid (Sigma, E4378). Suspended 1.902 gm of EGTA in 30-40 ml of sterile H_2O by warming on a magnetic stirrer. pH was adjusted to 7.0 by adding 10 M NaOH drop-wise while stirring. Made volume to 50 ml. Autoclaved and stored at room temperature

Enzymes and dNTP |
1. dNTP set, 100 mM each (Fermantas, #R0181)

2. dNTPs individual set. each 100 mM (Promega, U-

1330)

3. M-MLV Reverse Trnascriptase, 10,000U (Promega, M-1701)

4. M-MuLV Reverse Transcriptase (NEB, M0253S)

5. Recombinant RNasin® Ribonuclease inhibitor, 2500U (Promega, N-2511)

6. RNase Inhibitor (NEB, M0307S)

7. Taq DNA Polymerase (NEB, M0273L)

EtBr (10 mg/ml)	Added 10 mg of ethidium bromide (EtBr) (Sigma, E-8751) in 1.0 ml double distilled water. Stored at 4°C.
H_2O_2 (30%)	Hydrogen per oxide (H_2O_2) Merck Germany, #61754405001730. Stored at 4°C.
Ketamine	Anket®, 50mg/ml, Neon Laboratories Limited. Stored at 4°C.
Leupeptin (1 mg/ml)	Made in double distilled water at a concentration of 1.0 mg/ml and stored in aliquots at -20°C.
Mercaptoethanol-β	β-Mercaptoethanol, 14.4 M (Sigma, M-3149). Stored at 4°C.
$MgCl_2$, 1 M	Dissolved 20.33 g of Magnisium Chloride ($MgCl_2.6H_2O$) (Qualigens-ExcelaR) in 80.0 ml of double distilled water and final volume made upto 100 ml and autoclaved. Stored at RT.
Milk, non-fat (5%)	1.0 g skimed milk powder (CDH, #024363) added in 10.0 ml 1X PBS-T and heated at 60°C for 20 min. Cooled at RT to use.
NaCl, 5 M	14.6 g sodium chloride (NaCl) (Merck) added into 50 ml double distilled water and autoclaved. Stored at RT.

NaF (0.5M)	Sodium fluoride (Sigma, S1504). Made 0.5M stock solution in autoclaved ddw. Stored at -20°C in aliquots of 50 µl.
Neosporin	Neosporin powder from Johnson & Johnson®
Nitrocellulose membrane	Trans-Blot Transfer Medium (BIO-RAD, #162-0115). Pure Nitrocellulose Membrane 0.45 µm, use for westernblot. Stored at RT.
PBS (10X), pH 7.4	20 g NaCl (1.3 M) (Merck), 0.5 g KCl (20 mM)(Qualigen ExcelaR, #19255), 3.6 g $Na_2HPO_4.2H_2O$ (78 mM) (Sigma, S-7907), 0.6 g KH_2PO_4 (14 mM) (Merck Germany, MI5M552654) mixed in 200 ml double distilled water, pH adjusted to 7.4 with 1 N naOH, final volume made upto 250 ml and autoclaved. Stored at RT.
PBS-T	1 x PBS, pH 7.4 with 0.1% Tween-20.
PMSF, 100 mM	Dissolved 174.2 mg PMSF (phenylmethanesulfonylfluoride) (Sigma, P-7626) in final volume of 10 ml ethanol/isopropanol. Stored at -20°C up to six months.
Ponceau S	100 mg Ponceau S (Hi-media, RM-977) dissolved in 49.0 ml double distilled water and 1.0 ml acetic acid. Stored at RT.
SDS (10%)	Dissolve 2 g of sodium dodecyl sulphate (SDS) (Sigma, S-4390) to 18 ml 10 mM Tris.HCl (pH 8.0) and final volume made upto 20 ml. To dissolve it properly, keep the solution at 37°C for 3-4 hrs. Stored at RT.
SDS-PAGE Running buffer (1X)	Freshly prepared by 18.8 g Glycine GR (Merck, MC-9M583649), 3.0 g Trizma (Sigma, T-1503) and 1.0 g SDS (Sigma, S-4390) was added in 800 ml double distilled water and mixed well. Final volume made upto 1 L by adding double distilled water. Stored at RT.
SDS-PAGE dye (2X)	125 mM Tris.Cl (pH 6.8), 4% SDS, 20% Glycerol, 0.02% Bromophenol Blue (Aldrich Inc., 62625.28.9) and 200 mM

DTT or 10% β-Mercaptoethanol was added just prior to use. Stored at RT.

Sodium acetate, 3 M

pH 5.2

20.4 g Sodium Acetate (Qualigen ExcelaR, #13905) added to 30 ml double distilled water and pH adjusted to 5.2 by glacial Acetic Acid. Final volume made upto 50 ml and autoclaved. Stored at RT.

Sodium deoxycholate (10% w/v)

(Sigma D-6750, M-414.6 g/mol). Dissolved 10% (w/v) in autoclaved double-distilled H_2O. Stored at 4°C protected from light.

Sodium orthovanadate

(Sigma S-6508, M-183.91 g/mol). Prepared 200 mM stock in autoclaved double-distilled H_2O, adjusted the pH to 9.0 with 1N HCl, boil until colorless, cooled to RT. Repeat the cycle untill solution remains at pH 9.0 after boiling and cooling. Stored as 20 μl aliquots at −20ºC.

TAE (50X)

Tirs-Acetate-EDTA (TAE) buffer made by adding 60.5 g Trizma (Sigma, T-1503), 14.3 ml glacial Acetic Acid (Merck) and 4.7 g EDTA (Sigma, E-5134) to double distilled water, final volume made upto 250.0 ml and autoclaved. Stored at RT.

TBE (5X)

Tris-Borate-EDTA (TBE) buffer made by adding 54.0 g Trizma (Sigma, T-1503), 27.5 g Boric Acid (Sigma, B-6768) and 3.72 g EDTA (Sigma, E-5134) to double distilled water, final volume made upto 1.0 L and autoclavd. Stored at RT away from light.

TEMED

N,N,N',N', Tetra methyl ethylene diamine. (Sigma, T-7024), stored at 4ºC in a dark bottle.

Testosterone

For Mice studies: Sustanone 250mg, Each ml contained 30 mg testosterone propionate, 60 mg testosterone phynylpropionate and 100 mg testosterone decanoate, From

Organone (India) Limited. Stored at 4oC.

For cell culture Studies: Testosterone. Himedia, RM-1848

Tris.HCl, 0.5 M pH 6.8	6.1 g of Trizma (Sigma, T-1503) dissolved in 80 ml double distilled water, pH adjusted to 6.8 with conc. HCl, final volume made upto 100 ml and autoclaved. Stored at RT.
Tris.HCl, 1 M pH 7.0	6.1 g of Tris Buffer GR (Merck, MC-8M580254) dissolved in 30 ml double distilled water and pH adjusted to 7.0 with conc. HCl, fnal volume made upto 50 ml and autoclaved. Stored at RT.
Tris.HCl, 1.5 M pH 8.8	18.2 g of Trizma (Sigma, T-1503) dissolved in 80 ml double distilled water, pH adjusted to 8.8 with conc. HCl, final volume made upto 100 ml and autoclaved. Stored at RT.
Triton X- 100	(Sigma, T-8787), diluted to 10% in water and stored at RT.
Western blot transfer buffer	Freshly prepared by adding 2.9 g Glycine GR (Merck, MC-9M583649), 5.8 g Trizma (Sigma, T-1503) and 0.4 g SDS (Sigma, S-4390) to 850 ml double distilled water. 150 ml methanol was added to make the final volume 1 L. Stored at 4°C.
X-ray flim	XBT-5 (Kodak, #4909958). Stored at RT in dark place.
X-ray flim developer	Dissolved 17.8 ml Part A liquid with 1.4 g Part B powder (Kodak, #4908216) in 100 ml double distilled water and made final volume upto 150 ml, prepared fresh just prior to use. Stored at 4°C in dark bottle.
X-ray flim fixer	Dissolved 21.4 g of X-ray acid fixing salts (Kodak, #4908232 or #9000720) in 80 ml double distilled water, mxed well and final volume made upto 100 ml. Stored at 4°C in dark bottle.
Xylaxin	Xylaxin Hydrochloride (2% Solution)

V.1.2 Primers

S.No.	Primer	Sequence (5`→ 3`)	Annealing temp (°C)	Amplicon size (bp)
1.	Oligo-(dT)$_{15}$	TTTTTTTTTTTTTTT	42	-
2.	RNase L Fwd	CTGCAACCACAAAACATCTTAATA	60	644
3.	RNase L Rev	AGATCTGGAAATGTCTTCTGAAAATA		
4.	Nkx3.1 Fwd	GGAGACACCGACTGAACCC	60	311
5.	Nkx3.1 Rav	AGACTCCCAGGTCTTCCGAC		
6.	GAPDH Fwd	ACCACAGTCCATGCCATCAC	60	452
7.	GAPDH Rev	TCCACCACCCTGTTGCTGTA		

V.1.3 Experimental animals and cell lines

Male, 8-10 week old Swiss Albino mice were obtained from the University animal house facility. Mice were kept in a temperature-controlled room with a 12 hrs light/dark cycle and provided with food and water. Care was taken to ensure animals remained healthy. Mice were euthanized by cervical dislocation or anaesthetized using ketamine and xylazine.

Prostate cancer cell DU145 was acquired from the cell repository of National Centre for Cell Sciences. 22Rv1cells were kind gift from Dr R. P. Singh's laboratory, which was acquired from ATCC, USA.

V.2. METHODS

V.2.1. Analysis of RNaseL mRNA expression in different tissues

V.2.1.1. RNA isolation

RNA was isolated from the mouse tissues (prostate, liver, kidney, heart, spleen, thymus, brain, testis and lungs) using Tri-Reagent. Fifty to hundred mg of tissue was crushed and powdered in liquid nitrogen using a mortar and a pestle. One ml Tri-Reagent was added and the mixture. Homogenized samples were incubated for 15 min at room temperature. 0.3 ml of chloroform was added and the mixture was vortexed vigorously for 15 sec. The mixture was further incubated at room temperature for 15 min. Then the samples were centrifuged at 12,000 rpm for 15 min at $4^{\circ}C$. The homogenate was separated into three phases, the upper aqueous phase containing RNA, the interphase containing DNA and the lower organic phase containing protein. The upper aqueous phase was collected and again extracted with 0.3 ml of chloroform for further deprotenization. The aqueous phase was transferred in to a fresh tube. 0.5 ml of isopropanol was added and the mixture was inverted several times to mix thoroughly. The samples were kept at room temperature for 10 min to allow the RNA to precipitate, and then centrifuged at 12,000rpm for 15 min at $4^{\circ}C$. The supernatant was discarded and 1ml cold 80% ethanol was added to wash the RNA pellet which was again centrifuged at 10000 for 10 min at $4^{\circ}C$ for recovery. RNA pellet was air-dried and re-suspended in DEPC-treated water. For prostate RNA, an additional step of phenol chloroform treatment was give after dissolving the RNA pellets 500 µl dissolving Buffer (200mM Na-Acetate, 0.2% SDS, 1mM EDTA pH 8.0). The RNA concentration was spectrophotometrically determined at 260 nm. The ratio at $A_{260\ nm}$ / $A_{280\ nm}$, the spectrum from 200-300 nm and the gel picture of the 28S and 18S rRNAs were used to determine the RNA quality.

V.2.1.2. Reverse transcription

In 0.5 ml eppendorf tube, 500ng oligo $(dT)_{15}$ primer and 2.0 µg RNA were denatured in DEPC-treated water in a total volume 15 µl for 5 min at $70^{\circ}C$ in thermocycler and chilled on ice immediately. Ten µl of reaction mix was added to the denatured RNA as follows:

Components	Stock conc.	Volume (µl)	Final conc.
DEPC-treated water	-	2.25	-
5X MMLV-RT Buffer	5X	5.00	1X
dNTP	10 mM	1.25	0.5 mM
RNasin	40 U/µl	0.5	20 U/µl
MMLV-RT	200 U/µl	1.0	200 U/reaction
Total			10

The sample was incubated in a thermal cycler at 42 °C for 60 min.

V.2.1.2. PCR

The single-stranded cDNAs synthesized as above served as the template for PCR using gene specific primers for mouse RNaseL (mRNaseL) and Glyceraldehyde 3-Phosphate Dehydrogenase (GAPDH). The composition of the reaction mix for the mRNaseL and GAPDH PCR reactions were as follows:

Components	Stock conc.	Volume (µl) (mRNaseL)	Volume (µl) (GAPDH)	Final conc.
Deionized water	-	17.5	19.0	-
PCR buffer (With 2mM MgCl$_2$)	10X	2.5	2.5	1X
dNTP mix	10 mM	0.5	0.5	0.2 mM
Forward Primer	25 pmol/µl	0.5	0.5	12.5 pmol/reaction
Reverse Primer	25 pmol/µl	0.5	0.5	12.5 pmol/reaction
Taq polymerase	1 U/µl	1.0	1.0	1U/µl
cDNAs (1st strand reaction)	-	2.5	1.0	-
Total		25.0	25.0	

The PCR conditions for RNase L and GAPDH were as follows:

Step 1: 95 °C, 5 min.
Step 2: 95 °C, 45 sec.
Step 3: 60 °C, 45 sec.
Step 4: 72 °C, 1 min.
Step 5: Repeat steps 2-4 for 30 cycles for RNase L and 30 cycles for GAPDH.
Step 6: 72 °C, 10 min.

V.2.1.3. Agarose gel electrophoresis

0.5X TBE, 1.5% agarose gel containing 0.5 µg/ml of ethidium bromide was prepared. DNA samples were loaded in 6X Gel Loading Buffer and electrophoresed in 0.5X TBE buffer at 25 mA for 1 hr. The DNA was visualized using an UV transilluminator and photographed by AlphaImager 3400 gel documentation machine. Integrated Density Value (IDV) calculated by AlphaImager software was used for quantification.

V.2.2. Effect of testosterone on the expression of RNase L in mouse prostate

V.2.2.1. Mouse surgery

Anaesthetized the 8 week old swiss albino mice with 100 µl ketamine and xylazine (10 mg/ml ketamine, 1 mg/ml xylazine) per 10gm of the body weight. Wiped the scrotal sac region of mouse with spirit. Made a small incision and cut open the scrotal sac. To cut open scrotal sac, first cut open the dermis then cut open the muscle layer. Push testis slightly sideways so that it comes out of the scrotal sac. Then make a small incision on the thin membrane covering the testis. Slightly push the testis so that it comes out of the membrane covering. Tie the red coloured renal vein with help of needle and black thread. Tied the second knot tying all other connection to testis then dissect out the testis. Similarly other testis was also removed. Made 3-4 stiches to the scrotal sac to close the cut and open area. Sprinkled the Neosporin powder over the operated area and waited till it recovers from anaesthesia. After recovery when movement of mouse is normal then it is transferred back to the mouse cage.

V.2.2.2. Mouse care

Mouse was kept in animal room with 12 hr day-night cycle. Sufficient food and water were provided in cage. Neosporin was sprinkled over operated area for next three days after surgery. Mice were allowed to fully recover from surgery for 10 days.

V.2.2.3. Mouse treatment with testosterone

Injected 50 µl (2 mg) of working solution (40 mg/ml) of sustanone 250 intra-peritoneally to castrated mice. Labelled these mice as 'Treated'. Injected 50µl of Sesame oil to castrated mice and labelled 'Untreated'. Uncastrated mice were kept as 'Control',

and were not injected with either sustanone or sesame oil. The injections were given for five days.

V.2.2.4. Sacrifice of mice and Sample collection

On the Sixth day mice were sacrificed by cervical dislocation, tissues collected, snap freezed in liquid nitrogen and stored at -80°C. Picture of the mouse prostate was taken before snap freezing into liquid nitrogen.

V.2.2.5. RT-PCR

Reverse transcription and PCR for RNase L and GAPDH was done as described earlier. PCR for Nkx3.1 was done as follows

Components	Stock conc.	Volume(µl) (NKx3.1)	Final conc.
Deionized water	-	18.05	-
10X buffer (With 1.5mM MgCl$_2$)	10X	2.5	1X
MgCl$_2$	50mM	0.25	2 mM (Including 10X buffer MgCL$_2$)
dNTP mix	10 mM	0.5	0.2 mM
Forward Primer	25 pmol/µl	0.5	12.5 pmol/reaction
Reverse Primer	25 pmol/µl	0.5	12.5 pmol/reaction
Taq polymerase	5 U/µl	0.2	1 U/rection
cDNAs (1st strand reaction)	-	2.5	-
Total		25.0	

The PCR condition for Nkx3.1 was as follows:

Step 1: 95 °C, 5 min.

Step 2: 95 °C, 45sec.

Step 3: 61 °C, 45sec.

Step 4: 72 °C, 1 min.

Step 5: Repeat steps 2-4 for 30 cycles.

Step 6: 72 °C, 10 min.

V.2.2.6. Statistical analysis

For RNA expression by RT-PCR, the DNA band (amplicon) in the agarose gel was quantified by densitometry to obtain the integrated density value (IDV) using software AlphaImager 3400. IDV of RNase L and Nkx3.1 was normalized by IDV of GAPDH to express the relative expression of the RNase L or Nkx3.1 mRNA as the normalized IDV ratio. Statistical analysis of mRNA expression or cell proliferation was carried out by Student's t-test for comparing two groups using Sigma Plot (version 8.0) software. Values represented in graphs are mean ± SEM calculated from at least three independent observations. $p < 0.05$ was considered significant.

V.2.3. Analysis of mRNase L sequence for androgen receptor binding site

Upstream sequence (upto -1661) of mouse RNase L transcription start site was downloaded from NCBI Gene database. This sequence was aligned with Androgen receptor binding consensus sequence (5'-AGAACAnnnTGTTCT-3') using EBI EMBOSS software (http://www.ebi.ac.uk/Tools/emboss/align/index.html).

V.2.4. 22Rv1 and DU145 cell culture

Seeded 1-2 million cells in 5 ml RPMI-1640 with 10% FBS and 1X antibiotic in T-25 flask. Allowed to grow the cells in incubator at 37 °C, 5% CO_2. Monitored the growth/ confluency under microsope everyday. Did not disturb 22Rv1 cells for first 24h because these cells adhere very loosly and slowly. Monitor the change in colour of media visually and change media accordingly.

V.2.4.1.Trypsinization

Aspirateed spent media from T-25 flask. Washed the cells with 5 ml PBS twice. Add 1 ml Trypsin solution to T-25 flask. Incubate it at 37 °C for 1 min Observe under Microscope for detached cells. Add 4 ml media to T-25 flask. Transfer the media (having cell suspension) to 15 ml falcon tube and spin the falcon at 2000 rpm in swinging bucket rotor for 3 min. Discard supernatant and resuspend the cells in 1 ml media.

V.2.4.2. Cell counting

Clean the Haemocytometer and cover slip with 70% ethanol. Place the cover slip on haemocytometer. Mix 50 µl of cells with 50 µl trypan blue, Add a small volume of

trypan blue stained cell suspension to the haemocytometer. Focus the microscope on the grid lines of the haemocytometer using the 10X objective of the microscope. Focus on one set of 16 corners square. Count the number of live cells in this area of 16 squares. Move the haemocytometer to another set of 16 corner squares and carry on counting until all 4 sets of 16 corner squares are counted.

The concentration in cells per ml = (cells in four squares/4) $\times$ 2 $\times$ 10,000

V.2.4.3. Sub culturing

Seed new T-25 flask with 1-2 million cells in 5 ml RPMI-1640 media having 10% FBS and 1X antibiotic. Cells were observed everyday for confluency. Media were changed typically at in 2 days in case of DU145 cells and in 3 days in 22Rv1 cells. Once confluent, the cells were trypsinized, as mentioned above and either seeded in new flask or frozen in vapour phase of liquid nitrogen, as described below.

V.2.4.4. Freezing and thawing of cells

Healthy growing DU145 or 22Rv1 cells were harvested by trypsinization and cell pellets were resuspended at a concentration of 1.0×10^6 cells/ml freezing medium (10% DMSO and 90% FBS). The cryovials were wrapped in parafilm and aluminum foil, put on ice and transferred to -80°C for overnight and stored at liquid nitrogen for long term storage. Revival of frozen cells was done as quickly as possible. The frozen cells were thawed at 37°C, resuspended in 4 ml RPMI-1640 with 10% FBS. The cells were harvested by centrifugation, the medium containing DMSO was discarded, and the cells were resuspended gently in 5 ml RPMI-1640 with 10% FBS medium and seeded in T-25 flask. The cells are allowed to grow at 37°C, 5% CO_2 for overnight. On the next day the medium with floating cells were discarded and RPMI-1640 with 10% FBS was added, allowed to grow up to 80% confluency and maintained as described above.

V.2.4.5. MTT-assay

This MTT (3-(4, 5-dimethylthiasol-2-yl)-2, 4,-diphenyltetrazolium bromide) assay is a colorimetric assay that measures the reduction of MTT by succinate dehydrogenase enzyme in mitochondria where it is reduced to an insoluble, colored, formazan product from a soluble uncoloured substrate. The cells were then solubilised with (DMSO) and the released, solubilized formazan reagent is measured

spectrophotometrically (Mosmann, 1983). MTT assay was done as describe previously with some modification (Mishra et al., 2011). DU145 and 22Rv1 cells were seeded in to 24-well plate at three different densities for viz. 10×10^3, 20×10^3 and 40×10^3 per well in triplicate in three different plate for 24 hrs, 48 hrs and 72 hrs and kept at 37°C and 5% CO_2. After 24 hr, 48 hr or 72 hr, 100 µl of 5 mg/ml MTT was added in to each well and plate was again placed back in incubator for the next 2 hr. MTT is light sensitive, hence maintain dark or wrap the plate in aluminum foil such that proper aeration take place. After 2 hr, observe the cells under phase contrast microscope to visualize the dark violet coloured crystal inside the cells. Next, aspirate the media and added 300 µl DMSO in each well and kept for 10 min at RT with gentle shaking by hands. Colourless DMSO turned in to violet coloured. Transfer 200 µl from each well in to 96-well plate and absorbance was read at 590 nm, which has a photometric range from 0.0 to 4.0 O.D.

V.2.5. Testosterone treatment of DU145 cells for growth curve analysis

Du145 cells were seeded at density of 10000 cells per well (in 0.5 ml media) of 24 well plate in triplicate. After 24 hr the media (10% FBS and 1X antibiotic in RPMI 1640) was removed and the cells were treated with 10 nM and 100 nM of testosterone in culture media having 10% dextran-charcoal treated fetal bovine serum and 1X antibiotic in RPMI-1640 for the time point of 24 hr, 48 hr and 72 hr. After each time point, MTT assay was carried out as described earlier.

V.2.5.1. Testosterone treatment of 22Rv1 cells for growth curve analysis

22Rv1 cells were seeded at density of 20000 cells per well (in 0.5 ml media) of 24 well plate in triplicate. After 24 h the media (10% FBS and 1X antibiotic in RPMI 1640) was removed and the cells were treated with 0 nM, 10 nM and 100 nM of testosterone in culture media having 10% dextran-charcoal treated fetal bovine serum and 1X antibiotic in RPMI-1640 for the time point of 24 hr, 48 hr and 72 hr. After each time point, MTT assay was carried out as described earlier.

V.2.5.2. Testosterone treatment for expression analysis of RNase L mRNA in DU145 and 22Rv1 cells

50000 cells of DU145 and 100000 cells of 22Rv1 were seeded in 2 ml culture media (RPMI-1640 with 10% FBS and 1X antibiotic) in each well of 6 well plates. Cells

were allowed adhere and grow for 24 hr. After 24 hr, the media was replaced with a treatment media (RPMI-1640 with 10% dextran-charcoal treated FBS and 1X antibiotic) having 10nM testosterone for a period of 48 hr. After 48 h of treatment, media was removed. DU145 and 22Rv1 cells were washed in 1X PBS and were harvested in 0.5 ml Tri-reagent. Total RNA of the cells was isolated as described earlier. RT-PCR was done for RNase L and GAPDH mRNA as described earlier.

V.2.5.3. Testosterone treatment for expression analysis of RNase L protein in DU145 and 22Rv1 cells

50000 cells of DU145 and 100000 cells of 22Rv1 were seeded in 2ml culture media (RPMI-1640 with 10% FBS and 1X antibiotic) each well of 6 well plates. Cells were allowed adhere and grow for 24 h. After 24 h, The media was replaced with a treatment media (RPMI-1640 with 10% dextran-charcoal treated FBS and 1X antibiotic) having 0nM or 10nM testosterone for a period of 48 h. DU145 and 22Rv1 cells were harvested by mild trypsinization and scraping in ice cold Phosphate buffer saline. Cells were washed in PBS and centrifuged at 2000 rpm for 3 min to remove the media content. The cell pellet was either stored at -80 °C or processed for protein extraction for western blotting.

V.2.5.3.1. Protein extract preparation

Cell pellet was resuspended in 1 ml lysis buffer/ 1 million cells. Lysis buffer was made fresh and was composed of 50 mM Tris-Cl pH 7.5, 150 mM NaCl, 5 mM EDTA pH 8.0, 2.5 mM EGTA pH 7.5, 1 mM sodium orthovanadate, 1% Triton X-100, 0.5% sodium deoxycholate, 0.1% SDS, 2 mM NaF, 2 mM PMSF, 5 µg/ml leupeptin, 5 µg/ml aprotinin, 0.5 mg/ml benzamidine. Agitated the cells in lysis buffer at ice for 30min. Centrifuged the cells at 12000 rpm for 15 min, collected the supernatant and stored at -80°C.

V.2.5.3.2. Protein estimation

Bradford's method (Bradford, 1976) was used for estimation of protein conc. in the tissue extracts. A standard curve of BSA was made by using a serial dilution of BSA (1 µg/ml) from 0, 2, 4, 6, 8, 10 and 12 µg in a final vol of 0.8 ml in 1.5 ml Eppendorf tubes. Each conc. was taken in duplicates. Two hundred µl of 5X Bradford's reagent was added to each tube and allowed to react for 5 min. The O.D. was measured at 595 nm in

a spectrophotometer. A standard curve was plotted for the mean $O.D._{595nm}$ to estimate the conc. of BSA. Two µl of the protein extract in 0.8 ml was added with 200 µl of 5X Bradford reagent, O.D. at 595 nm was estimated using the standard curve.

V.2.5.3.3. Sample preparation

The protein extract (30 µg) was boiled with equal volume of 2X SDS-PAGE sample buffer (100 mM TrisCl, pH 6.8, 4% w/v SDS, 0.2% w/v bromophenol blue, 20% glycerol, 200 mM DTT, in H_2O) in boiling water bath for 5 min then chilled on ice.

V.2.5.3.4. SDS-PAGE

Sodium Dodecyl Sulphate Polyacrylamide Gel Electrophoresis (SDS-PAGE) was carried out according to Laemeli's method (Laemmli, 1970). Stacking and resolving gel solutions were made as follows:

Solution component	10% resolving gel (ml)	5% stacking gel (ml)
H_2O	4.0	2.1
30% acrylamide mix	3.3	0.5
1.5 M Tris (pH 8.8)	2.5	-
1.0 M Tris (pH 6.8)	-	0.38
10% SDS	0.1	0.03
10% APS	0.1	0.03
TEMED	0.006	0.003
Total	10	3

The solution was swirled gently to avoid formation of bubbles and quickly added with freshly prepared 10% APS and TEMED, poured in sealed vertical glass plates (Bio-Rad miniprotean III apparatus), covered with thin layer of isopropanol. It was allowed to polymerize for 30 min at RT, and after polymerization, the upper layer of isopropanol was completely removed and 5% stacking gel solution was poured and the 1.5 mm thick comb was put in to make the wells. After the stacking gel was polymerized, the comb was removed and the slots were washed well with 1X gel buffers to remove any unpolymerized acrylamide. The gel was placed in the vertical gel apparatus ensuring that there was no air bubble trapped between the buffer and the bottom of the gel. The cell

extract sample was loaded into the well and electrophoresed in 1X Tris-Glycine-SDS Buffer at 80V at RT till the bromophenol blue dye migrated out of the gel.

V.2.5.3.5. Western blotting

The gel was trimmed to remove the stacking gel. The gel was washed with the transfer buffer (39 mM glycine, 48 mM Tris, .037% SDS, 10 or 20% methanol, pH 8.3) to remove SDS. The gel and the nitrocellulose membrane were sandwiched between two sheets of Whatman 3MM sheets and packed into the Western blotting apparatus cassette. The transfer was carried out by electroblotting at 40V in the transfer buffer overnight in the cold room with constant mixing of the buffer. The gel was removed and the nitrocellulose membrane was stained with Ponceu-S. All the lanes with markers were visible. The markers were marked with a ball-point pen on the nitrocellulose membrane. The membrane was washed with PBST to remove the Ponceu-S, freshly washed in 1X PBST, incubated in 5% non fat milk in PBST for 3h at room temp with mild shaking. Then it was washed with 1X PBST gently and incubated with the primary antibody (Monoclonal anti human RNase L (at 1:3000 dilution) or anti-β-actin antibody (at 1:5000 dilution)) in 1X PBST for 2 h at room temperature. Then the membrane was washed in 1X PBST thrice, 10 min each on a rotating platform to wash away all non-specifically bound antibodies. The membrane was then incubated with horseradish peroxidase (HRP)-conjugated secondary antibody (anti mouse IgG, Sigma) in 2.5% nonfat milk in 1X PBST for 2 h at room temp, again washed in 1X PBST thrice, 10 min each on the rotating platform to wash away all non-specifically bound antibodies.

V.2.5.3.6. Developing

All the subsequent steps were carried out in a dark room with photographic safe light. In a clean container 1 ml ECL solution (equal volumes of ECL solution I and II) was added and swirled to mix, the blot was placed in the ECL solution mixture and swirled for 1min taking care to ensure that the entire blot is constantly in contact with the solution. The membrane was blotted on tissue paper to remove all extra ECL, wrapped in saran wrap and placed on intensifying screen and exposed to Kodak X-ray film for varying time, 5 sec, 30 sec, 1 min, 2 min or more and then developed the film with X-ray developing and fixing solution with intermediate wash in water. The film was dried and aligned with the blot and marked with the position of the markers. The image was obtained by scanning of the X-ray film. The blot was stored at 4°C.

V.2.6. H_2O_2 treatment of DU145 cells for growth curve analysis

Du145 cells were seeded at density of 20000 cells per well (in 0.5ml media) of 24 well plate in triplicate. After 24 h the media (10% FBS and 1X antibiotic in RPMI 1640) was removed and the cells were treated with different H_2O_2 concentrations for different time points. After each time point, MTT assay was carried out as described earlier.

V.2.7. H_2O_2 treatment of 22Rv1 cells for growth curve analysis

22Rv1 cells were seeded at density of 20000 cells per well (in 0.5ml media) of 24 well plate in triplicate. After 24 h the media (10% FBS and 1X antibiotic in RPMI 1640) was removed and the cells were treated with different H_2O_2 concentrations for different time points. After each time point, MTT assay was carried out as described earlier.

V.2.7. Effect of hydrogen peroxide on expression of RNase L in DU145 and 22Rv1 cells

1×10^5 cells of DU145 and 22Rv1 cells were seeded in each well of 6 well plates. Cells were allowed to adhere and grow or next 24 h. After 24 h cells were treated with hydrogen peroxide diluted in PBS at final concentration of 200 μM for 4 h. After 4 h, the cells were harvested for RT-PCR and western blotting and processed for same, as described earlier.

VI

Results

VI. RESULTS

VI.1. Expression of RNase L mRNA in mouse tissues

Expression of RNase L mRNA was analysed in nine different tissues of 8-10 week old Swiss Albino male mice. All nine tissues, that is, spleen, thymus, heart, liver, kidney, testis, prostate, brain and lung showed the constitutive expression of RNase L mRNA amplicon of the size of 644 bp (Fig. 1). Spleen showed highest level of expression (2.655±0.480) followed by thymus (1.546±0.161). The other tissues showed similar basal levels of expression. Some tissues like lung and kidney showed variations in the expression even among the individual mice. For example RNase L mRNA expression of lung in Fig. 1B and 1C shows much higher expression than in that of Fig. 1A. Also, kidney in Fig. 1A shows much higher expression of RNase L mRNA amplicon than in the kidney of Fig. 1B and 1C. These variations may be due to individual physiological or environmental variations affecting these tissues, as all these mice were analysed for RNase L mRNA expression independently and at different points of time. GAPDH is a house keeping gene constitutively expressed in all the tissues, it was used as a control. All the tissues showed nearly same level of expression of GAPDH mRNA. The relative expression of RNase L mRNA was about three fold higher in spleen and two fold higher in the thymus of mouse compared to the average level of expression in the other tissues (Fig. 2). Thus, RNase L mRNA is constitutively expressed in the mouse tissues under normal physiological conditions and the expression is higher in the immunological tissues like the spleen and thymus.

VI.2. Effect of castration and testosterone treatment on mouse prostate

To study the effect of endogenous and exogenous androgen on the RNase L expression in the mouse prostate, the castration experiment was carried out. The 8 to 10 week old mice were castrated as described in the methods section. Mouse prostate tissue was dissected out along with the seminal vesicle and urinary bladder. The picture was taken immediately after the tissue was dissected out and placed in ice cold normal saline in a petri-dish. Below the petri-dish a scale was placed to help comparison of the size of the tissue. Fig. 3A shows normal mouse prostate gland tissue along with the seminal vesicle and urinary bladder. Fig. 3B shows the prostate tissue after castration, 10 days of recovery period and 5 days of treatment with sesame oil (vehicle) intra-peritoneally. Fig.
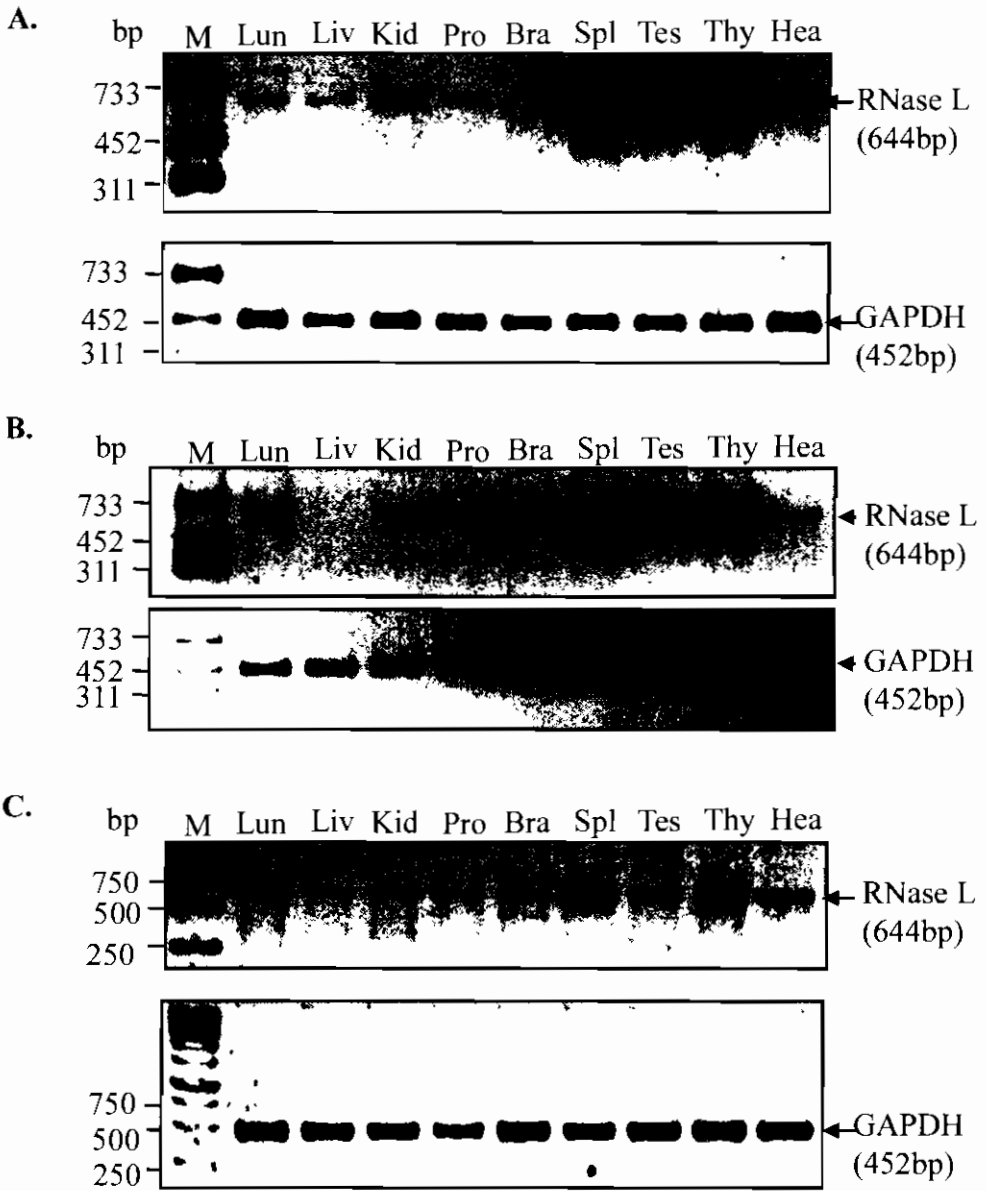
Fig. 1. Expression of RNase L mRNA in nine different tissues of the mouse as maesured by RT PCR. The 1.5% agarose (0.5X TBE buffer) gel electrophoresis shows the 644 bp RNase L and 452 bp GAPDH amplicons. A, B and C panels represent the independent experiments using total RNA isolated from three individual mice. Lun- lungs, Liv-liver, Kid- kidney, Pro- prostate, Bra- brain, Spl- spleen, Tes- testis, Thy- thymus, M- marker DNA (bp).
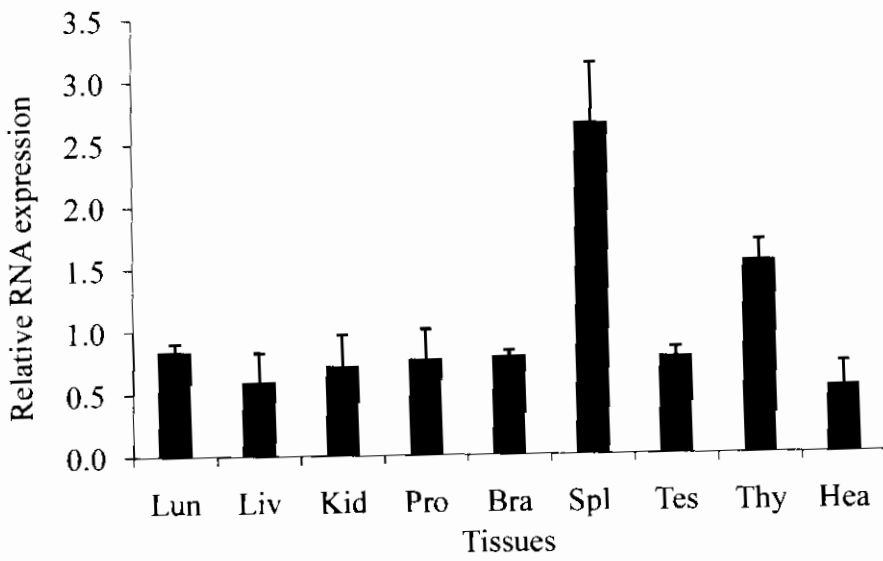
Fig. 2. Relative RNA expression (RNase L mRNA / GAPDH mRNA) in the nine mouse tissues. The IDVs (Mean ± SEM) are from the data shown in Fig. 1 (n=3). IDV- Integrated density values.

A. Normal

B. Castrated

C. Castrated + Androgen
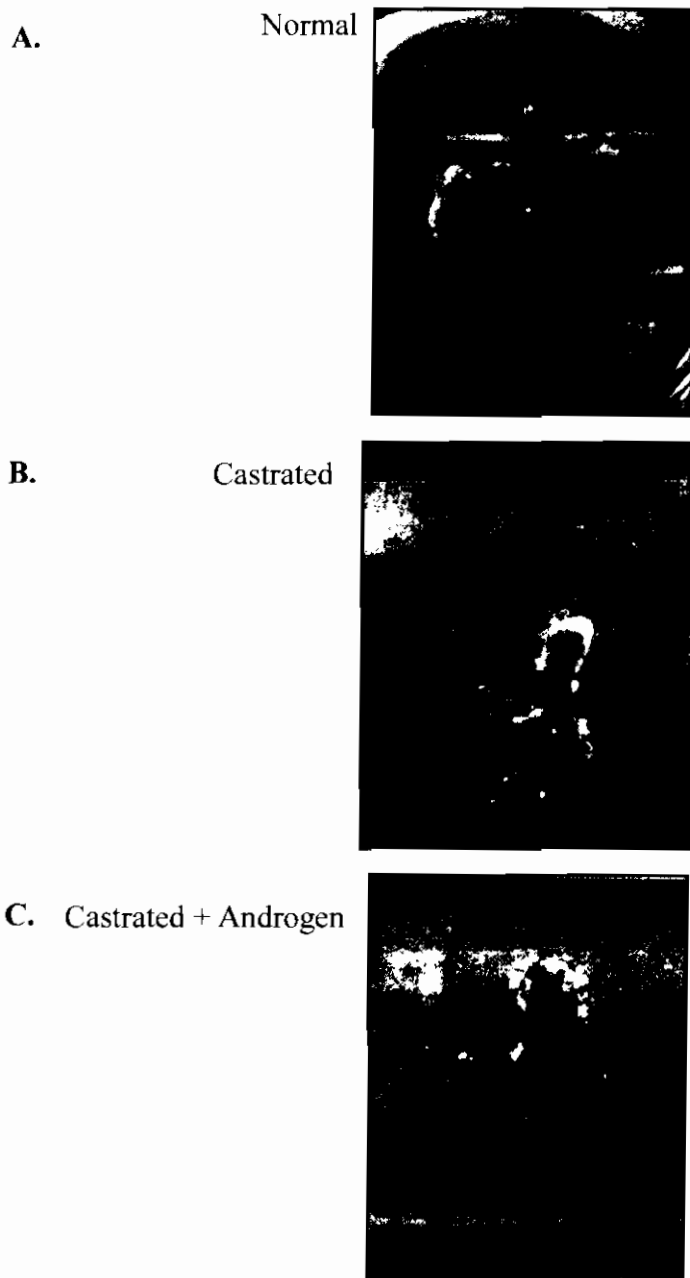
Fig. 3. Effect of androgen on mouse prostate tissue. A. Normal mouse prostate tissue along with seminal vesicle and urinary bladder. B. Atrophied mouse prostate tissue after castration (10 days recovery period and 5 days treatment with sesame oil intraperitoneally). C. Mouse prostate tissue of regaining in size after castration and androgen treatment (10 days recovery period and 5 days treatment with testosterone (2 mg/mice) in sesame oil intraperitoneally). P= Prostate, S= Seminal Vesicle, B= Bladder.

3C shows the prostate tissue after castration. 10 days of recovery period and 5 days of treatment with testosterone (2 mg/mice) in sesame oil intra-peritoneally. Fig. 3A clearly shows the developed mouse prostate tissue along with the grown flaccid seminal vesicle. While after castration in Fig. 3B, the prostate as well as seminal vesicle tissues are visually reduced in size, thus atrophied. But after the treatment with testosterone (2 mg/mice) in Fig. 3C, the prostate as well as seminal vesicle tissues have again grown to more or less normal shape and size. This shows that the castration experiments and the exogenous testosterone administration were working fine in respect of its effects on the maintenance and growth of the mouse prostate gland size, morphology and function under the control of the testis and androgen (endogenous testosterone) secreted from the testis as well as the exogenously administered androgen under in vivo conditions in the mouse.

VI.3. Effect of castration and testosterone treatment on expression of Nkx3.1 mRNA

NKx3.1 is a prostate-specific homeodomain transcription factor positively regulated by androgen (Meeks and Schaeffer, 2011). This gene's mRNA expression has been used here as the positive marker for androgen response in the mouse prostate at transcriptional mRNA level. The normal mouse prostate shows expression of the Nkx3.1 mRNA amplicon of 311 bp. After castration, the expression of Nkx3.1 mRNA decreases due to androgen depletion while the expression of Nkx3.1 mRNA again increases when the androgen is given exogenously (Fig. 4). Paired t-test analysis of GAPDH normalized values for the normal (N) and castrated (C) mouse showed P-value of less than 0.05 (P= 0.004) showing that the castration significantly decreased the level of NKx3.1 mRNA by nearly 66% (Table 1). Also, the paired t-test between the castrated (C) and castrated & androgen treated (C+T) showed a P-value of less than 0.05 (P= 0.013). Furthermore there is no significant difference in the levels of the Nkx3.1 mRNA between the normal (N) and castrated & androgen treated (C+T) (Fig. 5), showing that the exogenous treatment of testosterone was almost sufficient to attain the response at the molecular level. This response of the Nkx3.1 mRNA shows that our model system of castration in the mouse and hormone replacement was working at the molecular level of the mRNA under the in vivo conditions. Thus, the Nkx3.1 mRNA served as a good positive control in this case.
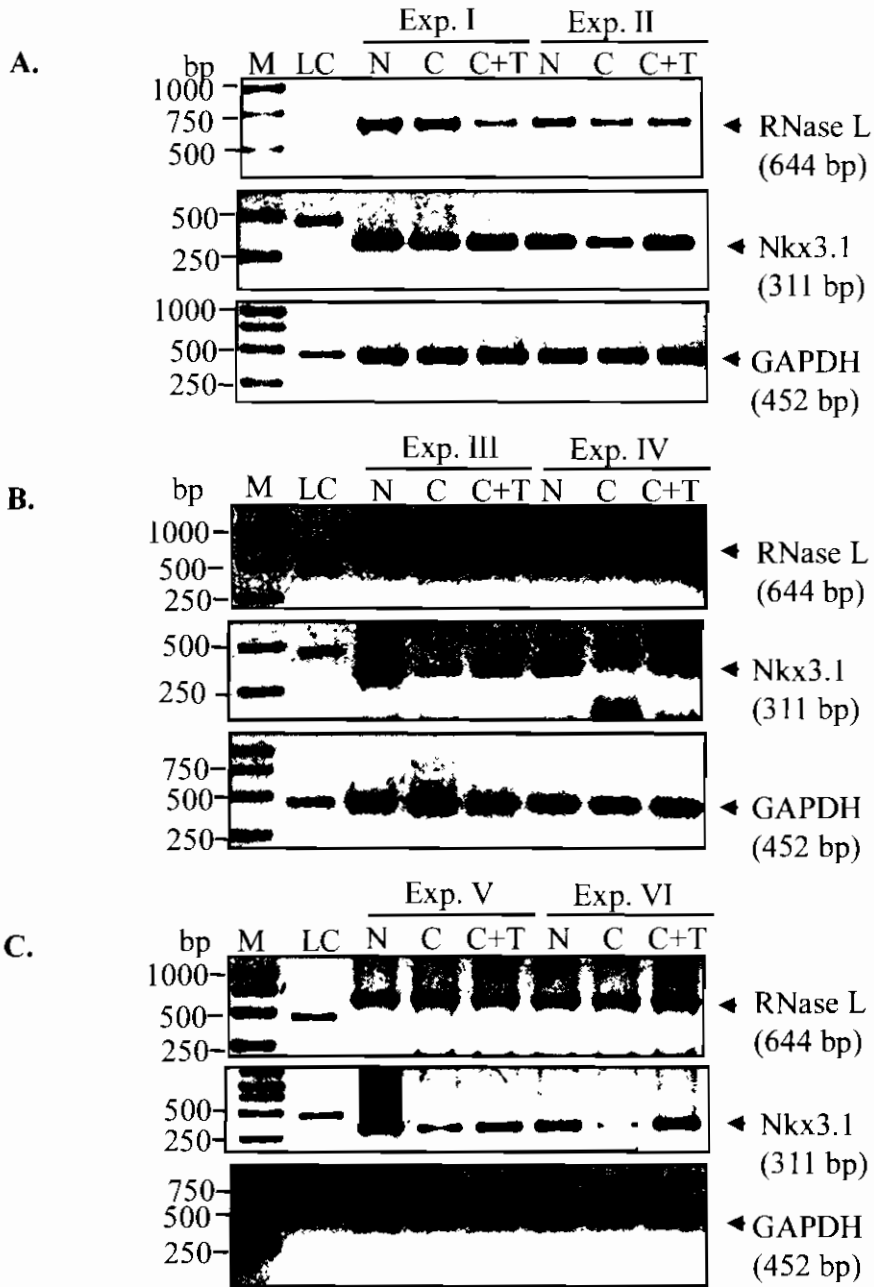
Fig.4. Expression of RNase L, Nkx3.1 and GAPDH mRNAs measured by RT-PCR in the normal mouse prostate (N), castrated mouse prostate treated with sesame oil only (C), and castrated mouse prostate and treated with testosterone (C+T). A total of six independent experiments (I- VI) are shown in A, B and C. Exp. (I- VI) = Experiment I- VI, LC = a 452 bp DNA fragment (20 ng) used as a loading control for the densitometry purpose. Nkx3.1 is an androgen responsive gene in the mouse prostate.

Table 1. Paired t-test of Nkx3.1 normalized values using software Sigmaplot 8.0. Underlined values are less the 0.05 thus significant

	Mean ±SEM	P- Value	% Change compared to N
N	1.661±0.267	Vs C=**0.004**	0.0
		Vs C+T= 0.257	
C	0.556±0.114	Vs N= **0.004**	-66.4
		Vs C+T= **0.013**	
C+T	1.300±0.207	Vs N= 0.257	-21.7
		Vs C= **0.013**	

N= Normal, C= Castrated, C+T= Castrated and treated with testosterone
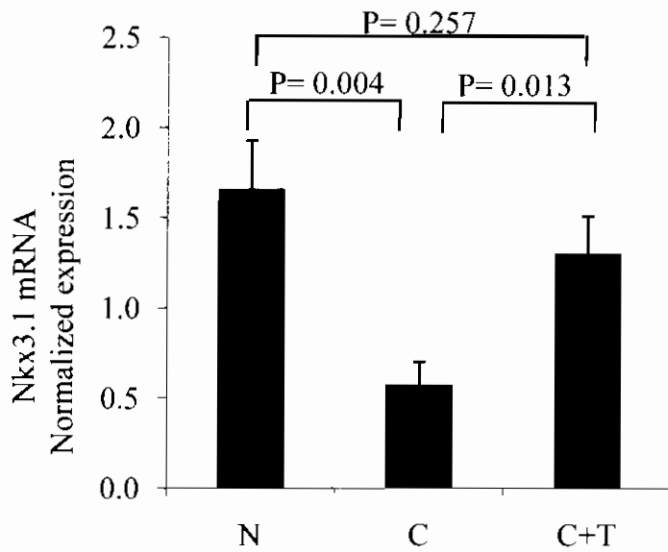
Fig. 5. Nkx3.1 mRNA expression in the prostate of the mouse after castration and androgen administration. IDV value of each band was divided by the loading control to normalize the gel to gel variations. Loading control normalized values of Nkx3.1 were again normalized with loading control normalized value of GAPDH. These values were then plotted for Nkx3.1. N= Normal, C= Castrated, C+T= Castrated and treated with testosterone. The data represents mean ± SEM, (n= 6). P-value shows the level of significance.

VI.4. Effect of castration and testosterone treatment on expression of RNase L mRNA

RNase L mRNA expression in the normal (N), castrated (C) and castrated & androgen treated (C+T) mouse prostates was analysed in the six independent sets of experiments (Fig. 4, Exp. 1-6) conducted at different times. Each experiment contained one normal (N), one castrated and one castrated & androgen treated (C+T) mice. The expression was found to vary in different sets of experiments. The experiment 3 and 4 showed a relative increase in the RNase L mRNA expression from the castrated mouse (C) to the normal mouse (N) prostate while the experiments 1, 2, 4 and 5 showed nearly no difference in RNase L mRNA levels. The experiments 1, 3, 4 and 5 showed a relative decrease in the expression of RNase L mRNA after testosterone replacement (C+T), when compared to the respective castrated mice (C) controls. After statistical analysis of the relative IDVs (RNase L/GAPDH) of all the experiments combined it was found that there was a decrease of approximately 35% in the RNase L mRNA level in the C+T when compared to the N. Although, when the two values (N vs C+T) were tested for significance by using t-test, the value was found to be more than 0.05 thus it is insignificant. None or very little difference (-6.4%) was found between the N and C (Fig. 6, Table 2). The variations in the results of different experiments could be due to physiological, genetic, experimental handling or environmental factor. Therefore, if at all anything, RNase L mRNA expression in the prostate of the mouse under in vivo conditions may be either not influenced by testosterone or it may be potentially negatively influenced. Next, it was therefore investigated, if mouse RNase L gene promoter has any androgen receptor (AR) binding site.

VI.5. Mouse RNase L gene promoter sequence analysis for Androgen Receptor binding site

Mouse RNase L gene promoter sequence was obtained from the NCBI gene database (http://www.ncbi.nlm.nih.gov/gene/24014). The sequence from -1 to -1661 of the mouse RNase L gene with reference to the transcriptional start site (+1) was downloaded and used to look for any possible androgen receptor consensus binding site. The AR binding consensus sequence is comprised of two 6-bp asymmetrical elements separated by a 3-bp spacer, 5'-AGAACAnnnTGTTCT-3' (TRANSFAC database, http://www.gene-regulation.com/cgi-bin/pub/databases/transfac/search.cgi).   This

Table 2. Paired t-test of normalized values for RNase L using software Sigmaplot 8.0.

	Mean ±SEM	P- Value	% Change compared to N
N	0.732±0.204	Vs C=0.704	0.0
		Vs C+T=0.216	
C	0.685 ±0.107	Vs N=0.704	-6.4
		Vs C+T=0.189	
C+T	0.475±0.103	Vs N=0.216	-35.0
		Vs C=0.189	

N= Normal, C= Castrated, C+T= Castrated and treated with testosterone
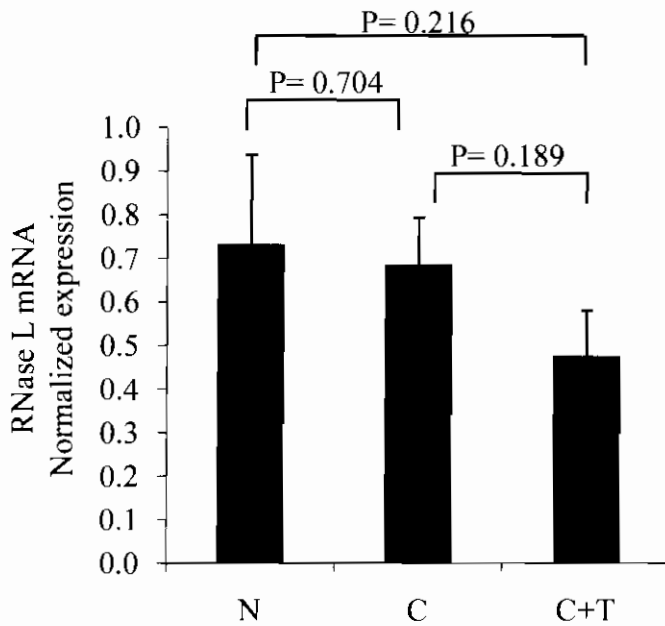
Fig. 6. RNase L mRNA expression in the prostate of the mouse after castration and androgen administration. IDV value of each band from RT-PCR gel was divided by the loading control to normalize. Loading control normalized values of RNase L were again normalized with loading control normalized values of GAPDH. These values were then plotted for RNase L. N= Normal, C= Castrated, C+T= Castrated and treated with testosterone. The data represents mean ± SEM (n= 6). P-value shows level of significance.

consensus sequence was aligned with the mouse RNase L promoter sequence using align online software (http://www.ebi.ac.uk/Tools/psa/emboss_water/nucleotide.html). One such partial consensus sequence was found from the -51 to -63 nucleotide of the promoter region (sequence) of mouse RNase L gene. This sequence is identical in one of the two 6-bp asymmetrical elements separated by a 3-bp spacer i.e. AGAACA. Three nucleotides of the other asymmetrical element are also identical, having three spacer nucleotides (Fig. 7). This, therefore, seems to be like a partial AR binding sequence. Next, the study was undertaken in the human prostate cancer cells. Two such cell lines were selected DU145 (androgen-unresponsive) and the 22Rv1 (androgen-responsive) cell lines. It was investigated whether RNase L gene expression is influenced by androgen in these two types of human prostate cancer cell lines. Phase contrast picture of the two cells seeded at low density is given in Fig. 8.

VI.6. Growth curve of DU145 cells

Growth curve of DU145 cells was plotted using MTT assay. About 5000, 10000, 20000 and 40000 cells/well were seeded in triplicates in 24 well plates for 24 hr, 48 hr, and 72 hr time period of cell growth and proliferation. After completion of each time point the MTT assay was carried out as described in the methods, The cells showed nearly 1.5 fold growth up to 48 hr and nearly 2.5 fold growth up to 72 hr compared to 24 hr (Table 3). The cells at all the four cell densities showed linear growth up to 48 hr while at 72 hr time point, the wells seeded at 40000 cells/well started showing decrease in growth. The cells seeded at 5000, 10000 and 20000 cells/well showed near linear growth up to 72 hr (Fig. 9). Next, the cell growth/proliferation was checked in response to androgen treatment.

VI.7. Effect of testosterone on growth curve of DU145 cells

DU145 cells were seeded at the density of 10000 cells per well of 24 well plates in triplicates. After 24 hr the media was removed and the cells were treated with, 10 nM and 100 nM of testosterone in the culture media having 10% dextran-charcoal treated foetal bovine serum in the RPMI-1640. The cells did not show any statistically significant (based on p-value) difference in cell growth at 24 hr, 48 hr or 72 hr (Table 4, Fig. 10). This showed that DU145 human prostate cancer cells are androgen-independent with respect to cell growth/proliferation.

```
(-1661)
AGAACTCTCAGATCTGCCTGCACCATGCCTGCCTGGATACTGCCATGCTCCCACCTTGA
TGATAATGGACTGAACCTCTGAATCTGTAAGCCAGCCCCAATTAAATGTTGTTTTATTA
AGACTTGCCTTGGTCATGGTGTCTGTTCACAGCAGTAAAACCCTAACTAAGACACTATG
TTTACCCCACAGAGTGGCACTATTAGGAGGTGAGGCCTTGTTGGAGTAGGTGTGTCACT
GTGGGCATGGGATTTAAGACCCTCATCCTAGCTACCTGAGAGCAAGTCTTTTCCTAGCA
GCCTGAAGATAAAGATGTAGAATTCTCGACTCTTCCTGCACCATGCCTGCCTGGACACT
GCCATGCTCCCACCTTGATGATAATGGACTGAATCTCTGAACCTGTAAGCCAGTCCTAA
TTAAATGTCCTTATAAGACTTGCCTTGGTCATGGTGTGTGTTCACAGCAGTAAATTCTA
AGACAAGATGGCTACATAGTAGATTGTGCGTTCATTTCCTTGTTTCCTTCCAAGAACAC
AGGCGACTTGTGATAACAGAGAAGGCACAAGCCTATCATATCTGTCCTCTGAGGTCAGG
GGACAGCCCTTGTCTTCCTCCAGGAGGTGAAGATTGCTCAGGCTGTGCCCGGATTGACG
CTGCACCCATGACTTCTGTTCTTCCGTTTTCTCACTCCTTTCTTGGCTCCTCCCTGATG
GCTCAGCGACTCACCACAAGGAAGCATTTTCTGTAGGGGTTGTTGCAGCCAAAGGAATG
CCTGCTGAGAAGAGGAGTAGAAGGTAGGCTAGAGGAGAGCTGGCTGTGGAGGTGTTCCT
TGCCTAATCTCTCTCAGCCTGGGTCGGGGCAAGGATGAAGAGGTCTGGAGGACTGGGGA
GCTGGGACTGATAGCAACTTGGCTGTGTCCCTGTGCTCCTAAGCGCTTCCACGGGTGCT
GTCACGGTTCTTACACTGTTTATTTATGTCCTCTGCTTCTGGCGCAGCTCTGAACCGAG
GAAGGAGAAAATGAAAGTGAGCTCGGGCTTGTTTGCTGCAGGGCTCTGTTCTGGAGTGG
GCTTTTCCCTCCCATATCAGAGTCCCCTGATTTTCTTCCCTCCTCTGTTCTTTTCATTA
CACCAACTCACCTCACAGCCAGTGGCAGTTAGGACCCATTACACAAATGCTTTGGACAA
CAACTTTGGTGCTTCGTATTCAGAATATACTGCAGATGTAGATCTCAGAGAATGAGGTT
TTGCACAGTTTGTAGCAGATACAGCTATTTAGATGTTCAGGTTAACAAGGGGTGCCTGA
TGAGTGAACCTGGAGCTAAGTGAGGCCCCTGGGCTAAATGGCACTCCCTGCAGTGGTGA
GTGGGTGTGGGGGGAGTATTTGCTATATTCCCTAAGACACTGTCTGCAATGGCCCTGTT
TACTGTTGTCCTCCGATGAGGAAACAAAATTGTGAGTCAGCCATTTATGAATGTGCAAT
GAGGAAGTGACAGCCAAAAGTTGCATTCCCAGAAACTCAAAGCTGAGTTCGTACTTCAA
CTTTCTTTTTTCAACCGCACTGCTTCAATAAAAACTCGCAGGGGGACGGAGAGAACGAA
CAGAA**AGAACAGTGTGT**GGGGGTGACCAGCCTCACCTGGGATAAAGTCAGATGGACCAA
GATTACCAG(-1)
```

AR consensus Sequence= AGAACAnnnTGTTCT


```
EMBOSS_001      -63 AGAACAGTGTGT  -51
                    | || ||| ··· |||
EMBOSS_001       1 AGAACAnnnTGT  12
```


Fig. 7. Possible presence of androgen receptor (AR) consensus
sequence in mouse RNase L promoter sequence. The mouse RNase L
promoter sequence (NP_036012.1) was analyzed by the EBI EMBOSS
bioinformatics tool to find possible AR binding sites.
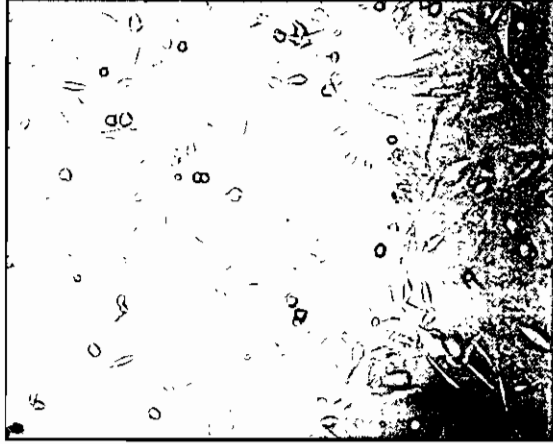
Fig. 8. Phase contrast micrograph of A. DU145 and B. 22Rv1 human prostate cancer cells. (100X magnification).

Table 3. Growth of DU145 prostate cancer cells in 24 well plate at different cell densities for 24, 48 and 72 hr by MTT assay. The OD 590 nm is shown for triplicate wells.

24 hr

Cells/well	OD$_{590}$	OD$_{590}$	OD$_{590}$	Mean ±SEM	Fold Induction
5000	0.148	0.154	0.179	0.160±0.009	1.00
10000	0.329	0.340	0.322	0.330±0.005	1.00
20000	0.694	0.721	0.740	0.718±0.013	1.00
40000	1.369	1.440	1.338	1.382±0.030	1.00

48 hr

Cells/well	OD$_{590}$	OD$_{590}$	OD$_{590}$	Mean ±SEM	Fold Induction
5000	0.238	0.266	0.309	0.271±0.021	1.69
10000	0.540	0.543	0.602	0.562±0.020	1.70
20000	1.071	1.047	1.090	1.069±0.012	1.48
40000	1.833	1.874	1.820	1.842±0.016	1.33

72 hr

Cells/well	OD$_{590}$	OD$_{590}$	OD$_{590}$	Mean ±SEM	Fold Induction
5000	0.437	0.441	0.418	0.432±0.007	2.70
10000	0.830	0.853	0.850	0.844±0.007	2.55
20000	1.471	1.439	1.449	1.453±0.009	2.02
40000	2.123	2.102	2.083	2.103±0.012	1.52

A.

B.
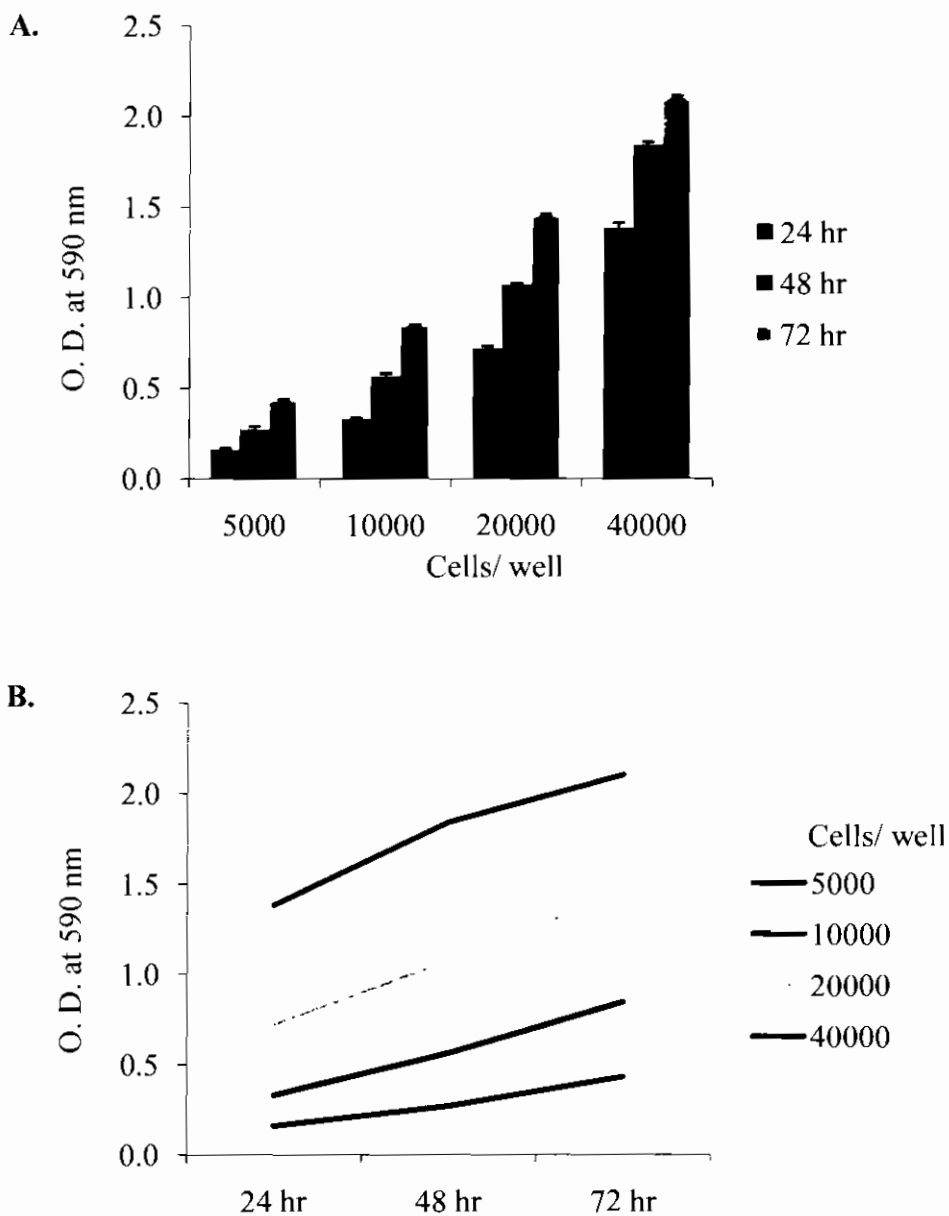
Fig. 9. Growth of DU145 human prostate cancer cells in 24 well plate at different cell densities for 24, 48 and 72 hr by MTT assay. The data represents Mean ± SEM (n= 3) from triplicate wells in A and B.

Table 4. Growth of DU145 cells at cell density of 10000 cells, in 24 well plate, after 0 nM, 10 nM and 100 nM testosterone (T) treatment for 24, 48 and 72 hr by MTT assay. OD at 590 nm values are shown for triplicate wells

24 hr

OD_{590}\T nM	Control	10 nM	100 nM
	0.530	0.562	0.626
	0.624	0.571	0.579
	0.608	0.604	0.558
Mean ±SEM	0.587 ±0.029	0.579 ±0.012	0.588 ±0.020
Fold Induction	1.00	0.98	1.00

48 hr

OD_{590}\T nM	Control	10 nM	100 nM
	0.780	0.824	0.923
	1.014	1.175	1.183
	0.950	1.272	0.922
Mean ±SEM	0.915 ±0.069	1.090 ±0.136	1.009 ±0.086
Fold Induction	1.0	1.19	1.10

72 hr

OD_{590}\T nM	Control	10 nM	100 nM
	1.478	1.538	1.264
	1.428	1.192	1.184
	1.410	1.279	1.207
Mean ±SEM	1.439 ±0.020	1.336 ±0.103	1.218 ±0.023
Fold Induction	1.00	0.92	0.84

Fig. 10. Growth of DU145 human prostate cancer cells at cell density of 10000 cells/well, in 24 well plate after 10 nM and 100 nM testosterone treatment for 24, 48 and 72 hr by MTT assay. The data represents mean± SEM (n= 3) from triplicate wells from A and B.

VI.8. Growth curve of 22Rv1 cells

Growth curve of 22Rv1 cells was plotted using MTT assay. About 5000, 10000, 20000 and 40000 cells/well were seeded in triplicates in 24 well plate for 24 hr, 48hr, and 72hr time periods. After completion of each time point, the MTT assay was carried out as described in the methods. Cells showed growth upto 2.7 fold at 48 hr and up to 2 fold at 72 hr (Table 5). Cells seeded at a density of 5000 cells per well of the 24 well plate did not grow at all, thus showing the density-dependent growth of this cell line. Cells at the all other densities (10000, 20000 and 40000) showed linear growth up to 48 hr. At 72 hr all the cell densities showed a little decline in growth suggesting some factors other than the contact inhibition/ confluency was a limiting factor after 48 hr in the growth of these cells (Fig. 11).

VI.9. Effect of testosterone on growth curve of 22Rv1 cells

The 22Rv1 cells were seeded at a cell density of 20000 cells per well of 24 well plate in triplicates. After 24 hr the media was removed and the cells were treated with 10 nM and 100 nM of testosterone in the culture media having 10% dextran-charcoal treated foetal bovine serum in the RPMI-1640 medium. After 24 hr, the difference in the cell growth of the control to the 10 and 100 nM testosterone-treated cells was clearly observed (1.2 fold), which further increased at 48 and 72hr to nearly 1.5 fold (Table 6). There was not any difference in the growth of cells with respect to 10 nM and 100 nM testosterone treatment at 48 and 72 hr, while at 24 hr 100 nM testosterone treatment had slightly higher growth compared to 10 nM testosterone treated cells, indicating the possibility of comparatively faster action of testosterone at the higher concentration. Not much cell growth was observed in the testosterone untreated cells from 24 hr to 72 hr time points indicating that testosterone is required for normal growth of the 22Rv1 cells (Fig. 12). Thus 22Rv1 is a testosterone-dependent human prostate cancer cell line. Next, the effect of testosterone on the RNase L mRNA expression was checked.

VI.10. Effect of testosterone on the expression of RNase L mRNA in DU145 and 22Rv1 cells

Based on the growth curve of the DU145 and 22Rv1 cells/well, 10000 cells for DU145 and 200000 cells/well for 22Rv1 cells were considered as suitable cell densities for 24 well plate. The experiments of RNase L mRNA expression analysis was carried
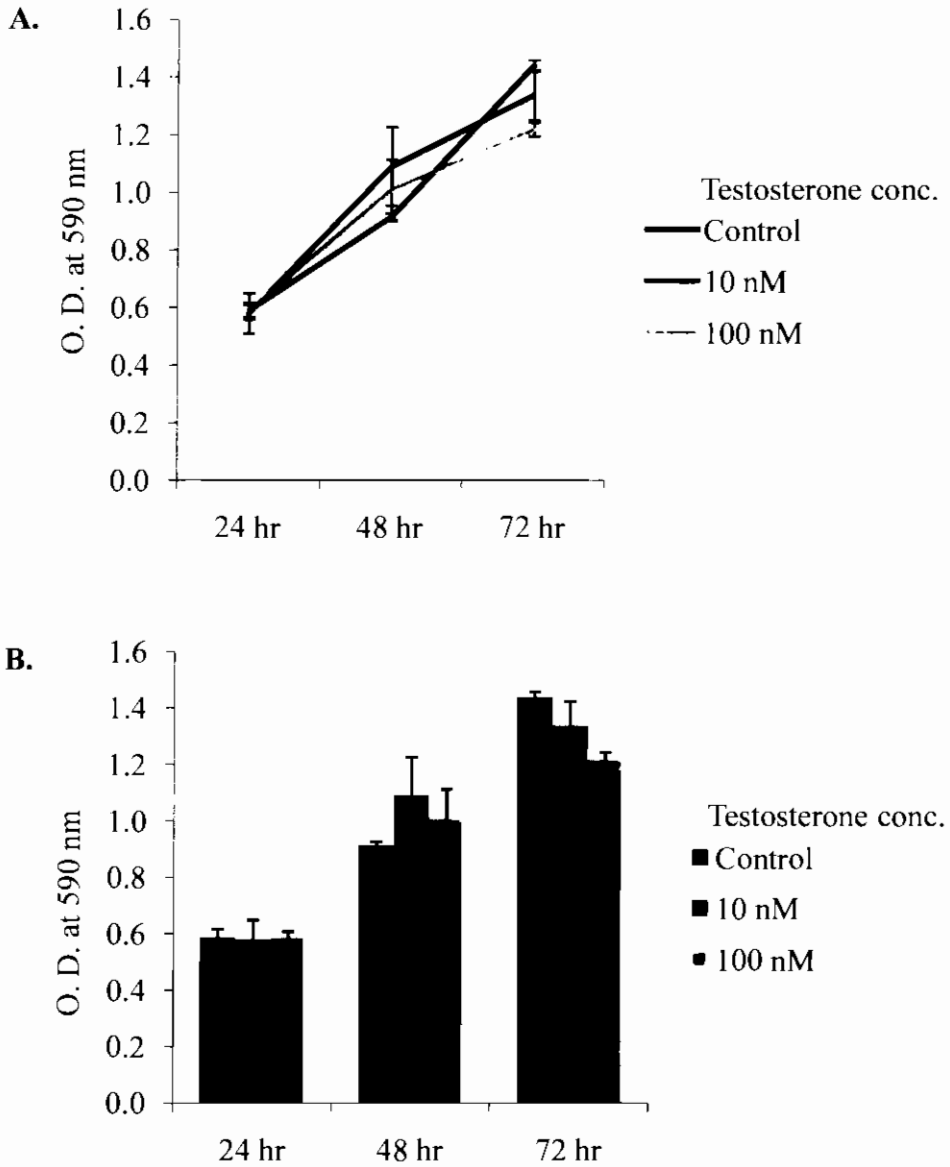
Table 5. Growth of 22Rv1 human prostate cancer cells at different cell densities in 24 well plate for 24, 48 and 72 hr by MTT assay. The data represents triplicate wells

24 hr	Cells	OD_{590}	OD_{590}	OD_{590}	Mean ±SEM	Fold Induction
	5000	0.025	0.015	0.016	0.019±0.003	1.00
	10000	0.159	0.180	0.133	0.157±0.014	1.00
	20000	0.591	0.496	0.500	0.529±0.031	1.00
	40000	1.184	1.148	1.081	1.138±0.030	1.00
48 hr	5000	0.015	0.030	0.030	0.025±0.005	1.31
	10000	0.430	0.466	0.388	0.428±0.023	2.72
	20000	1.218	1.078	1.172	1.156±0.041	2.18
	40000	1.895	2.004	1.915	1.938±0.034	1.70
72 hr	5000	0.038	0.035	0.040	0.038±0.001	2.00
	10000	0.454	0.552	0.456	0.487±0.032	3.01
	20000	1.456	1.271	1.319	1.349±0.055	2.55
	40000	2.252	2.228	2.320	2.267±0.028	1.99
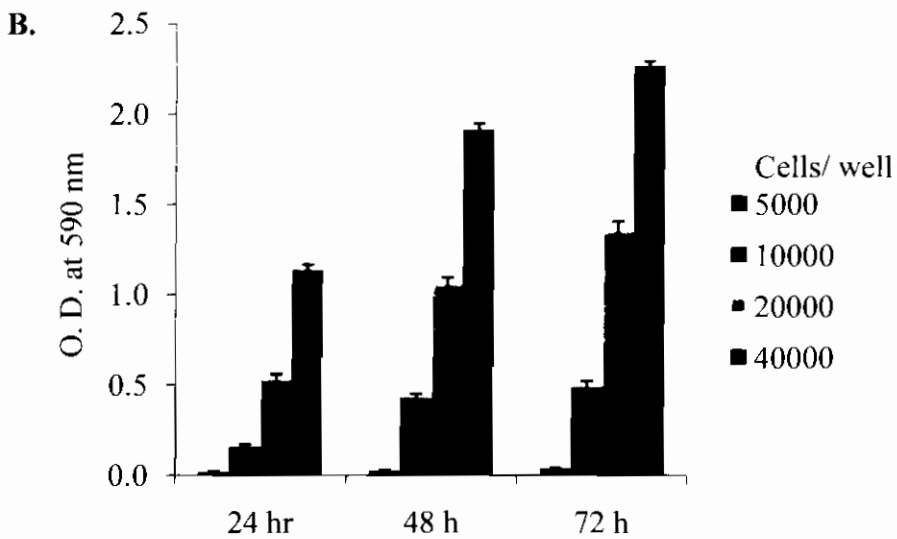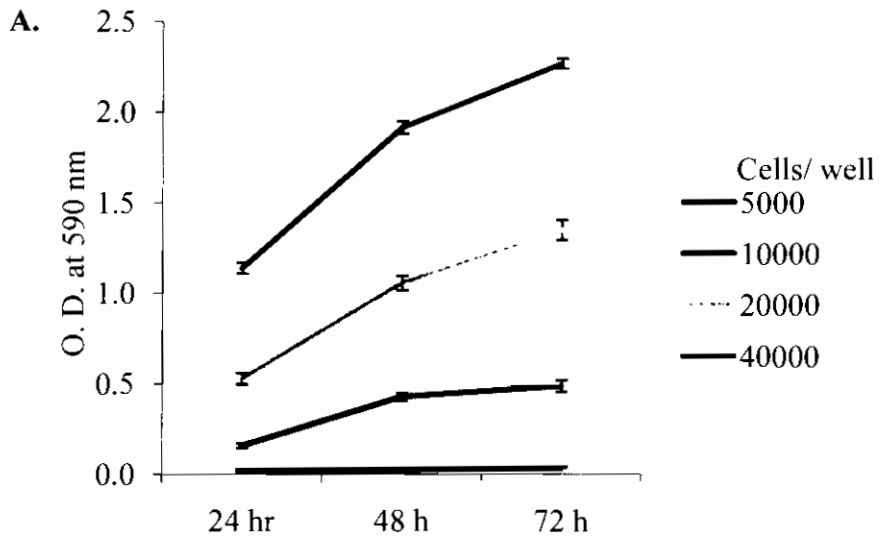
Fig. 11. Growth of 22Rv1 human prostate cancer cells at different cell densities in 24 well plate for 24, 48 and 72 hr by MTT assay. The data represents mean ± SEM (n= 3) from triplicate wells in A and B.

Table 6. Growth of 22Rv1 human prostate cancer cells at cell density of 20000 cells/well, After 10 nM and 100 nM testosterone treatment for 24, 48 and 72 hr.

	T	OD_{590}	OD_{590}	OD_{590}	Mean ±SEM	Fold Induction
24 hr	Control	0.872	0.806	0.786	0.821±0.026	1.00
	10 nM	0.927	0.904	0.968	0.933±0.019	1.13
	100 nM	0.831	1.029	1.118	0.993±0.085	1.20
48 hr	Control	0.900	0.829	1.087	0.939±0.077	1.00
	10 nM	1.315	1.324	1.361	1.333±0.014	1.41
	100 nM	1.356	1.328	1.411	1.365±0.024	1.45
72 hr	Control	0.958	0.971	0.996	0.975±0.011	1.00
	10 nM	1.407	1.434	1.387	1.409±0.014	1.44
	100 nM	1.395	1.389	1.491	1.425±0.033	1.46

T= Testosterone
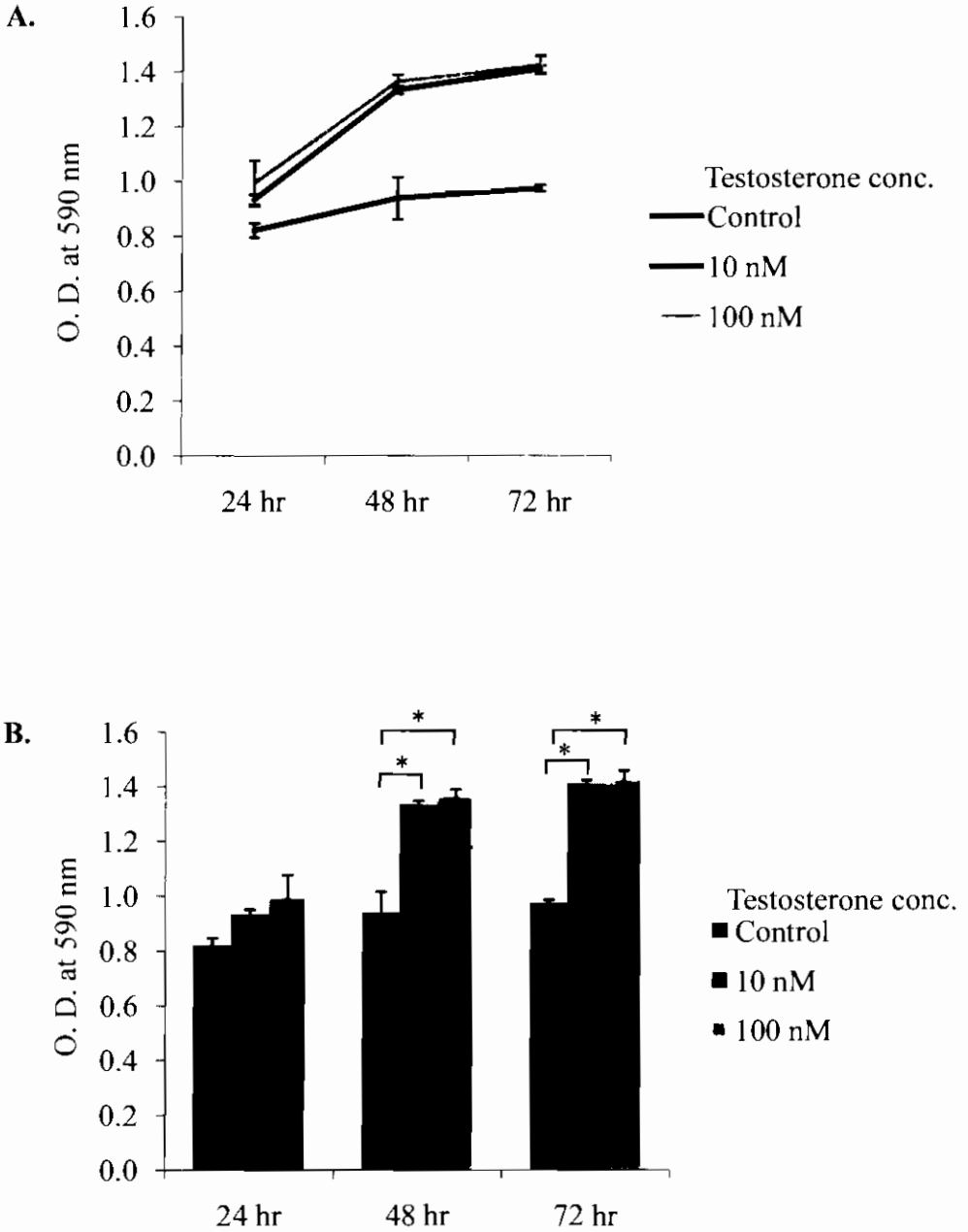
Fig. 12. Growth of 22Rv1 human prostate cancer cells at cell density of 20000 cells/well, after 10 nM and 100 nM testosterone treatment for 24, 48 and 72 hr. The data represents mean ± SEM from triplicate wells in A and B. * Shows P-value < 0.05.

out in 6 well plate. Each well of 24 well plate contain 2 cm^2 area while each well of 6 well plate contains 10 cm^2 area for cell growth. Thus to upscale the experiment, 50000 cells of DU145 and 100000 cells of 22Rv1 were seeded in each well of 6 well plate. After seeding the cells were allowed to adhere and grow for 24 hr. After 24 hr, the media was replaced with the androgen-treated media (RPMI-1640 with 10% dextran-charcoal treated FBS and 1X antibiotics) having either no testosterone or 10 nM testosterone for a period of 48 hr. After 48 hr, the cells were lysed in the Tri-Reagent and total RNA was isolated. After preparing first strand from the total RNA of each sample, PCR analysis for the RNase L mRNA expression and GAPDH mRNA expression was carried out (Fig. 13). From the densitometry of RT-PCR band, IDV of RNase L mRNA amplicon of 644 bp was normalized with corresponding IDV of GAPDH amplicon of 452 bp to find out the relative expression. The statistical analysis (t-test using Sigma plot) showed that, after treatment with 10 nM testosterone, the mRNA level of RNase L did not show any significant change (P=0.325). While 22Rv1 cells showed statistically significant decrease (0.46 fold) in the RNase L mRNA level after treatment with 10 nM testosterone for 48 hr (P= 0.029) (Table 7 and Fig. 14). Therefore, testosterone negatively regulated RNase L mRNA expression in 22Rv1 human prostate cancer cells.

VI.11. Effect of testosterone on expression of RNase L protein in DU145 and 22Rv1 cells

About 50000 cells of DU145 and 100000 cells of 22Rv1 were seeded in each well of 6 well plate. After seeding the cells were allowed to adhere and grow for 24 hr. After 24 hr, the media was replaced with the treatment-media (RPMI-1640 with 10% dextran-charcoal treated FBS with antibiotic) having 10 nM testosterone for a period of 48 hr. After 48 hr the cells were mildly trypsinized and scraped in ice cold 1X PBS. The cells were washed in PBS and centrifuged at 2000 rpm for 3 min to remove the medium. The protein extract was made as described in the methods. Equal quantities of the protein extracts (30 µg) were used to analyse the expression of RNase L protein by immunoblot analysis using an anti-human RNase L monoclonal antibody in the 10 nM testosterone-treated DU145 and 22Rv1 cells. DU145 cells treated with no testosterone and 10 nM testosterone showed the RNase L protein bands of nearly 83 kDa of nearly equal intensities, thereby showing no effect of testosterone-treatment on the RNase L protein level. While 22Rv1 cells, which have much higher level of endogenous RNase L protein compared to DU145 cells, showed a decrease in RNase L protein level after 10 nM
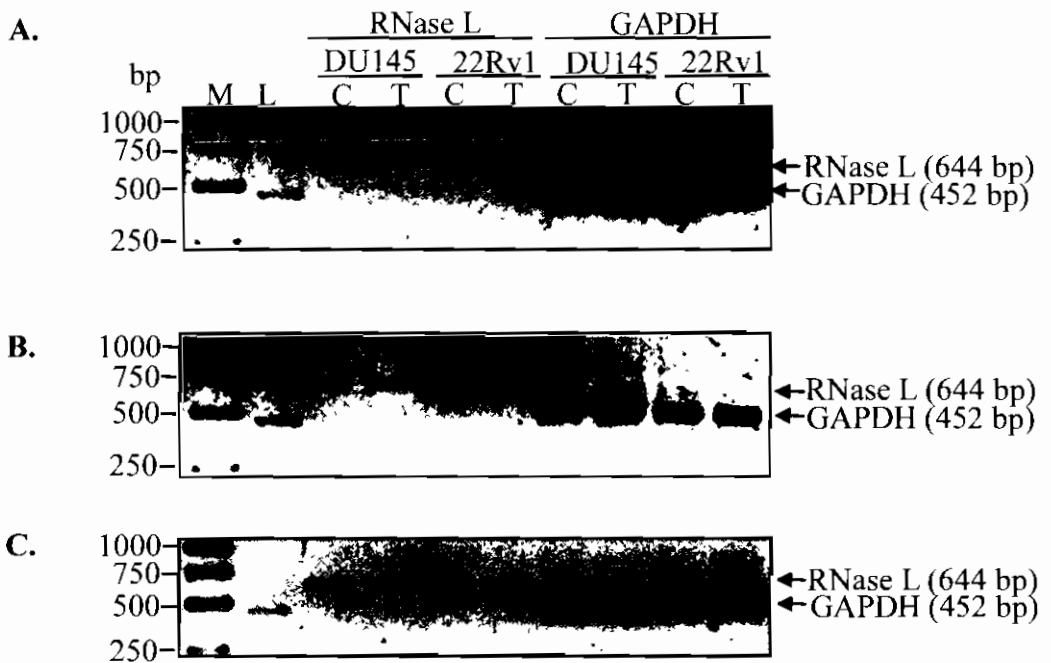
Fig. 13. Expression of RNase L and GAPDH mRNAs as measured by RT-PCR in DU145 and 22Rv1 human prostate cancer cells after testosterone treatment for 48 hr without (control, C) or with (testosterone treated, T) 10 nM testosterone. A, B and C represents three independent experiments. LC: Loading control (20 ng) of a 462 bp for densitometry. M: Molecular size marker

Table 7A. From the RT-PCR experiments shown in Fig. 12, the IDV value of each band was divided by the loading control to normalize the variation. The loading control normalized values of RNase L were again normalized with the loading control normalized values of GAPDH. These values were then plotted for RNase L. C= Control, T= Treated with 10 nM testosterone

	RNL	GAPDH	LC	RNL/LC	GAPDH/ LC	RNL/ GAPDH
DU-C1	14700	66885	22675	0.648	2.950	0.220
DU-T1	11760	65415	22675	0.519	2.885	0.180
Rv-C1	25050	72030	22675	1.105	3.177	0.348
Rv-T1	9555	68355	22675	0.421	3.015	0.140
DU-C2	18375	57330	22675	0.810	2.528	0.321
DU-T2	18375	66150	22675	0.810	2.917	0.278
Rv-C2	30870	61740	22675	1.361	2.723	0.500
Rv-T2	14905	64680	22675	0.657	2.852	0.230
DU-C3	20240	53130	21505	0.941	2.471	0.381
DU-T3	15180	55660	21505	0.706	2.588	0.273
Rv-C3	29095	51865	21505	1.353	2.412	0.561
Rv-T3	16505	59455	21505	0.767	2.765	0.278

C= Control, T= Treated with 10 nM testosterone, RNL= RNase L. C1, T1; C2, T2 and C3, T3 represents three independent experiments (Set 1-3).

Table 7B. Summary of the three experiments

	Set 1	Set 2	Set 3	Mean ±SEM	Fold Change	P- Value
DU-C	0.220	0.321	0.381	0.307±0.047	0.79	0.325
DU-T	0.180	0.278	0.273	0.243±0.032		
Rv-C	0.346	0.500	0.561	0.469±0.064	0.46	0.029
Rv-T	0.140	0.230	0.278	0.216±0.040		

Fig. 14. From the experiments shown in fig. 12 and table 7, IDV value of each band was divided by the loading control to normalize the variation. Loading control normalized values of RNase L were again normalized with loading control normalized values of GAPDH. The final values were then plotted for RNase L. C= Control, no testosterone, T= Treated with 10 nM testosterone. DU= DU145 cells, Rv= 22Rv1 cells.
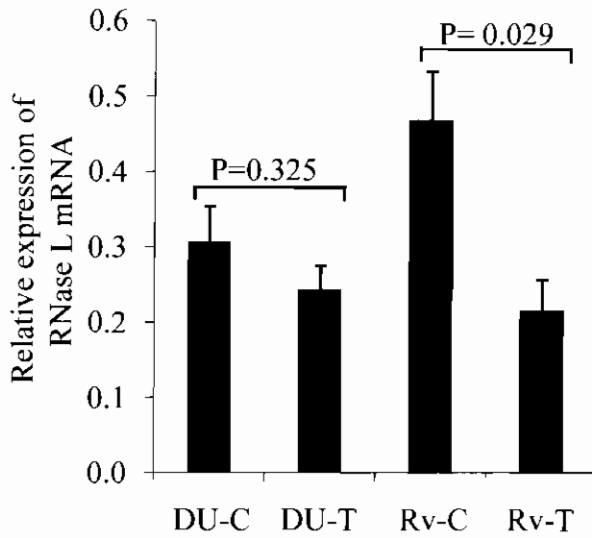
testosterone treatment after 48 hr. The control (no testosterone-treated) 22Rv1 cells also showed 2 extra bands, one slightly higher and one slightly lower than the 80 kDa RNase L protein. These two bands could be different forms of the RNase L due to post translational modifications (Fig. 15). This showed that RNase L protein expression is negatively influenced by exogenous androgen in 22Rv1 cells. Next, it was investigated if H_2O_2 treatment of the cells showed any effect on RNase L expression.

VI.12. Effect of hydrogen peroxide on growth curve of DU145 cells

DU145 cells were seeded at a density of 10000 cells per well of 24 well plate in triplicates. After 24 hr, the medium was removed and the cells were treated with 5 μM and 50 μM of H_2O_2 in the culture media having 10% foetal bovine serum in the RPMI-1640 for the time points of 24, 48 and 72 hr. At these time points the cells did not show any statistically significant (based on p-value) difference in the cell growth at 24 hr, 48 hr or 72 hr (Fig. 16 and Table 8). In another experiment, when the 10,000 DU145 cells/well of 24 well plate were treated with 200 μM H_2O_2, nearly all the cells were found to be dead (data not shown). Thus it was concluded that while 50 μM did not show any effect at 24 hr and 200 μM showed nearly 100% cell death, the effective concentration should be somewhere in between 50 to 200 μM within 24 hr. Then it was decided to use a higher cell density of 20000 cells per well and the H_2O_2 concentrations of 100 and 200 μM for a time period of 2, 4, 6 and 8 hr. At 2 hr and 4 hr both 100 and 200 μM H_2O_2 showed negative cell growth by MTT assay. But at 6 and 8 hr time points the cells treated with 100 μM H_2O_2 showed some recovery in cell growth, while the cells treated with 200 μM H_2O_2 showed a further decrease in the MTT assay (Fig. 17). Thus from this experiment it was found that 200 μM of H_2O_2 for 4 hr is suitable concentration and time period respectively for further study of H_2O_2 mediated oxidative stress. The extent of cell growth inhibition at 200 μM was 0.68 fold at 2 hr, 0.45 fold at 4 hr, 0.18 fold at 6 hr and 0.16 fold at 8 hr (Table 9).

VI.13. Effect of hydrogen peroxide on growth curve of 22Rv1 cells

Taking advantage of the experience gained in the H_2O_2 treatment of DU145 cells, the experiment was designed to use 0, 50, 100 and 200 μM of H_2O_2 for a time period of 2, 4, 6 and 8 hr. 22Rv1 cells were seeded at a density of 20000 cells per well of 24 well plate in triplicates. After 24 hr the media was removed and the cells were treated with 50 μM, 100 μM and 200 μM of H_2O_2 in culture media having 10% bovine serum in RPMI-
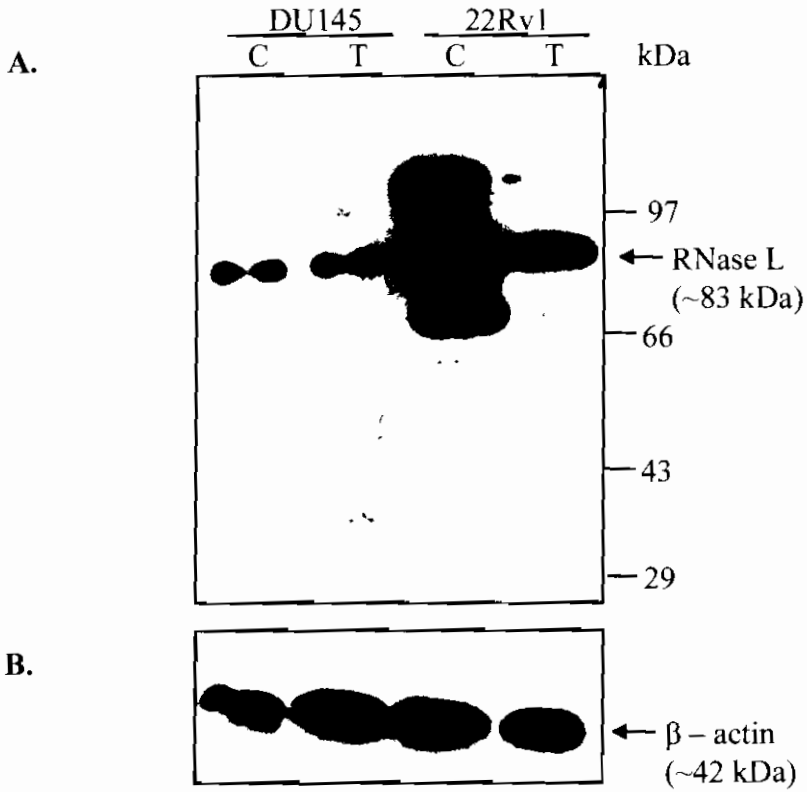
Fig. 15. A. Expression of RNase L, protein in DU145 and 22Rv1 human prostate cancer cells after 48 hr treatment with 10 nM testosterone (T), control, C= without T. 30 µg protein extract of the cells were resolved in 10% SDS-PAGE and immunoblotted against anti-human RNase L monoclonal antibody. B. Anti β-actin immunoblot.

Table 8. Treatment of DU145 human prostate cancer cells (10000 cells/well in 24 well plate) with different doses of H_2O_2. The data represents mean ± SEM of triplicate wells

	H_2O_2	OD_{590}	OD_{590}	OD_{590}	Mean ±SEM
24 h	Control	1.068	1.022	0.867	0.985±0.060
	5 μM	1.051	0.937	0.887	0.958±0.048
	50μM	0.982	0.91	1.112	1.001±0.059
48 hr	Control	1.351	1.508	1.539	1.466±0.058
	5 μM	1.485	1.444	1.531	1.486±0.025
	50 μM	1.531	1.495	1.517	1.514±0.010
72 hr	Control	1.889	1.863	1.714	1.822±0.054
	5 μM	1.922	1.81	1.84	1.857±0.033
	50 μM	1.885	1.896	1.691	1.824±0.066

Fig. 16. Treatment of DU145 human prostate cancer cells (20000 cells/well in 24 well plate) with different doses of H_2O_2

Table 9. Treatment of DU145 human prostate cancer cells (20000 cells/well in 24 well plate) with different doses of H_2O_2. The data represents mean ± SEM for triplicate wells.

	H_2O_2	OD_{590}	OD_{590}	OD_{590}	Mean ±SEM	Fold Change	P-value
2 hr	Control	1.521	1.566	1.530	1.539±0.013	1.00	-
	100 μM	1.185	1.175	1.116	1.158±0.021	0.75	0.000
	200 μM	1.076	1.048	1.017	1.047±0.017	0.68	0.000
4 hr	Control	1.622	1.62	1.661	1.634±0.013	1.06	0.007
	100 μM	0.995	0.925	0.945	0.955±0.020	0.62	0.000
	200 μM	0.709	0.726	0.685	0.706±0.011	0.45	0.000
6 hr	Control	1.744	1.759	1.743	1.748±0.005	1.13	0.000
	100 μM	1.067	1.039	1.045	1.050±0.008	0.68	0.000
	200 μM	0.371	0.248	0.228	0.282±0.044	0.18	0.000
8 hr	Control	1.832	1.822	1.830	1.828±0.003	1.18	0.000
	100 μM	1.299	1.219	1.204	1.240±0.029	0.80	0.000
	200 μM	0.236	0.263	0.255	0.251±0.008	0.16	0.000

A.

B.
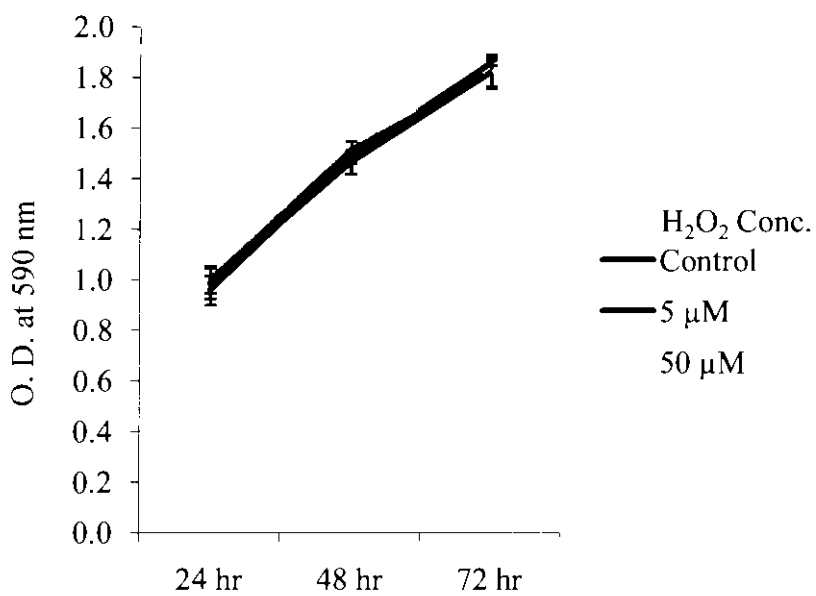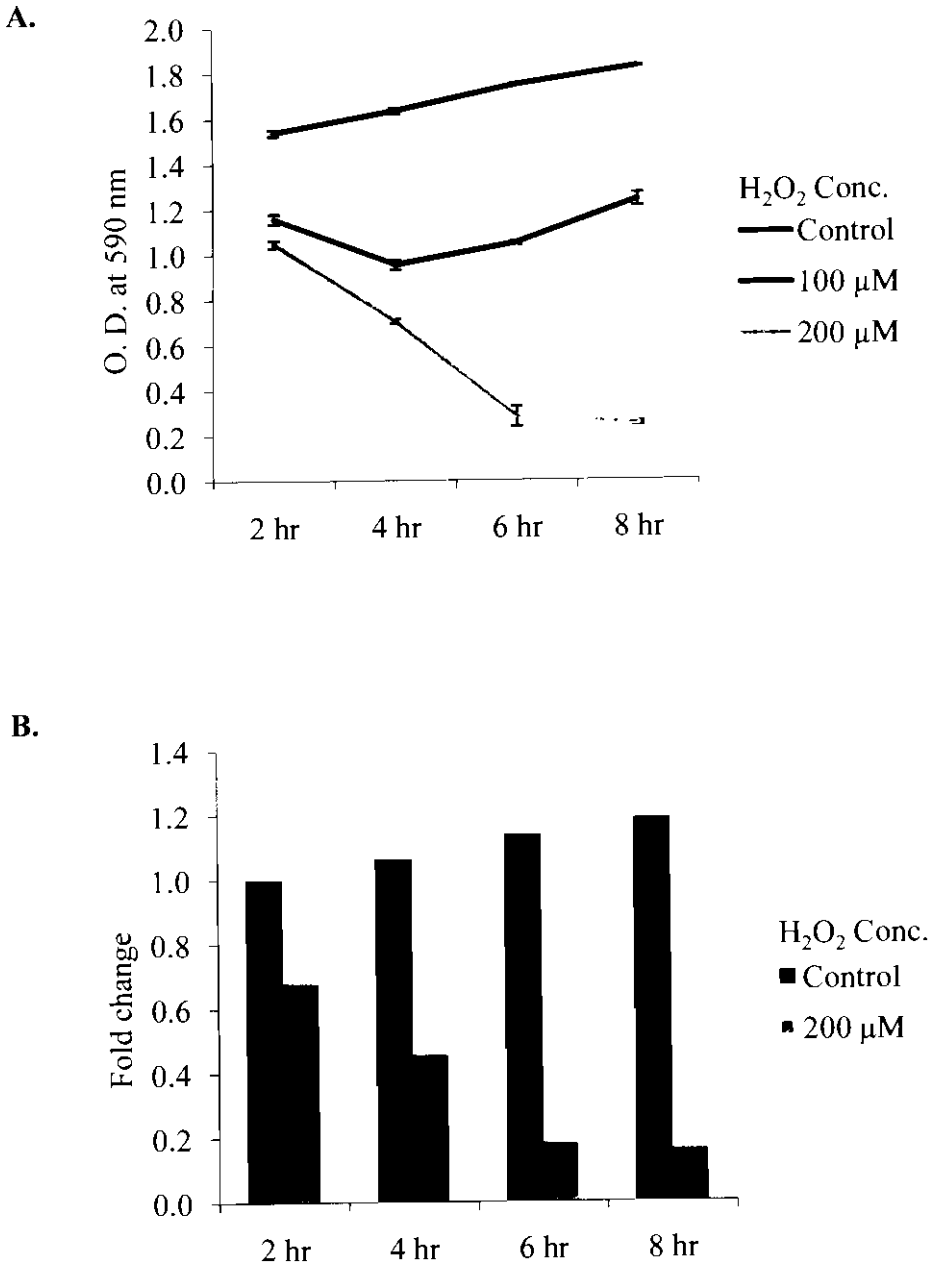

Fig. 17. Treatment of DU145 prostate cancer cells (20000 cells/well in 24 well plate) with different doses of H_2O_2. A. The data represents mean ± SEM for triplicate observations (n= 3). B. Fold inhibition of cell growth/ proliferation by H_2O_2.

1640 for the time points of 2, 4, 6 and 8 hr. The effect of H_2O_2 was evident as early as 2 hr at all concentrations, which continued upto 4 hr in all concentrations. After 4 hr, at 6 hr, at the concentrations of 50 and 100 μM, the cells started showing resistance to H_2O_2 mediated cell death (apoptosis). While cells treated with 50 μM H_2O_2 started showing the recovery of growth at 6 and 8 hr, the 100 μM H_2O_2-treated cells did not show any growth till 8 hr. The 200 μM H_2O_2 treated cells showed decreasing cell growth till 8 hr (Fig. 18). The extent of cell growth inhibition at 200 μM was 0.65 fold at 2 hr, 0.49 fold at 4 hr, 0.33 fold at 6 hr and 0.29 fold at 8 hr (Table 10).

VI.14. Effect of hydrogen peroxide on the expression of RNase L mRNA in DU145 and 22Rv1 cells

About 1×10^5 cells of DU145 and 22Rv1 cells were seeded in each well of 6 well plates. Cells were allowed to adhere and grow for the next 24 hr. After 24 hr, cells were treated with H_2O_2 diluted in PBS at final concentrations of 200 μM for 4 hr. After 4 hr, the cells were harvested and lysed in the Tri-Reagent and total RNA was isolated. After preparing the first strand cDNAs from the total RNA of each sample, PCR-analysis for the expression of RNase L mRNA and GAPDH mRNA was carried out (Fig. 19). The IDV of RNase L mRNA amplicon (644 bp) was normalized with the corresponding IDV of GAPDH amplicon (452 bp) to find the relative expression. The statistical analysis (t-test using Sigma plot) showed that after treatment with 200 μM, for 4 hr the mRNA level of RNase L was significantly increased in both DU145 (P= 0.003) and 22Rv1 cells (P= 0.027) (Fig. 20). There was an increase of 5.75 fold of DU145 and 1.51 fold for 22Rv1 in the RNase L mRNA expression in the response to H_2O_2 (Table 11A and B)

VI.15. Effect of hydrogen peroxide on expression of RNase L protein in DU145 and 22Rv1 cells

About 1×10^5 cells of DU145 and 22Rv1 cells were seeded in each well of 6 well plates. Cells were allowed to adhere and grow or next 24 hr. After 24 hr cells were treated with H_2O_2 diluted in PBS at final concentrations of 200 μM for 4 hr. After 4 hr, the cells were harvested for preparing the protein extracts for the western blot. About 30 μg of each cell extract was resolved in SDS-PAGE and transferred to the nitrocellulose membrane for western blotting against an anti-human RNase L monoclonal antibody. After developing the blot, as described in the methods section, the RNase L band at nearly 83 kDa was observed. This 83 kDa band of the RNase L protein showed up

Table10. Treatment of 22Rv1 human prostate cancer cells (20000 cells/well in 24 well plate) with different doses of H_2O_2. The data represents mean± SEM from triplicate wells

	H_2O_2	OD_{590}	OD_{590}	OD_{590}	Mean ±SEM	Fold Change	P-Value
2 hr	Control	0.761	0.731	0.712	0.735±0.014	1.00	-
	50 µM	0.652	0.663	0.691	0.669±0.012	0.91	0.022
	100 µM	0.521	0.571	0.540	0.544±0.015	0.74	0.000
	200µM	0.499	0.461	0.482	0.481±0.011	0.65	0.000
4 hr	Control	0.759	0.791	0.745	0.765±0.014	1.04	0.198
	50 µM	0.601	0.634	0.629	0.621±0.010	0.84	0.002
	100 µM	0.513	0.501	0.493	0.502±0.006	0.68	0.000
	200 µM	0.369	0.378	0.349	0.365±0.009	0.49	0.000
6 hr	Control	0.781	0.789	0.799	0.790±0.005	1.07	0.022
	50 µM	0.668	0.679	0.659	0.669±0.006	0.91	0.012
	100 µM	0.512	0.523	0.504	0.513±0.006	0.69	0.000
	200 µM	0.238	0.246	0.257	0.247±0.006	0.33	0.000
8 hr	Control	0.817	0.824	0.806	0.816±0.005	1.11	0.005
	50 µM	0.693	0.704	0.715	0.704±0.006	0.95	0.120
	100 µM	0.524	0.535	0.541	0.533±0.005	0.72	0.000
	200 µM	0.201	0.221	0.231	0.218±0.009	0.29	0.000
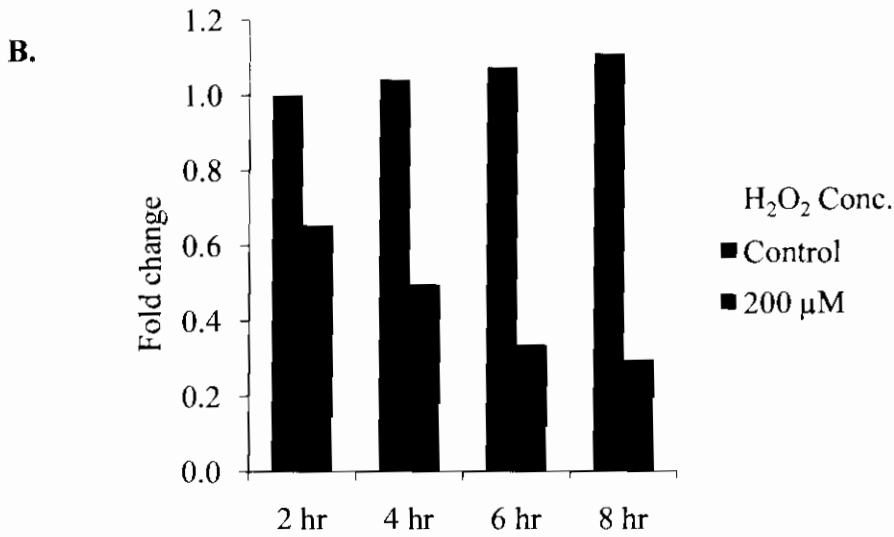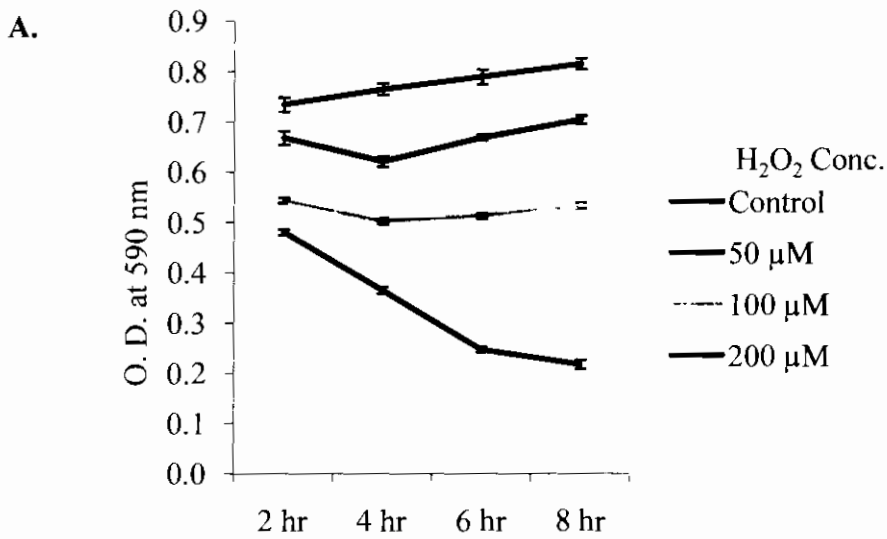
Fig. 18. Treatment of 22Rv1 human prostate cancer cells (20000 cells/well in 24 well plate) with different doses of H_2O_2. A. The data represents mean ± SEM for triplicate observation. B. Fold inhibition of cell growth/ proliferation by H_2O_2.
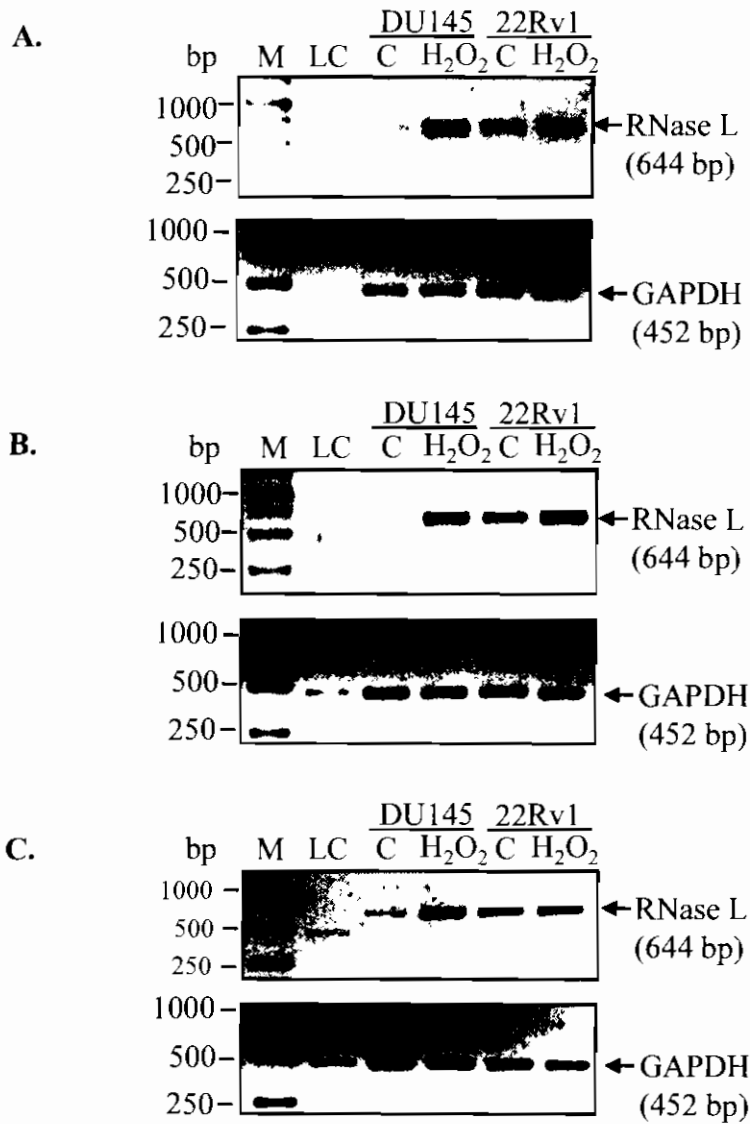
Fig. 19. Expression of RNase L and GAPDH mRNAs measured by RT-PCR in DU145 and 22Rv1 human prostate cancer cells after 4 hr treatment with 200 μM H_2O_2. A, B and C represents three independent experiments. C= Control, M= molecular size marker, LC= loading control, a 452 bp 20 ng DNA, used for densitometry.

Table 11A. From the RT-PCR experiments shown in fig. 18, the IDV value of each band was divided by the loading control to normalize the variation. The loading control normalized values of RNase L were again normalized with the loading control normalized values of GAPDH. These values were then plotted for RNase L. C= Control, H= Treated with 200 μM H_2O_2

|	RNL	LC	GAPDH	LC	RNL/LC	GAPDH/LC	RNL/GAPDH
DU-C1	6060	5684	19080	7155	1.066	2.667	0.400
DU-H1	27608	5684	20670	7155	4.857	2.889	1.681
Rv-C1	17864	5684	22260	7155	3.143	3.111	1.010
Rv-H1	36540	5684	27030	7155	6.429	3.778	1.702
DU-C2	6872	6496	29415	9540	1.058	3.083	0.343
DU-H2	39788	6496	28620	9540	6.125	3.000	2.042
Rv-C2	23548	6496	23850	9540	3.625	2.500	1.450
Rv-H2	44660	6496	32595	9540	6.875	3.417	2.012
DU-C3	6496	5684	32595	10335	1.143	3.154	0.362
DU-H3	41412	5684	28620	10335	7.286	2.769	2.631
Rv-C3	23548	5684	30210	10335	4.143	2.923	1.417
Rv-H3	35728	5684	30210	10335	6.286	2.923	2.150

C= Control, no H_2O_2, H= Treated with 200 μM H_2O_2, RNL= RNase L. C1, H1; C2, H2 and C3, H3 represents three independent experiments (Set 1-3).

Table 11B. Summary of the three experiments

	Set 1	Set 2	Set 3	Mean ±SEM	Fold Change	P- Value
DU-C	0.400	0.343	0.362	0.368±0.017	5.75	0.003
DU-H	1.681	2.042	2.631	2.118±0.277		
Rv-C	1.010	1.450	1.417	1.292±0.141	1.51	0.027
Rv-H	1.702	2.012	2.150	1.955±0.133		
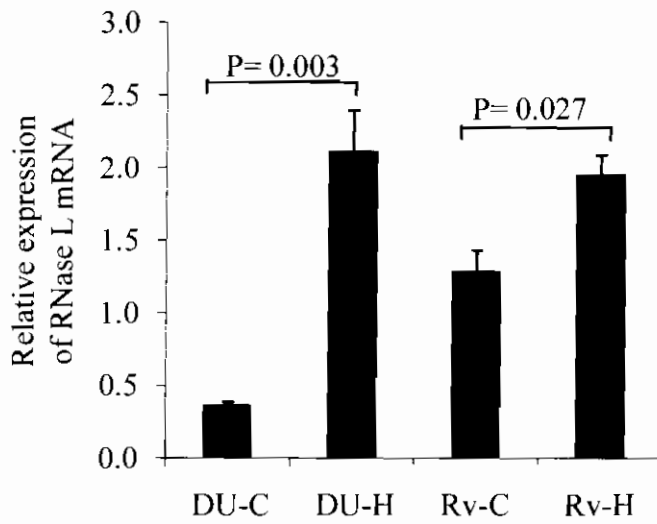
Fig. 20. Expression of RNase L mRNA in DU145 and 22Rv1 human prostate cancer cells after 4 hr treatment with 200 μM H_2O_2. DU= DU145 cells, Rv= 22Rv1 cells, C= Control, H= treated with 200 μM H_2O_2.

regulation after treatment with 200 μM H_2O_2 in both DU145 and 22Rv1 cells (Fig. 21). Another band at nearly 60 kDa was also observed, which could be an alternative form of the RNase L protein (Fig. 21). Thus H_2O_2 stimulated the expression of both RNase L mRNA and RNase L protein in both the types of the human prostate cancer cells.
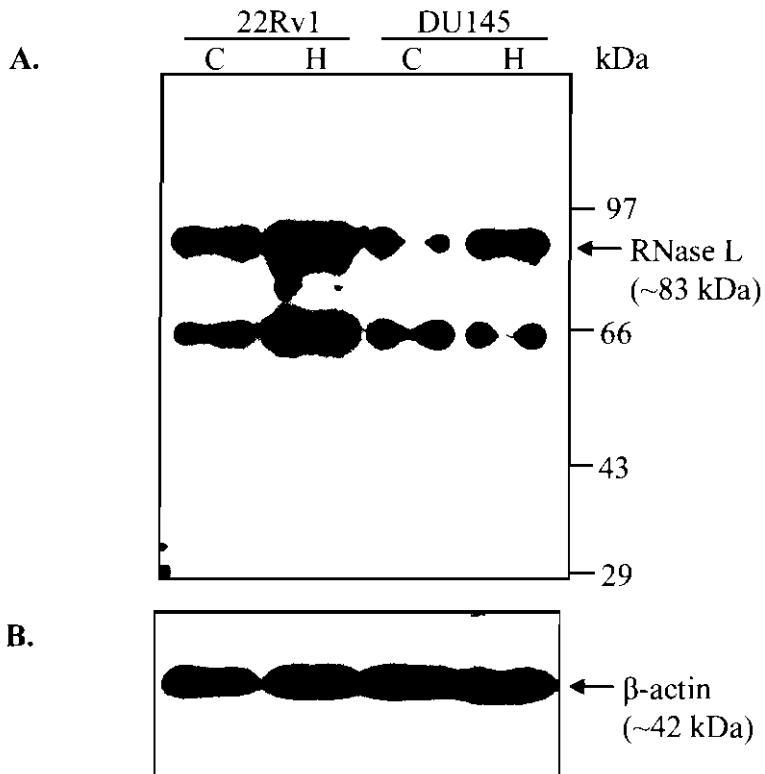
Fig. 21. A. Expression of RNase L protein in DU145 and 22Rv1 prostate cancer cells after 4 hr treatment with 200 μM H_2O_2 (H). 30 μg protein extract of the cells were resolved in 10% SDS-PAGE and immunoblotted against anti-human RNase L monoclonal antibody. B. Anti β- actin immunoblot. C= Control.

VII

Discussion

VII. DISCUSSION

VII.1 Expression of RNase L mRNA in mouse tissues

The present study was aimed to study the relative expression RNase L mRNA in 8-10 week old swiss albino mice in nine different mouse tissues viz; liver, kidney, brain, heart, prostate, testis, spleen thymus and lungs. The expression of RNase L in several mammalian tissues and cell lines has been reported by different researchers, even in the absence of interferon treatment. The earlier studies used radiolabelled 2-5A binding and cross-linking to RNase L molecule in tissue or cell extracts, indicating the level of native RNase L protein (Floyd-Smith and Denton, 1988; Nilsen et al., 1981; Silverman et al., 1988; Williams et al., 1979).

Different reports have shown varied results with respect to the tissues in which RNase L is found at higher level compared to other tissues. Nielsen et al., 1981 showed that RNase L is present in relatively higher amounts in the spleen, liver and lymphocytes followed by kidney while another study by Floyed-Smith and Denton in 1988 reported the spleen and lungs to contain higher amounts of RNase L compared to the intestine and liver. The 2-5A cross linking studies also showed that in new born mouse, RNase L level peaks between 2-14 days in several tissues with maximum amount in the kidney. The Spleen maintains its higher level after 2 days while in other tissues the level goes down gradually with age (Floyd-Smith and Denton, 1988; Pfeifer et al., 1993). In murine L929 cells, RNase L mRNA level was detected by northern blot to be increased by either interferon treatment or more potently by interferon in combination with cyclohexamide (Zhou et al., 1993). In recent past, 2-5A binding assay by UV cross linking was again performed in the extracts of tissues from seven different organs of the wild type mice, which showed highest expression in the spleen, thymus, lungs and testis compared to kidney, liver and heart. The RNase L knock out mice (RNase $L^{-/-}$) showed enlargement of the spleen and thymus, defect in interferon action and apoptosis (Zhou et al., 1997). Apart from Interferon, 100 µM glutamate exposure to the mouse cortical neurons for 15 min showed significant enhancement of RNase L mRNA expression as measured by semi quantitative RT-PCR at 2 hr post treatment, which was maintained at least upto 12 hr (Sugiyama et al., 2008).

In 1995, Wang el al., while studying the colorectal carcinogenesis and polyp formation found that, the expression of RNase L protein, as studied by the monoclonal

antibody, was highly increased as compared to the level of RNase L protein in the normal colonic mucosae (Wang et al., 1995). Zhou et al., in 2005, utilized a highly specific, radiobinding assay where a ^{32}P-labeled and bromine-substituted 2-5A analog was covalently cross-linked to RNase L under UV-light to measure RNase L levels in diffrent rodent and human cancer and normal cells. The rodent cells in which RNase L were present were as follows: mouse NIH3T3 (fibroblast), mouse SVT2 (SV40-transformed 3T3), mouse Baf-3 (pro-B cells), rat C6 (glioma cells), rat A10 (myoblast cells), mouse D5 (melanoma cells), mouse L929 fibroblasts, mouse RAW264.7 (monocytes) and mouse NIE115 (neuroblastoma) cell lines. Among these cell lines, the highest expression of RNase L, among the rodent cell types examined, was observed in the two blood cell lines, the mouse pro-B Baf-3 cell line and monocyte RAW264.7 cells. The human cell lines in which RNase L was measured were HeLa M (cervical carcinoma), U373 (malignant glioma), SW837 (rectal carcinoma), HT1080 (fibrosarcoma), HepG2 (hepatocellular carcinoma), HL-60 (promyelocytic leukemia cells), U937 (macrophage like cells), NCI-H292 (lung carcinoma), WI-38 (normal diploid fibroblast), Jurkat (T cell leukemia), and PC3 (prostate cancer cells). RNase L was observed in all these cells, with the highest expression in the SW837, HL-60, U937, Jurkat, and PC3 cells, spanning a wide variety of different human cancers (Zhou et al., 2005). High levels of expression found in the SW837 cells were consistent with the previously observed high levels of RNase L in human colorectal polyps and tumors (Wang et al., 1995).

Zhou et al. (2005) also determined levels of RNase L in normal human cell types and tissues by western blots and tissue microarrays with monoclonal antibody (mAb) to RNase L. The Western blot prepared from the human tissue extracts showed highest levels of RNase L in the lymph node and colon, followed by spinal cord and skeletal muscle, with lowest levels in the skin. Immunohistochemistry (IHC) showed presence of RNase L in the prostate epithelial cells and liver hepatocytes. Moreover in the lymph node, there were scattered, unidentified cells that stained strongly for the presence of RNase L. Our study, using RT-PCR as a tool, showed relative expression of RNase L mRNA in nine different tissues of the swiss albino mice namely spleen, thymus, kidney, testis, liver, brain, lungs, prostate and heart out of which the spleen showed highest level followed by the thymus. What is striking about these results, however, are not only the relative levels, but also the observation of ubiquitous expression of RNase L. The fact

that RNase L is so widely expressed suggests important functions as an innate immunity enzyme that controls viral infections. A more general role in RNA metabolism is also suggested by the wide- spread occurrence of the 2-5A/RNase L system in birds. reptiles. and mammals (Cayley and Kerr, 1982). An earlier study from our laboratory (Gupta. 2009) has also reported widespread and constitutive expression of RNase L mRNA in the nine different times of the mouse with high levels in the spleen, thymus and lungs, the immunological tissues. The present study confirms this observation.

VII.2. Effect of castration and testosterone treatment on mouse prostate

Prostatic structure and function are androgen-dependent. Castration induces rapid regression of the prostate gland to an atrophic state that is maintained until androgen is administered. Upon administration of androgen to a castrate, its atrophied prostate is rapidly restored morphologically and functionally. These hormonal influences on the prostate gland have been studied extensively by biochemical, histological, and physiological approaches (Sugimura et al.. 1986). Our study used this well-established procedure and effect to study the effect of androgen on expression of RNase L mRNA. The castration showed regression to atrophic state in the experimental mice. and its atrophic state was morphologically reversed upon testosterone administration for 5 days.

These effects have been described at molecular level in literature by different workers. Androgen withdrawal induces apoptosis of the secretory epithelium in normal prostate glands. Androgen receptors are present in the epithelial, stromal, and vascular smooth muscle cells (Johansson et al., 2005). Therefore the primary effects in all these cell types are possible. Studies in prostate tissue recombinants have shown that castration-induced glandular involution and epithelial cell apoptosis also occurs in chimeric prostate tissue that lacks androgen receptors in the epithelium (Kurita et al.. 2001). Thus, castration-induced prostate involution could be caused by primary changes in the androgen responsive cells in the prostate stroma (Kurita et al., 2001). Several growth and survival factors for the epithelial cells such as epidermal growth factors (EGFs), insulin-like growth factors (IGFs), fibroblast growth factors (FGFs), and transforming growth factor (TGF)-β are apparently produced in the prostate stroma cells (Culig et al., 1996: Cunha et al., 2003: Wong et al., 2003). Castration-induced regression of the ventral prostate (VP) lobe in the rats was preceded by a major decrease in the blood flow (Lekas et al., 1997) and increase in the endothelial cell apoptosis (Shabsigh et

al., 1998). Vascular regression caused tissue hypoxia and this may in turn trigger epithelial cell apoptosis and subsequent glandular involution (Lissbrant et al., 2004; Shabsigh et al., 1998)[Shabsigh et al, 1998, Lissbrant et al, 2001]. Prostate endothelial cells do not express androgen receptors suggesting indirect effects of castration on the endothelium (Johansson et al., 2005; Lissbrant et al., 2004; Shabsigh et al., 1998).

VII.3. Effect of castration and testosterone treatment on expression of Nkx3.1 mRNA in mouse prostate

Nkx3.1, a homeodomain transcription factor is one of the earliest proteins expressed in the prostate. Expression of Nkx3.1 is present at variable levels in all lobes of the prostate (Bhatia-Gaur et al., 1999). Bieberich et al (1996) localized Nkx3.1 to the luminal epithelium of the adult mouse prostate. Nkx3.1 expression appears to be strictly regulated by androgens, the mRNA levels of Nkx3.1 declined almost in 24 hours to 96 hours after castration (Bieberich et al., 1996). Mice with targeted disruption of Nkx3.1 have a significant reduction in the ductal morphology but not overall size of the prostate (Bhatia-Gaur et al., 1999). It is surprising that Nkx3.1 appears to play such an early role in prostate development yet is not required for prostate determination. In adulthood, Nkx3.1-deficient mice have decreased levels of prostate secretary proteins. Nkx3.1 also appears to mark prostate stem cells because the population of Nkx3.1-expressing cells is able to repopulate the prostate after castration and dihydrotestosterone (DHT) replacement (Wang et al., 2009). Loss of Nkx3.1 expression is a common finding in both prostate cancer and prostatic intraepithelial neoplasia (Abate-Shen et al., 2008).

In our experiment, castration of the mice did significantly decrease the level of Nkx3.1 mRNA, showing the results of effective androgen ablation by castration. Furthermore, intraperitoneal treatment with sustanone (a combination of testosterone propionate, testosterone phynylpropionate and testosterone decanoate) increased the level of Nkx3.1 mRNA, showing that hormone ablation and testosterone treatment in mouse prostate worked at the molecular level and both hormone ablation and exogenous supplementation can be used *in vivo* for further study under the given conditions.

VII.4. Effect of castration and testosterone treatment on expression of RNase L mRNA in mouse prostate

RNase L mRNA after castration and hormone replacement shows a decrease in the mouse prostate. However, this decrease is not statistically significant. The reason

behind not getting a statistically significant difffrence could be natural variation in the individual mouse with respect to RNase L mRNA expression and its unresponsiveness to androgen.

VII.5. Mouse RNase L promoter sequence analysis for androgen receptor binding site

The human RNase L gene, RNASEL, contains 7 exons and 6 introns , (Zhou et al., 2005). Silverman's group characterized and mapped the transcription start site in RNA isolated from human histiocytic U937 cells, chosen because of relatively high levels of RNase L by 5'-RACE. They amplified -881 to +48 bp and -202 to +48 bp. Treatments with 1000 U/ml IFN-α or IFN-γ, however, only slightly (not statistically significantly) increased the luciferase activity. Similarly, there was only a modest (2-fold) increase in the endogenous RNase L levels after IFN treatments of the HeLa M cells as determined in western blots probed with mAb against human RNase L. These results confirmed constitutive, basal expression of the human RNASEL promoter with, at best, modest stimulation by IFN-α or IFN-γ. They showed major and adjacent minor start sites at 190 and 188 nt upstream (5') of intron I. They also predicted several potential transcription factor binding sites by MatInspector Release 7.4 (Genomatix website: www.genomatix.de), which suggested a wide range of tissue-speeific as well as general transcription factors collectively contribute to the ubiquitous expression of RNase L. For example, there are potential binding sites for tissue-specific factors GKLF (gut), NGN1/3 (nervous system), IA-1 (pancreas), vErbA (thyroid), PTX1 (pituitary), TEF1, and MyoD (muscle). In addition, there are possible sites for a number of cytokine or growth factor-stimulated factors, including Stat5, Smad3, and c-Rel (Zhou et al., 2005). Although no IFN-stimulated response element (ISRE) was observed, a single canonical IFN-γ activation site (GAS) element is present (nucleotides -155 to -147) that could potentially lead to an induction by IFNs through Stat1 homodimer (Stark et al., 1998). The mouse RNase L gene promoter DNA sequences were characterized as restriction enzyme fragments and Southern hybridization to a 5'-proximal exon probe (Pandey and Rath, 2007).

It was investigated if there is any androgen receptor binding site in the mouse RNase L promoter sequence. For this purpose, the sequence from -1 to -1661 was analyzed for possible androgen receptor consensus binding site. One such partial consensus sequence was found at -51 to -63 nucleotides of the promoter region of mouse

RNase L gene which is in close proximity to the major and adjacent minor start sites at 190 and 188 nt upstream (5') of intron I (Zhou et al., 2005). This sequence may or may not be a functional androgen receptor binding sequence.

VII.6. Growth curve of DU145 cells

Growth curve of DU145 cells was plotted using MTT assay. 5000, 10000, 20000 and 40000 cells were seeded in triplicates in 24 well plate for 24 hr, 48 hr, and 72 hr time points. Cell at all the densities showed linear growth up to 48 hr while at 72 hr time point, the wells seeded with 40000 cells started showing decrease in cell growth. This may be due to arriving at a very high confluency or limitation of nutrients for further cell growth. The cells seeded at 5000, 10000 and 20000 per well showed nearly linear growth up to 72 hr. This was an optimisation experiment to find out the suitable cell density and time the time period for the testosterone treatment.

VII.7. Effect of testosterone on growth curve of DU145 cells

DU145 cells are androgen-nonresponsive cells. They do not express androgen receptor and does not respond to androgen treatment. The normal values for testosterone in the serum of adult males are 14 to 35 nM (Pinthus et al., 2007). We treated cells with 10 nM and 100 nM testosterone to observe the effect(s) of testosterone. The 10 nM dose is equivalent to the physiological levels of testosterone while 100 nM is a high dose of testosterone. Both the doses failed to show any stimulation in cell growth in DU145 cells. This confirmed the androgen-unresponsive nature of the cells.

VII.8. Growth curve of 22Rv1 cells

22Rv1 is an androgen-responsive human prostate carcinoma cell line derived from a primary prostate tumor. This cell line was isolated from a xenograft (CWR22R-2152) that was serially propagated in mice after castration-induced regression and relapse of the parental, androgen-dependent CWR xenograft (Sramkoski et al., 1999). 22Rv1 cells form tumors in nude mice and secrete prostate-specific antigen (PSA) into the circulation of tumor-bearing mice (Attardi et al., 2004). The 22Rv1 cells in our experiment showed density dependence on cell growth as low cell seeding density of 5000 cells/well in 24 well plates did not grow. Also, this experiment optimised the cell density and time period for the further experiments.

VII.9. Effect of testosterone on growth curve of 22Rv1 cells

22Rv1 is an androgen-responsive human prostate carcinoma cell line derived from a primary prostate tumor that expressed mutant (H874Y) androgen receptors (AR) and sceretes low levels of prostate specific antigen (PSA). Various androgens and other steroid hormones cause proliferation of 22Rv1 cells, PSA secretion, and transactivation. Incubation of 22Rv1 cells with various concentrations of testosterone have been shown to result in a dose-dependent 50–80%increase in cell growth over 72 hr (Barbara et al. 2004). In the present study androgen stimulated 22Rv1 cell growth proliferation at 10 nM conc. for 72 hr time upto 1.46 fold. Physiological levels of testosterone that is nearly 10 nM induces the androgen responsive cell line 22Rv1. While a high level of testosterone was not able to make a significant increase in cell growth compared to normal physiological level of 10 nM. This shows that probably 10 nM is saturating concentration of androgen for this particular set of experimental conditions. This may reflect the tumour growth from this cell line.

VII.10. Effect of testosterone on expression of RNase L mRNA and protein in DU145 and 22Rv1 cells

Our results show that after treatment with 10 nM testosterone, the mRNA level of RNase L did not show any significant change in DU145 cells, while, 22Rv1 cells showed statistically significant decrease (0.46 fold) in RNase L mRNA level after 48 hr. The abscence of any effect on the mRNA level of RNase L in DU145 cells by testosterone treatment shows that, in these cells due to the abscence of androgen receptor signalling axis, the cells are not showing any effect of testosterone on the RNase L mRNA level. 22Rv1 cells do express androgen receptor and show positive response in terms of cell growth to the androgen. In these cells, the decrease in mRNA level of RNase L compared to the untreated cells is associated with androgen treatment, which may act at transcriptional level or by reducing the stability of the RNase L mRNA. Here, there is a correlation between the reduction in the RNase L mRNA level and increase in the cell growth in response to androgen.

A similar effect was observed at the protein level in this testosterone treatment experiment. DU145 cells showed no effect while 22Rv1 cells showed decrease in the RNase L protein level in response to androgen. The androgen receptor is known to interact with RNase L (Bettoun et al., 2005). This interaction may be stabilising in

nature. After testosterone treatment, the androgen receptor may be activated, which may change its interaction with RNase L and make it unstable or vulnerable to degradation. More likely, androgen may influence its negative influence through the 3'-untranslated region (3'-UTR) of the RNase L mRNA. The 3'-UTR of RNase L has been well charecterized to play role in its short half-life and this is mediated through micro-RNA (Li et al., 2007; Malathi et al., 2007). It would be interesting to investigate, if wild type RNase L cDNA transfection and over expression can reduce the cell growth/proliferation and the tumour (xenograft) formation by the 22Rv1 cells in the cells and in the mice, respectively. Also, the RNase L mRNA and protein in the DU145 and 22Rv1 cells may or may not be of wild type sequence.

VII.11. Effect of hydrogen peroxide on growth curve of DU145 and 22Rv1 cells

Earlier study from our laboratory (Pandey et al., 2004) showed that RNase L gene is responsive to a wide variety of stressors, e.g., dsRNA (poly rI.rC), cyclohexamide, cisplatin, doxorubicin, doxorubicin, vincristine, vinblastin, H_2O_2, caleium chloride, tumour necrosis factor- α (TNF-α) in the human cervical cancer (HeLa) cells, such that all these agents induced the RNase L protein level in these cells. This correlated with RNA degradation, chromatin-DNA fragmentation and apoptosis of the HeLa cells by these stressors to variable extents. It was, therefore, decided to investigate the effects of H_2O_2 which causes oxidative stress and cytotoxicity, in terms of cytotoxicity and RNase L mRNA and protein expression in the DU145 and 22Rv1 prostate cancer cells. The initial experiments with hydrogen peroxide, of using low doses of hydrogen peroxide for long time periods resulted in no observation of the effect of hydrogen peroxide caused cytotoxicity. The reasons could be, build up of cellular response against the oxidative stress. While excess reactive oxygen species (ROS) are toxic, regulated ROS, however, play an important role in cellular signalling (Nacci et al., 2010). The ability of a cell to counteract stressful conditions, known as cellular stress response, requires the activation of pro-survival pathways and the production of molecules with anti-oxidant, anti-apoptotic or pro-apoptotic activities (Calabrese et al., 2007). Among the cellular pathways conferring protection against oxidative stress, a key role is played by heat shock proteins (Hsps) heme oxygenase-1 (HO-1) and Hsp70, as well as the thioredoxin/thioredoxin reductase system (Calabrese et al., 2008; Nacci et al., 2010). These systems may be activated in the case low hydrogen peroxide treatment for long duration. For obtaining a desired effect of oxidative stress/cytotoxicity higher doses of

hydrogen peroxide for shorter time duration was used. Even at these doses, cells which were seeded in higher density showed some recovery of cell growth. Thus it seems that in cell culture condition both time, dose and cell number is important in causing oxidative damage followed by cytotoxicity/apoptosis.

VII.12. Effect of hydrogen peroxide on expression of RNase L mRNA and protein in DU145 and 22Rv1 cells

Hydrogen peroxide induced RNase L at both mRNA and protein levels in both androgen-responsive 22Rv1 and androgen-nonresponsive DU145 cells. RNase L upregulation by stressors like hydrogen peroxide in human cervical carcinoma (HeLa) cells have been shown earlier (Pandey et al., 2004). Asparagine-233 in the ankyrin repeat number 6 of human RNase L is hydroxylated by a factor inhibiting hypoxia-inducible factor (HIF-1) alpha, the factor inhibiting hypoxia-inducible factor (FIH), suggesting that RNase L stability and/or activity could be regulated in response to oxygen-related signals (Cockman et al., 2009). It would be interesting to investigate whether the H_2O_2 –induced upregulation of RNase L mRNA and protein directly participated in the cytotoxity/apoptosis caused by H_2O_2 in these two human prostate cancer cells by a mechanism of cellular RNA-degradation.

Taken together, this study shows that the RNase L mRNA expression is constitutive in many tissues under normal conditions and it may be partially and negatively influenced by the androgen in the intact mouse. In the human prostate cancer cells (22Rv1), androgen negatively regulates RNase L mRNA expression and positively regulates cell growth/proliferation. This was not observed in the androgen-unresponsive human prostate cancer cells (DU145). However, an oxidative stress inducing agent, i.e. H_2O_2 stimulated/induced the RNase L mRNA as well as RNase L protein levels and caused cytotoxicity/apoptosis in both the types of human prostate cancer cells (DU145 and 22Rv1). Therefore, RNase L expression in the human prostate cancer cells responsive to oxygen may be exploited to cause inhibition of cell growth/proliferation and oxidative stress-inducing agents like H_2O_2 may be exploited to induce RNase L expression in order to cause cytotoxicity/apoptosis in both androgen-responsive and androgen-unresponsive human prostate cancer cells. Further investigation is necessary to dissect the molecular details of these cellular effects of androgen and H_2O_2 in the context of RNase L gene expression.

VIII

Conclusion

VIII. CONCLUSIONS

1. RNase L mRNA is constitutively expressed in the mouse tissues under normal physiological conditions, with higher levels in the spleen and thymus. suggesting housekeeping function(s) of RNase L in the tissues as well as its immunological role(s) in the spleen and thymus. This is a new information. as RNase L has been long known as an antiviral RNA-degrading enzyme induced by viruses. interferons and dsRNA in mammalian cells.

2. RNase L mRNA may not be primarily regulated by endogenous androgen in normal mouse prostate tissue, exogenous androgen also did not show any major significant effect on RNase L mRNA, at the best, it may negatively regulate RNase L expression to a small extent, possibly, through a cryptic androgen response element (ARE) in the RNase L promoter at -51 to -63 nucleotide. which needs to be established.

3. Human prostate cancer cell lines, e.g. the androgen-unresponsive DU145 and the androgen-responsive 22Rv1 cells showed diferential effects of androgen in regulating the levels of RNase L mRNA and protein. In 22Rv1 cells, androgen caused cell proliferation and down-regulation of the level of RNase L mRNA as well as protein, while in DU145 cells no effect of testosterone was observed either on cell proliferation or on expression of RNase L mRNA and protein.

4. Oxidative stress by H_2O_2 caused upregulation of both RNase L mRNA and protein in both the androgen-responsive and unresponsive cell lines. 22Rv1 and DU145.

5. Further investigation is necessary to establish the molecular details of these cellular effects.

IX

References

VIII. REFERENCES

Abate-Shen, C., Shen, M.M., and Gelmann, E. (2008). Integrating differentiation and cancer: the Nkx3.1 homeobox gene in prostate organogenesis and carcinogenesis. Differentiation *76*, 717-727.

Accola, M.A., Huang, B., Al Masri, A., and McNiven, M.A. (2002). The antiviral dynamin family member, MxA, tubulates lipids and localizes to the smooth endoplasmic reticulum. J Biol Chem *277*, 21829-21835.

Aebi, M., Fah, J., Hurt, N., Samuel, C.E., Thomis, D., Bazzigher, L., Pavlovic, J., Haller, O., and Staeheli, P. (1989). cDNA structures and regulation of two interferon-induced human Mx proteins. Mol Cell Biol *9*, 5062-5072.

Al-Ahmadi, W., Al-Haj, L., Al-Mohanna, F.A., Silverman, R.H., and Khabar, K.S. (2009). RNase L downmodulation of the RNA-binding protein, HuR, and cellular growth. Oncogene *28*, 1782-1791.

Almasan, A., and Ashkenazi, A. (2003). Apo2L/TRAIL: apoptosis signaling, biology, and potential for cancer therapy. Cytokine Growth Factor Rev *14*, 337-348.

Alvarez-Cubero, M.J., Entrala, C., Fernandez-Rosado, F., Martinez-Gonzalez, L.J., Alvarez, J.C., Suarez, A., Lorente, J.A., and Cozar, J.M. (2012). Predictive value in the analysis of RNASEL genotypes in relation to prostate cancer. Prostate Cancer Prostatic Dis *15*, 144-149.

Andersson, I., Bladh, L., Mousavi-Jazi, M., Magnusson, K.E., Lundkvist, A., Haller, O., and Mirazimi, A. (2004). Human MxA protein inhibits the replication of Crimean-Congo hemorrhagic fever virus. J Virol *78*, 4323-4329.

Ank, N., West, H., Bartholdy, C., Eriksson, K., Thomsen, A.R., and Paludan, S.R. (2006). Lambda interferon (IFN-lambda), a type III IFN, is induced by viruses and IFNs and displays potent antiviral activity against select virus infections in vivo. J Virol *80*, 4501-4509.

Arnheiter, H., Skuntz, S., Noteborn, M., Chang, S., and Meier, E. (1990). Transgenic mice with intracellular immunity to influenza virus. Cell *62*, 51-61.

Atanasiu, P., and Chany, C. (1960). [Effect of interferon originating in malignant cells on experimental infection of the newborn hamster with polyoma virus]. C R Seanees Soc Biol Fil *25*, 1687-1689.

Attardi, B.J., Burgenson, J., Hild, S.A., and Reel, J.R. (2004). Steroid hormonal regulation of growth, prostate specific antigen secretion, and transeription mediated by the mutated androgen receptor in CWR22Rv1 human prostate carcinoma cells. Mol Cell Endocrinol *222*, 121-132.

Austin, B.A., James, C., Silverman, R.H., and Carr, D.J. (2005). Critical role for the oligoadenylate synthetase/RNase L pathway in response to IFN-beta during acute ocular herpes simplex virus type 1 infection. J Immunol *175*, 1100-1106.

Bartsch, D.K., Fendrich, V., Slater, E.P., Sina-Frey, M., Rieder, H., Greenhalf, W., Chaloupka, B., Hahn, S.A., Neoptolemos, J.P., and Kress, R. (2005). RNASEL germline variants are assoeiated with pancreatic cancer. Int J Cancer *117*, 718-722.

Beattie, E., Denzler, K.L., Tartaglia, J., Perkus, M.E., Paoletti, E., and Jacobs, B.L. (1995). Reversal of the interferon-sensitive phenotype of a vaccinia virus lacking E3L by expression of the reovirus S4 gene. J Virol *69*, 499-505.

Benech, P., Mory, Y., Revel, M., and Chebath, J. (1985). Structure of two forms of the interferon-induced (2'-5') oligo A synthetase of human cells based on cDNAs and gene sequences. EMBO J *4*, 2249-2256.

Bettoun, D.J., Scafonas, A., Rutledge, S.J., Hodor, P., Chen, O., Gambone, C., Vogel, R., McElwee-Witmer, S., Bai, C., Freedman, L., *et al.* (2005). Interaction between the androgen receptor and RNase L mediates a eross-talk between the interferon and androgen signaling pathways. J Biol Chem *280*, 38898-38901.

Beuten, J., Gelfond, J.A., Franke, J.L., Shook, S., Johnson-Pais, T.L., Thompson, I.M., and Leach, R.J. (2010). Single and multivariate associations of MSR1, ELAC2, and RNASEL with prostate cancer in an ethnic diverse cohort of men. Cancer Epidemiol Biomarkers Prev *19*, 588-599.

Bhatia-Gaur, R., Donjacour, A.A., Sciavolino, P.J., Kim, M., Desai, N., Young, P., Norton, C.R., Gridley, T., Cardiff, R.D., Cunha, G.R., *et al.* (1999). Roles for Nkx3.1 in prostate development and cancer. Genes Dev *13*, 966-977.

Bieberich, C.J., Fujita, K., He, W.W., and Jay, G. (1996). Prostate-specific and androgen-dependent expression of a novel homeobox gene. J Biol Chem *271*, 31779-31782.

Bisbal, C., Martinand, C., Silhol, M., Lebleu, B., and Salehzada, T. (1995). Cloning and characterization of a RNAse L inhibitor. A new component of the interferon-regulated 2-5A pathway. J Biol Chem *270*, 13308-13317.

Bisbal, C., Silhol, M., Laubenthal, H., Kaluza, T., Carnac, G., Milligan, L., Le Roy, F., and Salehzada, T. (2000). The 2'-5' oligoadenylate/RNase L/RNase L inhibitor pathway regulates both MyoD mRNA stability and muscle cell differentiation. Mol Cell Biol *20*, 4959-4969.

Bradford, M.M. (1976). A rapid and sensitive method for the quantitation of microgram quantities of protein utilizing the principle of protein-dye binding. Anal Biochem *72*, 248-254.

Breeden, L., and Nasmyth, K. (1987). Similarity between cell-cycle genes of budding yeast and fission yeast and the Notch gene of Drosophila. Nature *329*, 651-654.

Calabrese, V., Mancuso, C., Sapienza, M., Puleo, E., Calafato, S., Cornelius, C., Finocchiaro, M., Mangiameli, A., Di Mauro, M., Stella, A.M., *et al.* (2007). Oxidative stress and cellular stress response in diabetic nephropathy. Cell Stress Chaperones *12*, 299-306.

Calabrese, V., Signorile, A., Cornelius, C., Mancuso, C., Scapagnini, G., Ventimiglia, B., Ragusa, N., and Dinkova-Kostova, A. (2008). Practical approaches to investigate redox regulation of heat shock protein expression and intracellular glutathione redox state. Methods Enzymol *441*, 83-110.

Carpten, J., Nupponen, N., Isaacs, S., Sood, R., Robbins, C., Xu, J., Faruque, M., Moses, T., Ewing, C., Gillanders, E., *et al.* (2002). Germline mutations in the ribonuclease L gene in families showing linkage with HPC1. Nat Genet *30*, 181-184.

Carter. B.S., Bova. G.S., Beaty, T.H., Steinberg, G.D., Childs, B., Isaacs, W.B.. and Walsh, P.C. (1993). Hereditary prostate cancer: epidemiologic and clinical features. J Urol *150*, 797-802.

Casey, G., Neville. P.J., Plummer, S.J., Xiang, Y., Krumroy, L.M.. Klein. E.A., Catalona, W.J., Nupponen, N.. Carpten, J.D., Trent, J.M., *et al.* (2002). RNASEL Arg462Gln variant is implicated in up to 13% of prostate cancer cases. Nat Genet *32*, 581-583.

Castelli, J.C., Hassel. B.A.. Wood, K.A.. Li, X.L., Amemiya, K., Dalakas, M.C.. Torrence, P.F.. and Youle, R.J. (1997). A study of the interferon antiviral mechanism: apoptosis activation by the 2-5A system. J Exp Med *186*, 967-972.

Castora, F.J., Erickson. C.E.. Kovacs, T., Lesiak, K.. and Torrence, P.F. (1991). 2',5'-oligoadenylates inhibit relaxation of supercoiled DNA by calf thymus DNA topoisomerase I. J Interferon Res *11*, 143-149.

Cayley, P.J., Davies, J.A., McCullagh, K.G., and Kerr, I.M. (1984). Activation of the ppp(A2'p)nA system in interferon-treated, herpes simplex virus-infected cells and evidence for novel inhibitors of the ppp(A2'p)nA-dependent RNase. Eur J Biochem *143*, 165-174.

Cayley, P.J., and Kerr, I.M. (1982). Synthesis, characterisation and biological significance of (2'-5')oligoadenylate derivatives of NAD+. ADP-ribose and adenosine(5')tetraphospho(5')adenosine. Eur J Biochem *122*, 601-608.

Chakrabarti, A., Ghosh. P.K., Banerjee, S., Gaughan, C., and Silverman, R.H. (2012). RNase L triggers autophagy in response to viral infections. J Virol *86*, 11311-11321.

Chandrasekaran, K., Mehrabian, Z., Li, X.L., and Hassel, B. (2004). RNase-L regulates the stability of mitochondrial DNA-encoded mRNAs in mouse embryo fibroblasts. Biochem Biophys Res Commun *325*, 18-23.

Chawla-Sarkar, M., Bauer, J.A., Lupica, J.A., Morrison, B.H.. Tang, Z., Oates, R.K.. Almasan, A., DiDonato, J.A.. Borden, E.C., and Lindner, D.J. (2003). Suppression of NF-kappa B survival signaling by nitrosylcobalamin sensitizes neoplasms to the anti-tumor effects of Apo2L/TRAIL. J Biol Chem *278*, 39461-39469.

Chebath, J., Benech, P., Revel, M., and Vigneron, M. (1987). Constitutive expression of (2'-5') oligo A synthetase confers resistance to picornavirus infection. Nature *330*, 587-588.

Chelbi-Alix, M.K., and Wietzerbin, J. (2007). Interferon, a growing cytokine family: 50 years of interferon research. Biochimie *89*, 713-718.

Chen, H., Griffin, A.R., Wu, Y.Q., Tomsho, L.P., Zuhlke, K.A., Lange, E.M., Gruber, S.B., and Cooney, K.A. (2003). RNASEL mutations in hereditary prostate cancer. J Med Genet *40*, e21.

Chen, Z.Q., Dong, J., Ishimura, A., Daar, I., Hinnebusch, A.G., and Dean, M. (2006). The essential vertebrate ABCE1 protein interacts with eukaryotic initiation factors. J Biol Chem *281*, 7452-7457.

Cockman, M.E., Webb, J.D., Kramer, H.B., Kessler, B.M., and Ratcliffe, P.J. (2009). Proteomics-based identification of novel factor inhibiting hypoxia-inducible factor (FIH) substrates indicates widespread asparaginyl hydroxylation of ankyrin repeat domain-containing proteins. Mol Cell Proteomics *8*, 535-546.

Colby, C., and Duesberg, P.H. (1969). Double-stranded RNA in vaccinia virus infected cells. Nature *222*, 940-944.

Culig, Z., Hobisch, A., Cronauer, M.V., Radmayr, C., Hittmair, A., Zhang, J., Thurnher, M., Bartsch, G., and Klocker, H. (1996). Regulation of prostatic growth and function by peptide growth factors. Prostate *28*, 392-405.

Cunha, G.R., Hayward, S.W., Wang, Y.Z., and Ricke, W.A. (2003). Role of the stromal microenvironment in carcinogenesis of the prostate. Int J Cancer *107*, 1-10.

Dagan, E., Laitman, Y., Levanon, N., Feuer, A., Sidi, A.A., Baniel, J., Korach, Y., Ben Baruch, G., Friedman, E., and Gershoni-Baruch, R. (2006). The 471delAAAG mutation and C353T polymorphism in the RNASEL gene in sporadic and inherited cancer in Israel. Fam Cancer *5*, 389-395.

Dar, A.C., Dever, T.E., and Sicheri, F. (2005). Higher-order substrate recognition of eIF2alpha by the RNA-dependent protein kinase PKR. Cell *122*, 887-900.

Defilippi, P., Huez, G., Verhaegen-Lawalle, M., De Clercq, E., Imai, J., Torrence, P., and Content, J. (1986). Antiviral activity of a chemically stabilized 2-5A analog upon microinjection into HeLa cells. FEBS Lett *198*, 326-332.

Demettre, E., Bastide, L., D'Haese, A., De Smet, K., De Meirleir, K., Tiev, K.P., Englebienne, P., and Lebleu, B. (2002). Ribonuclease L proteolysis in peripheral blood mononuclear cells of chronic fatigue syndrome patients. J Biol Chem *277*, 35746-35751.

Diaz-Guerra, M., Rivas, C., and Esteban, M. (1997). Inducible expression of the 2-5A synthetase/RNase L system results in inhibition of vaccinia virus replication. Virology *227*, 220-228.

Dong, B., Niwa, M., Walter, P., and Silverman, R.H. (2001). Basis for regulated RNA cleavage by functional analysis of RNase L and Ire1p. RNA *7*, 361-373.

Dong, B., and Silverman, R.H. (1995). 2-5A-dependent RNase molecules dimerize during activation by 2-5A. J Biol Chem *270*, 4133-4137.

Dong, B., and Silverman, R.H. (1997). A bipartite model of 2-5A-dependent RNase L. J Biol Chem *272*, 22236-22242.

Dong, B., and Silverman, R.H. (1999). Alternative function of a protein kinase homology domain in 2', 5'-oligoadenylate dependent RNase L. Nucleic Acids Res *27*, 439-445.

Dong, B., Xu, L., Zhou, A., Hassel, B.A., Lee, X., Torrence, P.F., and Silverman, R.H. (1994). Intrinsic molecular activities of the interferon-induced 2-5A-dependent RNase. J Biol Chem *269*, 14153-14158.

Dong, J.T. (2006). Prevalent mutations in prostate cancer. J Cell Biochem *97*, 433-447.

Dugan, J.W., Albor, A., David, L., Fowlkes, J., Blackledge, M.T., Martin, T.M., Planck, S.R., Rosenzweig, H.L., Rosenbaum, J.T., and Davey, M.P. (2009). Nucleotide oligomerization domain-2 interacts with 2'-5'-oligoadenylate synthetase type 2 and enhances RNase-L function in THP-1 cells. Mol Immunol *47*, 560-566.

Ehrenfeld, E., and Hunt, T. (1971). Double-stranded poliovirus RNA inhibits initiation of protein synthesis by reticulocyte lysates. Proc Natl Acad Sci U S A *68*, 1075-1078.

Flodstrom-Tullberg, M., Hultcrantz, M., Stotland, A., Maday, A., Tsai, D., Fine, C., Williams, B., Silverman, R., and Sarvetnick, N. (2005). RNase L and double-stranded RNA-dependent protein kinase exert complementary roles in islet cell defense during coxsackievirus infection. J Immunol *174*, 1171-1177.

Floyd-Smith, G., and Denton, J.S. (1988). Age-dependent changes are observed in the levels of an enzyme mediator of interferon action: a (2'-5')A(n)-dependent endoribonuclease. Proc Soc Exp Biol Med *189*, 329-337.

Floyd-Smith, G., Slattery, E., and Lengyel, P. (1981). Interferon action: RNA cleavage pattern of a (2'-5')oligoadenylate--dependent endonuclease. Science *212*, 1030-1032.

Fremont, M., El Bakkouri, K., Vaeyens, F., Herst, C.V., De Meirleir, K., and Englebienne, P. (2005). 2',5'-Oligoadenylate size is critical to protect RNase L against proteolytic cleavage in chronic fatigue syndrome. Exp Mol Pathol *78*, 239-246.

Gabaldon, T., and Huynen, M.A. (2004). Prediction of protein function and pathways in the genome era. Cell Mol Life Sci *61*, 930-944.

George, C.X., Thomis, D.C., McCormack, S.J., Svahn, C.M., and Samuel, C.E. (1996). Characterization of the heparin-mediated activation of PKR, the interferon-inducible RNA-dependent protein kinase. Virology *221*, 180-188.

Ghosh, A., Sarkar, S.N., Guo, W., Bandyopadhyay, S., and Sen, G.C. (1997). Enzymatic activity of 2'-5'-oligoadenylate synthetase is impaired by specific mutations that affect oligomerization of the protein. J Biol Chem *272*, 33220-33226.

Gil, J., and Esteban, M. (2000). The interferon-induced protein kinase (PKR), triggers apoptosis through FADD-mediated activation of caspase 8 in a manner independent of Fas and TNF-alpha receptors. Oncogene *19*, 3665-3674.

Gil, J., Garcia, M.A., Gomez-Puertas, P., Guerra, S., Rullas, J., Nakano, H., Alcami, J., and Esteban, M. (2004). TRAF family proteins link PKR with NF-kappa B activation. Mol Cell Biol *24*, 4502-4512.

Gresser, I., Bourali, C., Levy, J.P., Fontaine-Brouty-Boye, D., and Thomas, M.T. (1969). Increased survival in mice inoculated with tumor cells and treated with interferon preparations. Proc Natl Acad Sci U S A 63, 51-57.

Gribaudo, G., Lembo, D., Cavallo, G., Landolfo, S., and Lengyel, P. (1991). Interferon action: binding of viral RNA to the 40-kilodalton 2'-5'-oligoadenylate synthetase in interferon-treated HeLa cells infected with encephalomyocarditis virus. J Virol 65, 1748-1757.

Grivennikov, S.I., Greten, F.R., and Karin, M. (2010). Immunity, inflammation, and cancer. Cell 140, 883-899.

Gupta, A. (2009). Functional analysis of the Ribonuclease L (RNase L). In School of Life Sciences (New Delhi, Jawaharlal Nehru University).

Gupta, A., and Rath, P.C. (2012). Expression, purification and characterization of the interferon-inducible, antiviral and tumour-suppressor protein, human RNase L. J Biosci 37, 103-113.

Haller, O., Arnheiter, H., Lindenmann, J., and Gresser, I. (1980). Host gene influences sensitivity to interferon action selectively for influenza virus. Nature 283, 660-662.

Hartmann, R., Justesen, J., Sarkar, S.N., Sen, G.C., and Yee, V.C. (2003). Crystal structure of the 2'-specific and double-stranded RNA-activated interferon-induced antiviral protein 2'-5'-oligoadenylate synthetase. Mol Cell 12, 1173-1185.

Hartmann, R., Olsen, H.S., Widder, S., Jorgensen, R., and Justesen, J. (1998). p59OASL, a 2'-5' oligoadenylate synthetase like protein: a novel human gene related to the 2'-5' oligoadenylate synthetase family. Nucleic Acids Res 26, 4121-4128.

Hassel, B.A., Zhou, A., Sotomayor, C., Maran, A., and Silverman, R.H. (1993). A dominant negative mutant of 2-5A-dependent RNase suppresses antiproliferative and antiviral effects of interferon. EMBO J 12, 3297-3304.

Hearl, W.G., and Johnston, M.I. (1987). Accumulation of 2',5'-oligoadenylates in encephalomyocarditis virus-infected mice. J Virol 61, 1586-1592.

Hovanessian, A.G., and Justesen, J. (2007). The human 2'-5'oligoadenylate synthetase family: unique interferon-inducible enzymes catalyzing 2'-5' instead of 3'-5' phosphodiester bond formation. Biochimie *89*. 779-788.

Hovanessian, A.G., Wood. J., Meurs, E., and Montagnier, L. (1979). Increased nuclease activity in cells treated with pppA2'p5'A2'p5' A. Proc Natl Acad Sci U S A *76*, 3261-3265.

Hovanessian, A.G., and Wood, J.N. (1980). Anticellular and antiviral effects of pppA(2'p5'A)n. Virology *101*. 81-90.

Ikeda, H., Old. L.J., and Schreiber, R.D. (2002). The roles of IFN gamma in protection against tumor development and cancer immunoediting. Cytokine Growth Factor Rev *13*. 95-109.

Ireland, D.D., Stohlman, S.A., Hinton. D.R., Kapil, P., Silverman, R.H., Atkinson, R.A., and Bergmann, C.C. (2009). RNase L mediated protection from virus induced demyelination. PLoS Pathog *5*, e1000602.

Jacobs, M.D., and Harrison, S.C. (1998). Structure of an IkappaBalpha/NF-kappaB complex. Cell *95*, 749-758.

Jacobsen, H., Krause, D., Friedman, R.M., and Silverman, R.H. (1983). Induction of ppp(A2'p)nA-dependent RNase in murine JLS-V9R cells during growth inhibition. Proc Natl Acad Sci U S A *80*, 4954-4958.

Johansson, A., Rudolfsson, S.H., Wikstrom, P., and Bergh, A. (2005). Altered levels of angiopoietin 1 and tie 2 are associated with androgen-regulated vascular regression and growth in the ventral prostate in adult mice and rats. Endocrinology *146*, 3463-3470.

Justesen, J., Hartmann, R., and Kjeldgaard, N.O. (2000). Gene structure and function of the 2'-5'-oligoadenylate synthetase family. Cell Mol Life Sci *57*, 1593-1612.

Kerr, I.D. (2004). Sequence analysis of twin ATP binding cassette proteins involved in translational control, antibiotic resistance, and ribonuclease L inhibition. Biochem Biophys Res Commun *315*, 166-173.

Kerr, I.M., and Brown, R.E. (1978). pppA2'p5'A2'p5'A: an inhibitor of protein synthesis synthesized with an enzyme fraction from interferon-treated cells. Proc Natl Acad Sci U S A *75*, 256-260.

Kerr, I.M., Brown, R.E., and Ball, L.A. (1974). Increased sensitivity of cell-free protein synthesis to double-stranded RNA after interferon treatment. Nature *250*, 57-59.

Kerr, I.M., Brown, R.E., and Hovanessian, A.G. (1977). Nature of inhibitor of cell-free protein synthesis formed in response to interferon and double-stranded RNA. Nature *268*, 540-542.

Khabar, K.S., Siddiqui, Y.M., al-Zoghaibi, F., al-Haj, L., Dhalla, M., Zhou, A., Dong, B., Whitmore, M., Paranjape, J., Al-Ahdal, M.N., *et al.* (2003). RNase L mediates transient control of the interferon response through modulation of the double-stranded RNA-dependent protein kinase PKR. J Biol Chem *278*, 20124-20132.

Kim, S., Rusmevichientong, A., Dong, B., Remenyi, R., Silverman, R.H., and Chow, S.A. (2010). Fidelity of target site duplication and sequence preference during integration of xenotropic murine leukemia virus-related virus. PLoS One *5*, e10255.

Kispal, G., Sipos, K., Lange, H., Fekete, Z., Bedekovics, T., Janaky, T., Bassler, J., Aguilar Netz, D.J., Balk, J., Rotte, C., *et al.* (2005). Biogenesis of cytosolic ribosomes requires the essential iron-sulphur protein Rli1p and mitochondria. EMBO J *24*, 589-598.

Kochs, G., and Haller, O. (1999). Interferon-induced human MxA GTPase blocks nuclear import of Thogoto virus nucleocapsids. Proc Natl Acad Sci U S A *96*, 2082-2086.

Krause, D., Lesiak, K., Imai, J., Sawai, H., Torrence, P.F., and Silverman, R.H. (1986). Activation of 2-5A-dependent RNase by analogs of 2-5A (5'-O-triphosphoryladenylyl(2'---5')adenylyl(2'----5')adenosine) using 2',5'-tetraadenylate (core)-cellulose. J Biol Chem *261*, 6836-6839.

Krause, D., Mullins, J.M., Penafiel, L.M., Meister, R., and Nardone, R.M. (1991). Microwave exposure alters the expression of 2-5A-dependent RNase. Radiat Res *127*, 164-170.

Krause, D., Panet, A., Arad, G., Dieffenbach, C.W., and Silverman, R.H. (1985). Independent regulation of ppp(A2'p)nA-dependent RNase in NIH 3T3, clone 1 cells by growth arrest and interferon treatment. J Biol Chem *260*, 9501-9507.

Krause, D., and Silverman, R.H. (1993). Tissue-related and species-specific differences in the 2-5A oligomer size requirement for activation of 2-5A-dependent RNase. J Interferon Res *13*, 13-16.

Kruger, S., Silber, A.S., Engel, C., Gorgens, H., Mangold, E., Pagenstecher, C., Holinski-Feder, E., von Knebel Doeberitz, M., Moeslein, G., Dietmaier, W., *et al.* (2005). Arg462Gln sequence variation in the prostate-cancer-susceptibility gene RNASEL and age of onset of hereditary non-polyposis colorectal cancer: a case-control study. Lancet Oncol *6*, 566-572.

Kurita, T., Wang, Y.Z., Donjacour, A.A., Zhao, C., Lydon, J.P., O'Malley, B.W., Isaacs, J.T., Dahiya, R., and Cunha, G.R. (2001). Paracrine regulation of apoptosis by steroid hormones in the male and female reproductive system. Cell Death Differ *8*, 192-200.

Laemmli, U.K. (1970). Cleavage of structural proteins during the assembly of the head of bacteriophage T4. Nature *227*, 680-685.

Larson, B.T., Magi-Galluzzi, C., Casey, G., Plummer, S.J., Silverman, R., and Klein, E.A. (2008). Pathological aggressiveness of prostatic carcinomas related to RNASEL R462Q allelic variants. J Urol *179*, 1344-1348.

Latham, K.E., Cosenza, S., Reichenbach, N.L., Mordechai, E., Adelson, M.E., Kon, N., Horvath, S.E., Charubala, R., Mikhailov, S.N., Pfeiderer, W., *et al.* (1996). Inhibition of growth of estrogen receptor positive and estrogen receptor negative breast cancer cells in culture by AA-etherA, a stable 2-5A derivative. Oncogene *12*, 827-837.

Le Roy, F., Bisbal, C., Silhol, M., Martinand, C., Lebleu, B., and Salehzada, T. (2001). The 2-5A/RNase L/RNase L inhibitor (RLI) [correction of (RNI)] pathway regulates mitochondrial mRNAs stability in interferon alpha-treated H9 cells. J Biol Chem *276*, 48473-48482.

Le Roy, F., Laskowska, A., Silhol, M., Salehzada, T., and Bisbal, C. (2000). Characterization of RNABP, an RNA binding protein that associates with RNase L. J Interferon Cytokine Res *20*, 635-644.

Le Roy, F., Salehzada, T., Bisbal, C., Dougherty, J.P., and Peltz, S.W. (2005). A newly discovered function for RNase L in regulating translation termination. Nat Struct Mol Biol *12*, 505-512.

Le Roy, F., Silhol, M., Salehzada, T., and Bisbal, C. (2007). Regulation of mitochondrial mRNA stability by RNase L is translation-dependent and controls IFNalpha-induced apoptosis. Cell Death Differ *14*, 1406-1413.

Lee, T.Y., Ezelle, H.J., Venkataraman, T., Lapidus, R.G., Scheibner, K.A., and Hassel, B.A. (2013). Regulation of Human RNase-L by the miR-29 Family Reveals a Novel Oncogenic Role in Chronic Myelogenous Leukemia. J Interferon Cytokine Res *33*, 34-42.

Lekas, E., Johansson, M., Widmark, A., Bergh, A., and Damber, J.E. (1997). Decrement of blood flow precedes the involution of the ventral prostate in the rat after castration. Urol Res *25*, 309-314.

Li, G., Xiang, Y., Sabapathy, K., and Silverman, R.H. (2004). An apoptotic signaling pathway in the interferon antiviral response mediated by RNase L and c-Jun NH2-terminal kinase. J Biol Chem *279*, 1123-1131.

Li, X.L., Andersen, J.B., Ezelle, H.J., Wilson, G.M., and Hassel, B.A. (2007). Post-transcriptional regulation of RNase-L expression is mediated by the 3'-untranslated region of its mRNA. J Biol Chem *282*, 7950-7960.

Li, X.L., Blackford, J.A., and Hassel, B.A. (1998). RNase L mediates the antiviral effect of interferon through a selective reduction in viral RNA during encephalomyocarditis virus infection. J Virol *72*, 2752-2759.

Li, X.L., Blackford, J.A., Judge, C.S., Liu, M., Xiao, W., Kalvakolanu, D.V., and Hassel, B.A. (2000). RNase-L-dependent destabilization of interferon-induced mRNAs. A role for the 2-5A system in attenuation of the interferon response. J Biol Chem *275*, 8880-8888.

Li, X.L., Ezelle, H.J., Kang, T.J., Zhang, L., Shirey, K.A., Harro, J., Hasday, J.D., Mohapatra, S.K., Crasta, O.R., Vogel, S.N., *et al.* (2008). An essential role for the antiviral endoribonuclease, RNase-L, in antibacterial immunity. Proc Natl Acad Sci U S A *105*, 20816-20821.

Lindenmann, J. (1962). Resistance of mice to mouse-adapted influenza A virus. Virology *16*, 203-204.

Lissbrant, I.F., Hammarsten, P., Lissbrant, E., Ferrara, N., Rudolfsson, S.H., and Bergh, A. (2004). Neutralizing VEGF bioactivity with a soluble chimeric VEGF-receptor protein flt(1-3)IgG inhibits testosterone-stimulated prostate growth in castrated mice. Prostate *58*, 57-65.

Liu, W., Liang, S.L., Liu, H., Silverman, R., and Zhou, A. (2007). Tumour suppressor function of RNase L in a mouse model. Eur J Cancer *43*, 202-209.

Lopez de Silanes, I., Fan, J., Yang, X., Zonderman, A.B., Potapova, O., Pizer, E.S., and Gorospe, M. (2003). Role of the RNA-binding protein HuR in colon carcinogenesis. Oncogene *22*, 7146-7154.

Lopp, A., Kuusksalu, A., Reintamm, T., Muller, W.E., and Kelve, M. (2002). 2',5'-oligoadenylate synthetase from a lower invertebrate, the marine sponge Geodia cydonium, does not need dsRNA for its enzymatic activity. Biochim Biophys Acta *1590*, 140-149.

Lux, S.E., John, K.M., and Bennett, V. (1990). Analysis of cDNA for human erythrocyte ankyrin indicates a repeated structure with homology to tissue-differentiation and cell-cycle control proteins. Nature *344*, 36-42.

Ma, J., and Spremulli, L.L. (1996). Expression, purification, and mechanistic studies of bovine mitochondrial translational initiation factor 2. J Biol Chem *271*, 5805-5811.

Madsen, B.E., Ramos, E.M., Boulard, M., Duda, K., Overgaard, J., Nordsmark, M., Wiuf, C., and Hansen, L.L. (2008). Germline mutation in RNASEL predicts increased risk of head and neck, uterine cervix and breast cancer. PLoS One *3*, e2492.

Malathi, K., Dong, B., Gale, M., Jr., and Silverman, R.H. (2007). Small self-RNA generated by RNase L amplifies antiviral innate immunity. Nature *448*, 816-819.

Malathi, K., Paranjape, J.M., Ganapathi, R., and Silverman, R.H. (2004). HPC1/RNASEL mediates apoptosis of prostate cancer cells treated with 2',5'-oligoadenylates, topoisomerase I inhibitors, and tumor necrosis factor-related apoptosis-inducing ligand. Cancer Res *64*, 9144-9151.

Malathi, K., Saito, T., Crochet, N., Barton, D.J., Gale, M., Jr., and Silverman, R.H. (2010). RNase L releases a small RNA from HCV RNA that refolds into a potent PAMP. RNA *16*, 2108-2119.

Marcotte, E.M., Pellegrini, M., Yeates, T.O., and Eisenberg, D. (1999). A census of protein repeats. J Mol Biol *293*, 151-160.

Marie, I., Blanco, J., Rebouillat, D., and Hovanessian, A.G. (1997). 69-kDa and 100-kDa isoforms of interferon-induced (2'-5')oligoadenylate synthetase exhibit differential catalytic parameters. Eur J Biochem *248*, 558-566.

Marie, I., and Hovanessian, A.G. (1992). The 69-kDa 2-5A synthetase is composed of two homologous and adjacent functional domains. J Biol Chem *267*, 9933-9939.

Mashimo, T., Glaser, P., Lucas, M., Simon-Chazottes, D., Ceccaldi, P.E., Montagutelli, X., Despres, P., and Guenet, J.L. (2003). Structural and functional genomics and evolutionary relationships in the cluster of genes encoding murine 2',5'-oligoadenylate synthetases. Genomics *82*, 537-552.

Meeks, J.J., and Schaeffer, E.M. (2011). Genetic regulation of prostate development. J Androl *32*, 210-217.

Meurs, E., Chong, K., Galabru, J., Thomas, N.S., Kerr, I.M., Williams, B.R., and Hovanessian, A.G. (1990). Molecular cloning and characterization of the human double-stranded RNA-activated protein kinase induced by interferon. Cell *62*, 379-390.

Meyer, M.S., Penney, K.L., Stark, J.R., Schumacher, F.R., Sesso, H.D., Loda, M., Fiorentino, M., Finn, S., Flavin, R.J., Kurth, T., *et al.* (2010). Genetic variation in

RNASEL associated with prostate cancer risk and progression. Carcinogenesis *31*, 1597-1603.

Mishra, R.R., Chaudhary, J.K., Bajaj, G.D., and Rath, P.C. (2011). A novel human TPIP splice-variant (TPIP-C2) mRNA, expressed in human and mouse tissues, strongly inhibits cell growth in HeLa cells. PLoS One *6*, e28433.

Mosmann, T. (1983). Rapid colorimetric assay for cellular growth and survival: application to proliferation and cytotoxicity assays. J Immunol Methods *65*, 55-63.

Nacci, A., Dallan, I., Monzani, F., Dardano, A., Migliorini, P., Riente, L., Ursino, F., and Fattori, B. (2010). Elevated antithyroid peroxidase and antinuclear autoantibody titers in Meniere's disease patients: more than a chance association? Audiol Neurootol *15*, 1-6.

Naito, T., Yokogawa, T., Kim, H.S., Matsuda, A., Sasaki, T., Fukushima, M., Kitade, Y., and Wataya, Y. (2007). A novel apoptotic pathway of 3'-Ethynylcytidine(ECyd) involving the inhibition of RNA synthesis--the possibility of RNase L activated pathway as a target of ECyd. Nucleic Acids Symp Ser (Oxf), 435-436.

Naito, T., Yokogawa, T., Takatori, S., Goda, K., Hiramoto, A., Sato, A., Kitade, Y., Sasaki, T., Matsuda, A., Fukushima, M., *et al.* (2009). Role of RNase L in apoptosis induced by 1-(3-C-ethynyl-beta-D-ribo-pentofuranosyl)cytosine. Cancer Chemother Pharmacol *63*, 837-850.

Nakanishi, M., Tanaka, N., Mizutani, Y., Mochizuki, M., Ueno, Y., Nakamura, K.T., and Kitade, Y. (2005). Functional characterization of 2',5'-linked oligoadenylate binding determinant of human RNase L. J Biol Chem *280*, 41694-41699.

Nakanishi, M., Yoshimura, A., Ishida, N., Ueno, Y., and Kitade, Y. (2004). Contribution of Tyr712 and Phe716 to the activity of human RNase L. Eur J Biochem *271*, 2737-2744.

Nakazato, H., Suzuki, K., Matsui, H., Ohtake, N., Nakata, S., and Yamanaka, H. (2003). Role of genetic polymorphisms of the RNASEL gene on familial prostate cancer risk in a Japanese population. Br J Cancer *89*, 691-696.

Nanduri, S., Carpick, B.W., Yang, Y., Williams, B.R., and Qin, J. (1998). Structure of the double-stranded RNA-binding domain of the protein kinase PKR reveals the molecular basis of its dsRNA-mediated activation. EMBO J *17*, 5458-5465.

Nilsen, T.W., Wood, D.L., and Baglioni, C. (1981). 2',5'-Oligo(A)-activated endoribonuclease. Tissue distribution and characterization with a binding assay. J Biol Chem *256*, 10751-10754.

Pandey, M., Bajaj, G.D., and Rath, P.C. (2004). Induction of the interferon-inducible RNA-degrading enzyme, RNase L, by stress-inducing agents in the human cervical carcinoma cells. RNA Biol *1*, 21-27.

Pandey, M., and Rath, P.C. (2004). Expression of interferon-inducible recombinant human RNase L causes RNA degradation and inhibition of cell growth in Escherichia coli. Biochem Biophys Res Commun *317*, 586-597.

Pandey, M., and Rath, P.C. (2007). Organization of the interferon-inducible 2',5'-oligoadenylate-dependent ribonuclease L (RNase L) gene of mouse. Mol Biol Rep *34*, 97-104.

Patel, R.C., and Sen, G.C. (1998). PACT, a protein activator of the interferon-induced protein kinase, PKR. EMBO J *17*, 4379-4390.

Paucker, K., Cantell, K., and Henle, W. (1962). Quantitative studies on viral interference in suspended L cells. III. Effect of interfering viruses and interferon on the growth rate of cells. Virology *17*, 324-334.

Pavlovic, J., Haller, O., and Staeheli, P. (1992). Human and mouse Mx proteins inhibit different steps of the influenza virus multiplication cycle. J Virol *66*, 2564-2569.

Pestka, S., Krause, C.D., and Walter, M.R. (2004). Interferons, interferon-like cytokines, and their receptors. Immunol Rev *202*, 8-32.

Pfeifer, K., Ushijima, H., Lorenz, B., Muller, W.E., and Schroder, H.C. (1993). Evidence for age-dependent impairment of antiviral 2',5'-oligoadenylate synthetase/ribonuclease L-system in tissues of rat. Mech Ageing Dev *67*, 101-114.

Pinthus, J.H., Bryskin, I., Trachtenberg, J., Lu, J.P., Singh, G., Fridman, E., and Wilson, B.C. (2007). Androgen induces adaptation to oxidative stress in prostate cancer: implications for treatment with radiation therapy. Neoplasia 9, 68-80.

Rasmussen, S.B., Jensen, S.B., Nielsen, C., Quartin, E., Kato, H., Chen, Z.J., Silverman, R.H., Akira, S., and Paludan, S.R. (2009). Herpes simplex virus infection is sensed by both Toll-like receptors and retinoic acid-inducible gene- like receptors, which synergize to induce type I interferon production. J Gen Virol 90, 74-78.

Rayamajhi, M., Humann, J., Penheiter, K., Andreasen, K., and Lenz, L.L. (2010). Induction of IFN-alphabeta enables Listeria monocytogenes to suppress macrophage activation by IFN-gamma. J Exp Med 207, 327-337.

Rebouillat, D., and Hovanessian, A.G. (1999). The human 2',5'-oligoadenylate synthetase family: interferon-induced proteins with unique enzymatic properties. J Interferon Cytokine Res 19, 295-308.

Rebouillat, D., Hovnanian, A., Marie, I., and Hovanessian, A.G. (1999). The 100-kDa 2',5'-oligoadenylate synthetase catalyzing preferentially the synthesis of dimeric pppA2'p5'A molecules is composed of three homologous domains. J Biol Chem 274, 1557-1565.

Rebouillat, D., Marie, I., and Hovanessian, A.G. (1998). Molecular cloning and characterization of two related and interferon-induced 56-kDa and 30-kDa proteins highly similar to 2'-5' oligoadenylate synthetase. Eur J Biochem 257, 319-330.

Rennert, H., Bercovich, D., Hubert, A., Abeliovich, D., Rozovsky, U., Bar-Shira, A., Soloviov, S., Schreiber, L., Matzkin, H., Rennert, G., et al. (2002). A novel founder mutation in the RNASEL gene, 471delAAAG, is associated with prostate cancer in Ashkenazi Jews. Am J Hum Genet 71, 981-984.

Rivas, C., Gil, J., Melkova, Z., Esteban, M., and Diaz-Guerra, M. (1998). Vaccinia virus E3L protein is an inhibitor of the interferon (i.f.n.)-induced 2-5A synthetase enzyme. Virology 243, 406-414.

Robbins, C.M., Hernandez, W., Ahaghotu, C., Bennett, J., Hoke, G., Mason, T., Pettaway, C.A., Vijayakumar, S., Weinrich, S., Furbert-Harris, P., et al. (2008).

Association of HPC2/ELAC2 and RNASEL non-synonymous variants with prostate cancer risk in African American familial and sporadic cases. Prostate *68*, 1790-1797.

Roberts, W.K., Hovanessian, A., Brown, R.E., Clemens, M.J., and Kerr, I.M. (1976). Interferon-mediated protein kinase and low-molecular-weight inhibitor of protein synthesis. Nature *264*, 477-480.

Rokman, A., Ikonen, T., Seppala, E.H., Nupponen, N., Autio, V., Mononen, N., Bailey-Wilson, J., Trent, J., Carpten, J., Matikainen, M.P., *et al.* (2002). Germline alterations of the RNASEL gene, a candidate HPC1 gene at 1q25, in patients and families with prostate cancer. Am J Hum Genet *70*, 1299-1304.

Rusch, L., Zhou, A., and Silverman, R.H. (2000). Caspase-dependent apoptosis by 2',5'-oligoadenylate activation of RNase L is enhanced by IFN-beta. J Interferon Cytokine Res *20*, 1091-1100.

Rusmevichientong, A., and Chow, S.A. (2010). Biology and pathophysiology of the new human retrovirus XMRV and its association with human disease. Immunol Res *48*, 27-39.

Ruvolo, P.P., Gao, F., Blalock, W.L., Deng, X., and May, W.S. (2001). Ceramide regulates protein synthesis by a novel mechanism involving the cellular PKR activator RAX. J Biol Chem *276*, 11754-11758.

Rysiecki, G., Gewert, D.R., and Williams, B.R. (1989). Constitutive expression of a 2',5'-oligoadenylate synthetase cDNA results in increased antiviral activity and growth suppression. J Interferon Res *9*, 649-657.

Sabbah, A., Chang, T.H., Harnack, R., Frohlich, V., Tominaga, K., Dube, P.H., Xiang, Y., and Bose, S. (2009). Activation of innate immune antiviral responses by Nod2. Nat Immunol *10*, 1073-1080.

Sadler, A.J., and Williams, B.R. (2008). Interferon-inducible antiviral effectors. Nat Rev Immunol *8*, 559-568.

Saelens, X., Kalai, M., and Vandenabeele, P. (2001). Translation inhibition in apoptosis: caspase-dependent PKR activation and eIF2-alpha phosphorylation. J Biol Chem *276*, 41620-41628.

Saito, T., Owen, D.M., Jiang, F., Marcotrigiano, J., and Gale, M., Jr. (2008). Innate immunity induced by composition-dependent RIG-I recognition of hepatitis C virus RNA. Nature *454*, 523-527.

Samuel, M.A., Whitby, K., Keller, B.C., Marri, A., Barchet, W., Williams, B.R., Silverman, R.H., Gale, M., Jr., and Diamond, M.S. (2006). PKR and RNase L contribute to protection against lethal West Nile Virus infection by controlling early viral spread in the periphery and replication in neurons. J Virol *80*, 7009-7019.

Sarkar, S.N., Pal, S., and Sen, G.C. (2002). Crisscross enzymatic reaction between the two molecules in the active dimeric P69 form of the 2'-5' oligodenylate synthetase. J Biol Chem *277*, 44760-44764.

Sato, A., Naito, T., Hiramoto, A., Goda, K., Omi, T., Kitade, Y., Sasaki, T., Matsuda, A., Fukushima, M., Wataya, Y., *et al.* (2010). Association of RNase L with a Ras GTPase-activating-like protein IQGAP1 in mediating the apoptosis of a human cancer cell-line. FEBS J *277*, 4464-4473.

Scherbik, S.V., Paranjape, J.M., Stockman, B.M., Silverman, R.H., and Brinton, M.A. (2006). RNase L plays a role in the antiviral response to West Nile virus. J Virol *80*, 2987-2999.

Schroder, H.C., Natalio, F., Wiens, M., Tahir, M.N., Shukoor, M.I., Tremel, W., Belikov, S.I., Krasko, A., and Muller, W.E. (2008). The 2'-5'-oligoadenylate synthetase in the lowest metazoa: isolation, cloning, expression and functional activity in the sponge Lubomirskia baicalensis. Mol Immunol *45*, 945-953.

Schroder, H.C., Suhadolnik, R.J., Pfleiderer, W., Charubala, R., and Muller, W.E. (1992). (2'-5')Oligoadenylate and intracellular immunity against retrovirus infection. Int J Biochem *24*, 55-63.

Sedgwick, S.G., and Smerdon, S.J. (1999). The ankyrin repeat: a diversity of interactions on a common structural framework. Trends Biochem Sci *24*, 311-316.

Shabsigh, A., Chang, D.T., Heitjan, D.F., Kiss, A., Olsson, C.A., Puchner, P.J., and Buttyan, R. (1998). Rapid reduction in blood flow to the rat ventral prostate gland after castration: preliminary evidence that androgens influence prostate size by regulating blood flow to the prostate gland and prostatic endothelial cell survival. Prostate *36*, 201-206.

Shook, S.J., Beuten, J., Torkko, K.C., Johnson-Pais, T.L., Troyer, D.A., Thompson, I.M., and Leach, R.J. (2007). Association of RNASEL variants with prostate cancer risk in Hispanic Caucasians and African Americans. Clin Cancer Res *13*, 5959-5964.

Siddiqui, M.A., and Malathi, K. (2012). RNase L Induces Autophagy via c-Jun N-terminal Kinase and Double-stranded RNA-dependent Protein Kinase Signaling Pathways. J Biol Chem *287*, 43651-43664.

Silverman, R.H. (2003). Implications for RNase L in prostate cancer biology. Biochemistry *42*, 1805-1812.

Silverman, R.H. (2007). A scientific journey through the 2-5A/RNase L system. Cytokine Growth Factor Rev *18*, 381-388.

Silverman, R.H., Jung, D.D., Nolan-Sorden, N.L., Dieffenbach, C.W., Kedar, V.P., and SenGupta, D.N. (1988). Purification and analysis of murine 2-5A-dependent RNase. J Biol Chem *263*, 7336-7341.

Silverman, R.H., Nguyen, C., Weight, C.J., and Klein, E.A. (2010). The human retrovirus XMRV in prostate cancer and chronic fatigue syndrome. Nat Rev Urol *7*, 392-402.

Silverman, R.H., Skehel, J.J., James, T.C., Wreschner, D.H., and Kerr, I.M. (1983). rRNA cleavage as an index of ppp(A2'p)nA activity in interferon-treated encephalomyocarditis virus-infected cells. J Virol *46*, 1051-1055.

Sperling, J., Chebath, J., Arad-Dann, H., Offen, D., Spann, P., Lehrer, R., Goldblatt, D., Jolles, B., and Sperling, R. (1991). Possible involvement of (2'5')oligoadenylate synthetase activity in pre-mRNA splicing. Proc Natl Acad Sci U S A *88*, 10377-10381.

Sramkoski, R.M., Pretlow, T.G., 2nd, Giaconia, J.M., Pretlow, T.P., Schwartz, S., Sy, M.S., Marengo, S.R., Rhim, J.S., Zhang, D., and Jacobberger, J.W. (1999). A new human prostate carcinoma cell line, 22Rv1. In Vitro Cell Dev Biol Anim *35*, 403-409.

Stark, G.R., Kerr, I.M., Williams, B.R., Silverman, R.H., and Schreiber, R.D. (1998). How cells respond to interferons. Annu Rev Biochem *67*, 227-264.

Sugimura, Y., Cunha, G.R., and Donjacour, A.A. (1986). Morphological and histological study of castration-induced degeneration and androgen-induced regeneration in the mouse prostate. Biol Reprod *34*, 973-983.

Sugiyama, C., Kuramoto, N., Nagashima, R., Yoneyama, M., and Ogita, K. (2008). Enhanced expression of RNase L as a novel intracellular signal generated by NMDA receptors in mouse cortical neurons. Neurochem Int *53*, 71-78.

Suhadolnik, R.J., Peterson, D.L., O'Brien, K., Cheney, P.R., Herst, C.V., Reichenbach, N.L., Kon, N., Horvath, S.E., Iacono, K.T., Adelson, M.E., *et al.* (1997). Biochemical evidence for a novel low molecular weight 2-5A-dependent RNase L in chronic fatigue syndrome. J Interferon Cytokine Res *17*, 377-385.

Takaoka, A., and Yanai, H. (2006). Interferon signalling network in innate defence. Cell Microbiol *8*, 907-922.

Tanaka, N., Nakanishi, M., Kusakabe, Y., Goto, Y., Kitade, Y., and Nakamura, K.T. (2004). Structural basis for recognition of 2',5'-linked oligoadenylates by human ribonuclease L. EMBO J *23*, 3929-3938.

Ting, J.P., Duncan, J.A., and Lei, Y. (2010). How the noninflammasome NLRs function in the innate immune system. Science *327*, 286-290.

Truve, E., Kelve, M., Aaspollu, A., Schroder, H.C., and Muller, W.E. (1994). Homologies between different forms of 2-5A synthetases. Prog Mol Subcell Biol *14*, 139-149.

Turan, K., Mibayashi, M., Sugiyama, K., Saito, S., Numajiri, A., and Nagata, K. (2004). Nuclear MxA proteins form a complex with influenza virus NP and inhibit the transcription of the engineered influenza virus genome. Nucleic Acids Res *32*, 643-652.

Turpaev, K., Hartmann, R., Kisselev, L., and Justesen, J. (1997). Ap3A and Ap4A are primers for oligoadenylate synthesis catalyzed by interferon-inducible 2-5A synthetase. FEBS Lett *408*, 177-181.

Vilcek, J. (2003). Boosting p53 with interferon and viruses. Nat Immunol *4*, 825-826.

Wang, L., Zhou, A., Vasavada, S., Dong, B., Nie, H., Church, J.M., Williams, B.R., Banerjee, S., and Silverman, R.H. (1995). Elevated levels of 2',5'-linked oligoadenylate-dependent ribonuclease L occur as an early event in colorectal tumorigenesis. Clin Cancer Res *1*, 1421-1428.

Wang, X., Kruithof-de Julio, M., Economides, K.D., Walker, D., Yu, H., Halili, M.V., Hu, Y.P., Price, S.M., Abate-Shen, C., and Shen, M.M. (2009). A luminal epithelial stem cell that is a cell of origin for prostate cancer. Nature *461*, 495-500.

Wiklund, F., Jonsson, B.A., Brookes, A.J., Stromqvist, L., Adolfsson, J., Emanuelsson, M., Adami, H.O., Augustsson-Balter, K., and Gronberg, H. (2004). Genetic analysis of the RNASEL gene in hereditary, familial, and sporadic prostate cancer. Clin Cancer Res *10*, 7150-7156.

Williams, B.R. (1999). PKR; a sentinel kinase for cellular stress. Oncogene *18*, 6112-6120.

Williams, B.R., Golgher, R.R., Brown, R.E., Gilbert, C.S., and Kerr, I.M. (1979). Natural occurrence of 2-5A in interferon-treated EMC virus-infected L cells. Nature *282*, 582-586.

Witt, P.L., Spear, G.T., Helgeson, D.O., Lindstrom, M.J., Smalley, R.V., and Borden, E.C. (1990). Basal and interferon-induced 2',5'-oligoadenylate synthetase in human monocytes, lymphocytes, and peritoneal macrophages. J Interferon Res *10*, 393-402.

Wong, Y.C., Wang, X.H., and Ling, M.T. (2003). Prostate development and carcinogenesis. Int Rev Cytol *227*, 65-130.

Wreschner, D.H., James, T.C., Silverman, R.H., and Kerr, I.M. (1981). Ribosomal RNA cleavage, nuclease activation and 2-5A(ppp(A2'p)nA) in interferon-treated cells. Nucleic Acids Res *9*, 1571-1581.

Wreschner, D.H., Silverman, R.H., James, T.C., Gilbert, C.S., and Kerr, I.M. (1982). Affinity labelling and characterization of the ppp(A2'p)nA-dependent endoribonuclease from different mammalian sources. Eur J Biochem *124*, 261-268.

Xiang, Y., Wang, Z., Murakami, J., Plummer, S., Klein, E.A., Carpten, J.D., Trent, J.M., Isaacs, W.B., Casey, G., and Silverman, R.H. (2003). Effects of RNase L mutations associated with prostate cancer on apoptosis induced by 2',5'-oligoadenylates. Cancer Res *63*, 6795-6801.

Yin, H., Zhou, A., and Dai, Y. (2012). The association of elevated 2',5'-oligoadenylate-dependent RNase L with lung cancer correlated with deficient enzymatic activity and decreased capacity of RNase L dimerization. Lung Cancer *78*, 30-38.

Zhou, A., Hassel, B.A., and Silverman, R.H. (1993). Expression cloning of 2-5A-dependent RNAase: a uniquely regulated mediator of interferon action. Cell *72*, 753-765.

Zhou, A., Molinaro, R.J., Malathi, K., and Silverman, R.H. (2005). Mapping of the human RNASEL promoter and expression in cancer and normal cells. J Interferon Cytokine Res *25*, 595-603.

Zhou, A., Paranjape, J., Brown, T.L., Nie, H., Naik, S., Dong, B., Chang, A., Trapp, B., Fairchild, R., Colmenares, C., *et al.* (1997). Interferon action and apoptosis are defective in mice devoid of 2',5'-oligoadenylate-dependent RNase L. EMBO J *16*, 6355-6363.